GEOCHEMISTRY AND MIGRATION OF CONTAMINANTS AT THE WELDON SPRING CHEMICAL PLANT SITE, ST. CHARLES COUNTY, MISSOURI--1989-91

By John G. Schumacher

U.S. GEOLOGICAL SURVEY

Open-File Report 93-433

U.S. DEPARTMENT OF THE INTERIOR

BRUCE BABBITT, Secretary

U.S. GEOLOGICAL SURVEY

Robert M. Hirsch, Acting Director

CONTENTS

ILLUSTRATIONS

TABLES

CONVERSION FACTORS AND VERTICAL DATUM

Multiply	By	To obtain
inch	25.4	millimeter
foot	0.3048	meter
mile	1.609	kilometer
acre	0.4047	hectare
cubic foot per second	0.02832	cubic meter per second
million gallons per day	0.04381	cubic meter per second
ton, short	907.2	kilogram
pound, avoirdupois	0.4536	kilogram
cubic foot	0.02832	cubic meter

Temperature in degrees Celsius (°C) can be converted to degrees Fahrenheit (°F) as follows:

$$°F = (1.8 \times °C) + 32$$

Sea Level: In this report, "sea level" refers to the National Geodetic Vertical Datum of 1929 (NGVD of 1929)--a geodetic datum derived from a general adjustment of the first-order level nets of both the United States and Canada, formerly called Sea Level Datum of 1929.

GEOCHEMISTRY AND MIGRATION OF CONTAMINANTS AT THE WELDON SPRING CHEMICAL PLANT SITE, ST. CHARLES COUNTY, MISSOURI--1989-91

By John G. Schumacher

ABSTRACT

Investigations were conducted by the U.S. Geological Survey in cooperation with the U.S. Department of Energy at the Weldon Spring chemical plant site to determine the geochemistry of the shallow aquifer and geochemical controls on the migration of uranium and other constituents from the raffinate (waste) pits. Water-quality analyses from monitoring wells at the site and vicinity property indicate that water in the shallow aquifer is a calcium magnesium bicarbonate type that is at equilibrium with respect to calcite and slightly supersaturated with respect to dolomite.

Water samples from the surface of the raffinate pits contained various concentrations of the following major constituents (numbers in parentheses are constituent concentrations in milligrams per liter): calcium (11 to 1,400), magnesium (21 to 480), sodium (120 to 1,500), potassium (13 to 181), sulfate (70 to 990), and nitrite plus nitrate (less than 10 to more than 1,800, as nitrogen); and the following trace constituents (numbers in parentheses are concentrations in micrograms per liter): lithium (10 to 6,240), molybdenum (670 to 7,100), strontium (122 to 5,460), vanadium (70 to 3,200), and uranium (less than 10 to more than 4,000). Analysis of interstitial-water samples from raffinate pit 3 indicated that concentrations of most constituents increased with increasing depth below the water-sediment interface. Equilibrium-speciation calculations indicate that interstitial solutions generally are supersaturated with respect to carnotite and undersaturated with respect to uraninite. Shallow sludge samples (less than 4.5 feet deep) contained large quantities of apatite [$Ca_5(PO_4)_3$] and trace quantities of carnotite [$K_2(UO_2)_2(VO_4)_2 \cdot 3H_2O$]. Deeper sludge samples (4.5 to 9 feet deep) contained large quantities of gypsum ($CaSO_4 \cdot 2H_2O$, 40 to 75 percent) and sellaite (MgF_2, 10 to 40 percent), lesser quantities of apatite (5 to 15 percent), quartz (SiO_2, 5 to 10 percent), goethite [$FeO(OH)$, about 5 percent], and scattered grains of carnotite. No uranium (IV) minerals were identified. Equilibrium-speciation calculations indicate that nitrate and uranium were not chemically reduced or attenuated within the raffinate pits and can be expected to migrate into the underlying overburden.

No significant sorption of calcium, sodium, sulfate, nitrate, or lithium was observed in laboratory sorption experiments using samples of two overburden units at the site (Ferrelview Formation and clay till); however, significant quantities of molybdenum (VI) and uranium (VI) were sorbed. Sorption of molybdenum (VI) was dependent only on solution pH and sorption of uranium (VI) was dependent on solution pH and carbonate concentration. The sorption of molybdenum (VI) and uranium (VI) was consistent with sorption controlled by oxyhydroxides, rather than by clay minerals. At neutral pH values, the uranium (VI) distribution coefficient for solutions in contact with the Ferrelview Formation ranged from 330 to 437 milliliters per gram of solid as compared to 10.7 to 26 milliliters per gram of solid for solutions in contact with the clay till. The distribution coefficient values for uranium (VI) sorption by the clay till were small because of the formation of weakly sorbed uranium carbonate complexes.

The water quality of samples from lysimeters completed in the overburden near raffinate pit 4 can be obtained as a mixture of water from raffinate pits 3 and 4 and an uncontaminated component in a system at equilibrium with ferrihydrite and calcite. Concentrations of uranium are limited by dilution and sorption. The simulations also indicate that precipitation of calcite is likely when calcium-rich solutions migrating from raffinate pit 3 mix with bicarbonate-rich ground water and solutions from raffinate pit 4. Additional sources of sulfate other than the raffinate pits are indicated by the model. Potential sources of this sulfate include wastes from the manufacturing of military ordnance at the site before 1946.

Constituents that had no sorption in the laboratory experiments, such as nitrate, were detected most frequently, and in the largest concentrations, in monitoring wells near the raffinate pits and Ash pond. Increased uranium concentrations in monitoring wells near the raffinate pits indicates the presence of preferential flow paths, saturation of available sorption sites, or formation of weakly sorbed uranium carbonate complexes within the overburden. Computer simulations of water quality in several contaminated bedrock monitoring wells near the raffinate pits indicate that the water quality can be simulated by mixing water from raffinate pits 3 and 4 with an uncontaminated component, and allowing for equilibrium with calcite. The hydrologic and geochemical data indicate that raffinate pit 3 is the most likely source of increased concentrations of calcium, sodium, nitrite plus nitrate, and lithium in these wells, and raffinate pit 4 is the primary source of uranium.

Water-level, dye trace, discharge, and water-quality data and the results of geochemical simulations indicated that increased constituent concentrations in Burgermeister spring are the result of several sources. At low-base flow Burgermeister spring contains increased concentrations of sodium, chloride, nitrite plus nitrate, lithium, and uranium. Increased concentrations of sodium and chloride probably are the result of a subsurface connection between the spring and the east tributary of Schote Creek, which contains a road-salt storage facility. Schote Creek loses flow to the subsurface and has been shown by dye traces to be hydrologically connected to Burgermeister spring. Increased concentrations of nitrite plus nitrate,

lithium, and small quantities of uranium at base flow are the result of seepage from the raffinate pits (predominately raffinate pits 3 and 4) migrating through preferential pathways within bedrock troughs extending northward from the raffinate pit area to Burgermeister spring. Concentrations of uranium tended to increase at larger flows because runoff that contained large concentrations of uranium (from Ash pond) entered the east fork of the west tributary of Schote Creek.

INTRODUCTION

During 1955 the U.S. Atomic Energy Commission authorized the construction of the Weldon Spring uranium feed materials plant [locally known as the Weldon Spring chemical plant (WSCP)]. The 217-acre plant is situated on the eastern part of a 17,232-acre tract of land known as the Weldon Spring ordnance works (WSOW; fig. 1) formerly owned by the U.S. Army. The WSCP was operated by a private contractor under contract to the U.S. Atomic Energy Commission (AEC) from 1957 to 1966. The plant processed uranium (U) ore concentrates and recycled scrap into U-tetrafluoride, U-dioxide, and pure U metal (Harrington and Ruehle, 1959). Wastes from the plant, referred to as raffinate (Weidner and Boback, 1982), were slurried to four large disposal pits at the site (hereafter referred to as raffinate pits). The Weldon Spring uranium feed materials plant was designed to process 5,000 tons of ore concentrates per year; however, between 1958 and 1964, an average of 16,000 tons per year were processed (Ryckman and others, 1978). The excess production resulted in the radiologic contamination of the five major process buildings, support buildings, and adjacent property (MK-Ferguson Company and Jacobs Engineering Group, 1989e). The two existing raffinate pits (pits 1 and 2) were quickly filled, requiring the construction of two additional pits, pits 3 and 4 (fig. 2).

The disposal of low-level radioactive and associated wastes at the site has resulted in increased specific conductance values and concentrations of calcium (Ca), magnesium (Mg), sodium (Na), sulfate (SO_4), chloride (Cl), nitrite plus nitrate ($NO_2 + NO_3$), lithium (Li), strontium (Sr), U, and possibly molybdenum (Mo) in the shallow ground water (Kleeschulte and Emmett, 1987). In addition, large quantities of SO_4 and trace quantities of nitroaromatic
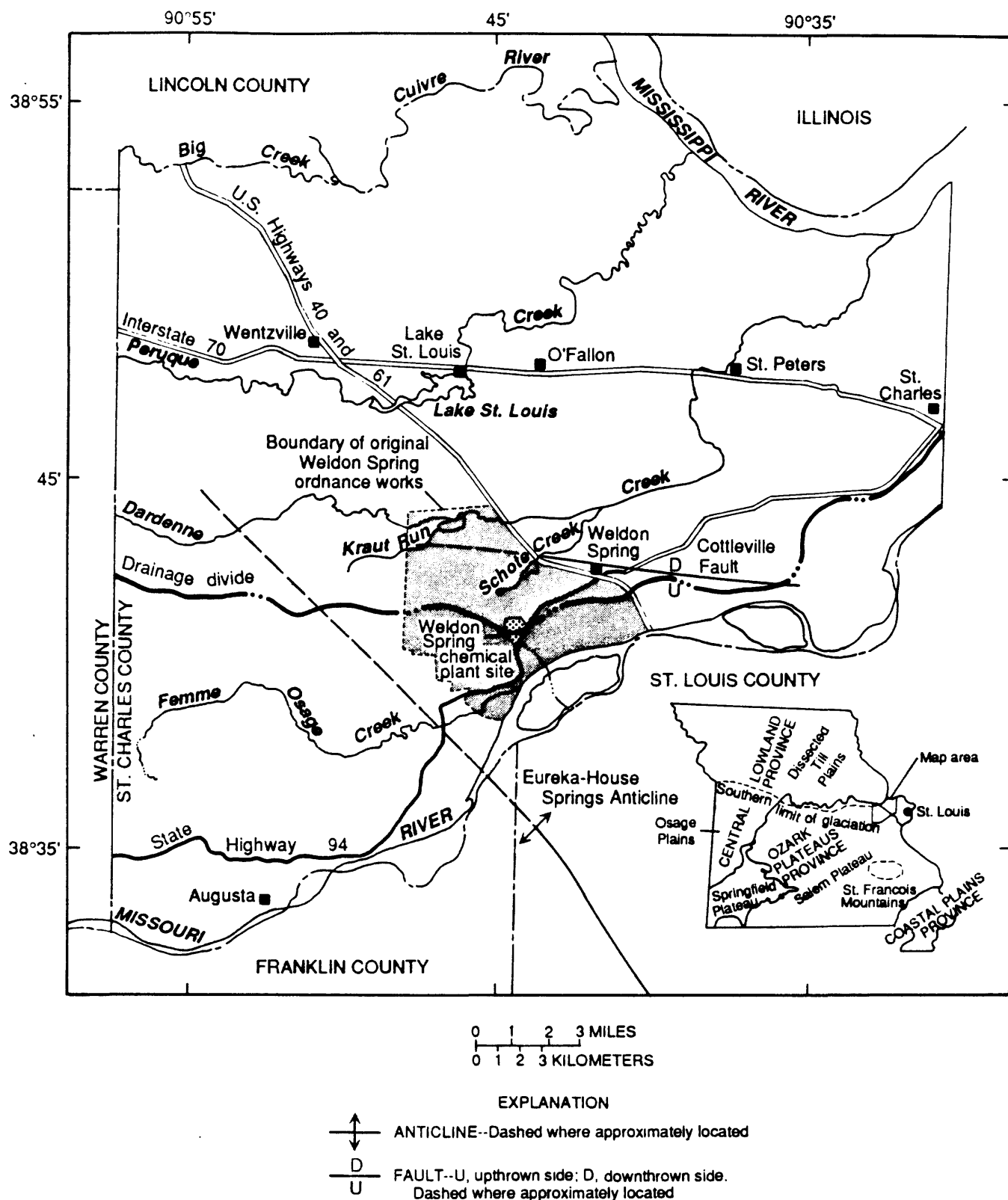
Figure 1. Location of the Weldon Spring chemical plant site, boundary of the original Weldon Spring ordnance works, and selected geologic structures (physiography from Fenneman, 1938).

Ordnance production lines modified from MK-Ferguson Company
and Jacobs Engineering Group (1989e)

EXPLANATION

GENERALIZED LOCATION OF ORDNANCE PRODUCTION LINES

—×——×——×— BOUNDARY OF THE WELDON SPRING CHEMICAL PLANT SITE

TNT   TRINITROTOLUENE
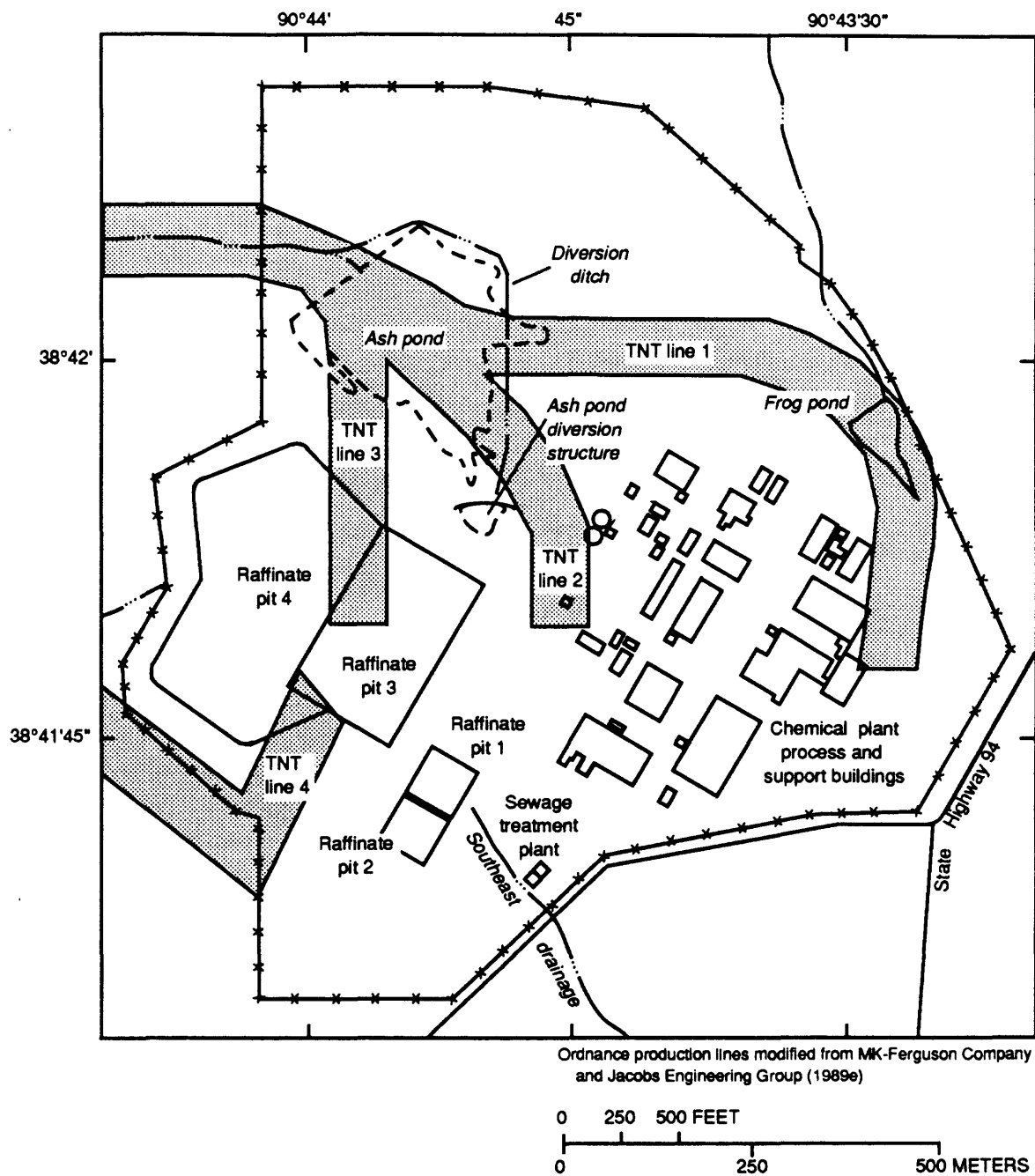
Figure 2. Major features of the Weldon Spring chemical plant site and the generalized location of former ordnance production lines.

compounds are associated with the former ordnance works operations (MK-Ferguson Company and Jacobs Engineering Group, 1989a).

The U.S. Geological Survey (USGS) began collecting hydrologic data at the WSCP during 1983. Results of the first year of study and results from previous investigations by others are presented in an interim progress report (Kleeschulte and Emmett, 1986). Water-quality data from the raffinate pits, vicinity streams, and shallow aquifer collected from 1984 through 1986 and seepage-run data for six area streams and discharge data for several vicinity springs are presented in a report by Kleeschulte and others (1986). Kleeschulte and Emmett (1987) gives a description of the hydrogeology and water quality of the Weldon Spring area.

Although a large quantity of data is available on the extent and magnitude of contamination at the WSCP site, little information exists on factors that may control the migration of contaminants within the overburden and shallow aquifer. Therefore, an investigation was conducted in cooperation with the U.S. Department of Energy (USDOE) to determine the geochemical controls on contaminant migration and provide additional information on the extent, magnitude, and source of ground-water contamination at the site and vicinity property.

Purpose and Scope

This report describes (1) the geochemistry of the shallow aquifer in the vicinity of the Weldon Spring chemical plant site, (2) the geochemical controls on the extent and magnitude of contaminant migration from the raffinate pits within the overburden, and (3) the source of increased contaminants in the shallow aquifer and Burgermeister spring. The hydrochemistry of the shallow aquifer at the site and vicinity property is presented, followed by a description of the geochemistry of the raffinate pits. This is follwed by a discussion of results from laboratory sorption experiments between a simulated raffinate pit leachate and various overburden units beneath the raffinate pits. Results of the laboratory experiments are compared to onsite data collected from lysimeters near the raffinate pits. The final section discusses the geochemical controls and sources of increased constituent concentrations in the shallow aquifer and Burgermeister spring.

From 1989 to 1991, water-quality samples were collected from 20 ground-water and 5 surface-water sites. Additional data from more than 360 water-quality samples collected from 57 wells, 19 springs, 17 surface-water sites, and 10 special sources (Kleeschulte and Cross, 1990) also were used in this investigation. Laboratory studies included more than 140 individual experiments interacting raffinate pit water with various overburden materials at the site. Mineralogic and chemical analysis were performed on about 70 overburden samples to determine the effects of overburden mineralogy on the results from laboratory sorption experiments and contaminant distributions in the shallow aquifer. Stratigraphic information specific to the site was obtained from reports published by the U.S. Department of Energy. Interpretation of ground-water geochemistry and contaminant migration was aided by the use of statistical and graphical techniques and by the geochemical codes SOLMINEQ.88 (Kharaka and others, 1988), WATEQ4F (Ball and Nordstrom, 1987), and PHREEQE (Parkhurst and others, 1980).

Acknowledgments

The author is grateful to the faculty and graduate students of the Department of Civil Engineering, University of Missouri-Rolla for their use and preparation of laboratory facilities. Special acknowledgment is given to graduate students Stephen Bader, Craig Borgmeyer, and Steven Fink; undergraduate students Robert Ford and Ralph Lemongelli; and their faculty advisor Dr. Purush TerKonda for their assistance with the laboratory sorption experiments. Without their contributions this investigation would not have been possible. The author gives special thanks to Jeff Carman and John Bogner of Jacobs Engineering Group and James Nishi and Stephen Sutley of the U.S. Geological Survey, Geologic Division for their technical assistance in identification of mineral phases and interpretation of U solid phase association in raffinate pit sludge.

Description of the Study Area

The WSCP site is located in the south-central part of St. Charles County in eastern Missouri (fig. 1). For purposes of this report, the WSCP site refers to the

217-acre tract owned by the USDOE and consists of the abandoned WSCP and associated raffinate pits (fig. 2). Average rainfall at the site is approximately 34 in. (inches) per year (National Oceanic and Atmospheric Administration, 1988). The site is located along an east-west trending ridge near the boundary of the Dissected Till Plains of the Central Lowland Province to the north and the Salem Plateau of the Ozark Plateaus to the south (fig. 1). The ridge approximates the surface- and ground-water divides between the Mississippi River to the northeast and the Missouri River to the south (Kleeschulte and Emmett, 1986). The topography of the site is characterized by a gently undulating surface of unconsolidated Quaternary glacial drift and loess deposited on weathered, undifferentiated Mississippian rocks of the Burlington and Keokuk Limestones. Immediately to the south of the site near the Missouri River, the topography changes to one of steeply dipping slopes.

HISTORY AND DESCRIPTION OF THE WELDON SPRING CHEMICAL PLANT SITE

The history of the WSCP site includes the production of military ordnance during the 1940's and refinement of U ores during the 1950's and 1960's. General background information on both of these production processes is important in understanding the complex distribution of contaminants detected at the site.

Operations at the Weldon Spring Ordnance Works

During 1941 the Department of the Army acquired 17,232 acres of land for the construction of the WSOW (fig. 1). This facility produced more than 710 million lbs (pounds) of trinitrotoluene (TNT) and lesser quantities of dinitrotoluene (DNT) during its operation from November 1941 to September 1945 (International Technology Corporation, 1989). Eighteen TNT production lines and two DNT production lines were constructed along surface-water drainages at the WSOW. Three of these production lines and part of a fourth were located across what would later become the 217-acre WSCP (fig. 2). Each production line consisted of numerous production and

support buildings interconnected by railways, hand-pushed tramways, and wooden wastewater pipelines. The U.S. Army declared the WSOW surplus property in 1946 and transferred ownership of 15,169 acres to various state and local agencies by 1949. Currently (1991), the U.S. Army owns 1,655 acres immediately west of the site known as the Weldon Spring Training Area. The rest of the original property currently (1991) is owned by the Missouri Department of Conservation, Francis Howell School District, the University of Missouri, a local residential subdivision, and the USDOE.

The TNT was manufactured by a three stage process using toluene, nitric acid, and sulfuric acid (catalyst) as the primary raw materials. The nitric and sulfuric acids were manufactured at the WSOW. Approximately 1 lb each of nitric acid and toluene was consumed to produce 1 lb of TNT.

The purification of impure TNT was accomplished by the sellite process (International Technology Corporation, 1989). In this process, the impure TNT washed with a solution of sodium bicarbonate and sellite (Na_2SO_3). This removed isomers other than 2,4,6-TNT and neutralized any remaining acid present. During this process the liquid became red. The waste liquid from this process, called "red water", contained various mixtures of water, inorganic salts, ash, sulfonate derivatives, and nitroaromatic compounds (International Technology Corporation, 1989).

Increased concentrations of SO_4, NO_3, lead (Pb), nickel (Ni), and nitroaromatic compounds attributable to ordnance production were detected in soil samples from isolated areas along former TNT production lines and in areas of fill at the site (MK-Ferguson Company and Jacobs Engineering Group, 1989b). Samples from many monitoring wells at the site and vicinity property contained detectable concentrations of nitroaromatic compounds (International Technology Corporation, 1989). Much of the surface- and ground-water contamination attributable to the WSOW probably is related to the disposal practices of the red water generated during the sellite process. Before mid-1942, the red water was discharged to settling lagoons at the site. Area springs and streams were observed to turn red shortly after the construction of the red water lagoons, indicating contamination from the ordnance works (V.C. Fishel and C.C. Williams, U.S. Geological Survey, written commun., 1944). Consequently, a large network of

underground wooden pipelines was constructed in mid-1942 to connect the TNT and DNT lines to three wastewater-treatment plants (Fraser-Brace Engineering Company, 1941). Several miles of underground wooden wastewater pipelines were constructed and about 61,000 ft (feet) currently (1991) are in place on the U.S. Army property west of the site (International Technology Corporation, 1989). Fishel and Williams (written commun., 1944) indicated that the gravity-flow lines often became clogged, causing the red water to back up and flow directly into gullies and streams on the vicinity property.

Operations at the Weldon Spring Chemical Plant

The WSCP was operated as the Weldon Spring uranium feed materials plant from 1957 to 1966. Uranium ore concentrates and recycled uranium scrap were converted into U-hexafluoride, U-dioxide, and pure U metal at the plant (Harrington and Ruehle, 1959). A flow chart showing the major stages in the operations of the AEC during the operation of the Weldon Spring uranium feed materials plant is given in figure 3. The processes outlined in the chart are those operations performed at feed materials plants. Many of these steps involved the use, or generation, of compounds that currently (1991) are environmental concerns at the site. In addition to feed materials operations, the plant also assayed ore materials. Much of the following discussion of the feed materials plant is derived from Harrington and Ruehle (1959).

The initial step in refining at the Weldon Spring feed material plant involved the digestion of ore concentrates in hot nitric acid to produce uranyl (UO_2^{2+}) nitrates, such as $UO_2(NO_3)_2$, in a mixture of nitric oxide and nitrogen dioxide. During the digestion process, relatively insoluble compounds, such as uranyl phosphates, molybdates, and vanadates, would not be recovered and these materials probably were discharged to the raffinate pits.

The second step in refining involved the solvent extraction of $UO_2(NO_3)_2$ from the acid slurry using tributyl phosphate (TBP) diluted in hexane. In this process, the U was partitioned between the acid phase and the organic phase. The $UO_2(NO_3)_2$-rich organic phase was subsequently mixed with pure water where the U was transferred to the aqueous phase. The raffinate from this process, which contained large

quantities of NO_3 and other impurities, was transferred to large tanks where it was neutralized with a lime slurry to a pH slightly greater than 7. The neutralized raffinate then was transferred to the raffinate pits (fig. 2) where the solids settled and the supernate drained off.

The third and fourth steps in refining involved the denitration and conversion of the $UO_2(NO_3)_2$ slurry to U trioxide (UO_3, orange oxide) and then into U dioxide (UO_2, brown oxide), which was used for the manufacture of fuel rods, but predominately used for the production of U metal. The production of U metal was accomplished by a two-stage heating process carried out in batch tanks. Small quantities of sulfuric acid often were added to improve the reactivity of the residual slurry in the tanks. The UO_3 produced from the denitration step underwent a process of hydrogen reduction where the UO_3 was reacted with hydrogen gas to form UO_2 and water (reaction 1).

$$UO_3(s) + H_2(g) = UO_2(s) + H_2O. \qquad (1)$$
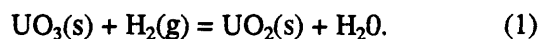
The hydrogen source in this reaction was derived from anhydrous ammonia (NH_3).

The final process steps in the production of U metal involved the conversion of the UO_2 into U tetrafluoride (UF_4, green salt) by the reaction of UO_2 with anhydrous hydrogen fluoride (HF) gas at high temperature. The UF_4 product then was cooled for conversion to U metal or U hexafluoride (UF_6) and the off-gas HF was collected for the production of commercial grade (70 percent) hydrofluoric acid. The UF_4 was reacted with Mg metal at high temperature producing U metal and sellaite (MgF_2), according to the general reaction:

$$UF_4 + 2Mg = U + 2MgF_2. \qquad (2)$$

This reaction, called "thermite reduction," was highly exothermic and was performed in steel reaction vessels insulated with a MgF_2 lining. The U metal was forged into ingots and surface impurities, such as adhered MgF_2 slag, were removed by washing with nitric acid. The slag and other wastes from this reaction were discharged to the raffinate pits.

An estimated 150 tons of U, 76 tons of Th, and 1.5 tons of slightly enriched U were discharged to the raffinate pits (Lenhard and others, 1967). The physical properties of the four raffinate pits are given in table 1. The liquids from the raffinate pits continuously overflowed into the plant-process sewer system. Lenhard and others (1967) estimated that the sewer

Mining

Mill concentrating

Operations performed at the
Weldon Spring uranium feed
materials plant

Refining

Uranium
tetrafluoride
production

Uranium
metal production

Uranium
hexafluoride
production

Reactor
operation

Isotope
separation

Plutonium

Uranium - 235
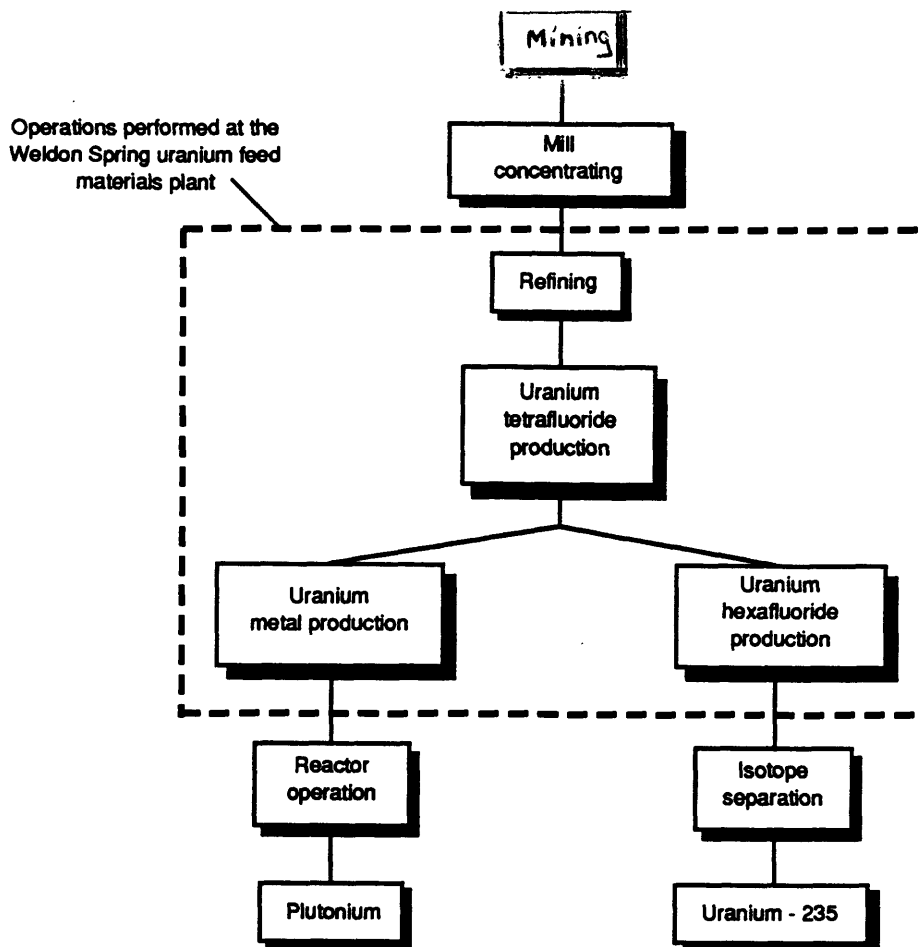
Figure 3. Generalized flow chart of U.S. Atomic Energy Commission operations during
the operation of the Weldon Spring uranium feed materials plant (modified from
Harrington and Ruehle, 1959).

system discharged 1 Mgal/d (million gallons per day) during plant operation and that one-half of this was from the raffinate pits. The sewer discharged into a small drainage southeast of the plant (locally known as the southeast drainage) and flowed approximately 1.5 mi (mile) before entering the Missouri River (fig. 2). Approximately 5.3 million ft^3 (cubic feet) of radiologically contaminated wastes are present within the raffinate pits (MK-Ferguson Company and Jacobs Engineering Group, 1989d). The raffinate pits are underlain by a variable thickness of overburden (loess, glacial till, and residuum) deposited on limestones of Mississippian age. The thickness of the overburden beneath the raffinate pits is estimated to range from less than 10 ft to more than 30 ft (Bechtel National, Inc., 1984) and from 25 to 45 ft (MK-Ferguson Company and Jacobs Engineering Group, 1990b).

The USDOE has detected increased concentrations of Mg, fluoride (F), NO$_3$, beryllium (Be), cadmium (Cd), chromium (Cr), and U in soils at the site (MK-Ferguson Company and Jacobs Engineering Group, 1989a). With the exception of increased NO$_3$ concentrations in soils near the raffinate pits, concentrations of these constituents do not persist with depth, indicating surficial soil contamination probably does not contribute substantial constituent concentrations to the shallow aquifer (MK-Ferguson Company and Jacobs Engineering Group, 1989b). Although widespread contamination of the shallow aquifer at the site by downward migration from contaminated soils is unlikely, the contamination of runoff from these areas can occur. Large concentrations of U [as much as 4,000 μg/L (micrograms per liter)] detected in Ash pond (Kleeschulte and Emmett, 1987) are thought to result from runoff from U contaminated soils and abandoned process equipment located along the south edge of Ash pond in an area referred to as the "south dump" (MK-

Table 1. Physical properties of the four raffinate pits

[Modified from Lenhard and others (1967); Bechtel National, Inc. (1984); MK-Ferguson Company and Jacobs Engineering Group (1989c); Jeff Carman, U.S. Department of Energy, oral commun., (1991)]

Raffinate pit number (fig. 2)	Surface area, in acres	Date used	Altitude of levee top, in feet above sea level	Altitude of pit bottom, in feet above sea level	Design capacity, in million cubic feet	Actual sludge volume, in million cubic feet	Altitude of top of sludge, in feet above sea level	Percent filled	Altitude of spillway, in feet above sea level	Destination of outflow
1	1.2	1958-60	664	648	0.500	0.483	661	97	662	process sewer
2	1.2	1958-60	664	648	.500	.513	661	103	662	process sewer
3	8.4	1959-64	663	638-647	4.500	3.488	654-660	78	656	process sewer
4	15.0	1964-66	663	628-650	12.000	.815	[a]	7	[b]656	pit 3

[a] Sludge unevenly distributed throughout the pit.
[b] Pit 4 was designed to overflow into pit 3 but altitude of water has never reached this level in pit 4; however, water in pit 3 has flowed into pit 4.

9

Ferguson Company and Jacobs Engineering Group, 1989a). Frog pond (fig. 2) receives runoff from some of the WSCP process and support buildings in the eastern part of the site, and outflow from this pond contains increased concentrations of U (200 to 410 μg/L; Kleeschulte and Cross, 1990).

Geology of the Weldon Spring Chemical Plant Site

The WSCP site lies on the northeast flank of the Ozark Uplift, which is the approximate boundary of the Ozark Plateaus physiographic province (fig. 1). Previous investigations by the USDOE (Bechtel National, Inc., 1984; MK-Ferguson Company and Jacobs Engineering Group, 1989a, 1989b, 1989c, and 1990a) have indicated that contamination from the WSCP site is restricted to overburden units at the site and the underlying Burlington and Keokuk Limestones at or near the site (fig. 4). The youngest consolidated rocks beneath the site include undifferentiated Burlington and Keokuk Limestones of Mississippian age.

In Missouri, the contact between the Burlington and Keokuk Limestones is transitional and often difficult or impossible to identify (Thompson, 1986) and the formations commonly are undifferentiated. The lithology of the Burlington and Keokuk Limestones generally is uniform, consisting of white to light gray, medium to coarsely crystalline, fossiliferous limestone. The limestones also contain abundant nodular chert that often has tripolitic borders. Structural features in the vicinity of the WSCP site include a northwest-southeast trending anticline known as the Eureka-House Springs Anticline and an east-west trending fault (locally referred to as the Cottleville Fault) about 1.5 mi to the north (fig. 1). The Cottleville Fault was described as a normal fault with a vertical displacement of about 60 ft (Whitfield and others, 1989). Generally, consolidated rocks in the region dip between 1 and 2° (degrees) to the northeast. The rocks in the region have two sets of distinct joints: one set trends from N. 30° E. to N. 72° E. and the other from N. 30° W. to N. 65° W. (Roberts, 1951). Several streams in the region seem to have developed along former fracture lines or solution channels (V.C. Fishel and C.C. Williams, written commun., 1944). Well logs from a well cluster installed by the USDOE immediately south and west of the site indicate the combined thickness of the Burlington and Keokuk Limestones is about 120 ft (C.E. Robertson, Missouri Department of Natural Resources, written commun., 1988).

Geophysical studies at the site by Bechtel National, Inc. (1984) indicated that the upper 35 to 40 ft of the Burlington and Keokuk Limestones is gradationally weathered and has an irregular upper surface. The studies also indicated that the upper 35 ft of the Burlington and Keokuk Limestones is highly fractured, contains iron (Fe) oxide stains, and has numerous small voids containing variable quantities of clay. More detailed core drilling at the site by the USDOE (MK-Ferguson Company and Jacobs Engineering Group, 1990a) has resulted in the separation of the Burlington and Keokuk Limestones into two units; an upper "weathered limestone" and a lower "unweathered limestone" based on the degree of weathering, number of fractures, and core loss.

The unweathered limestone is thinly to massively bedded, gray to light gray, fine to coarsely crystalline, fossiliferous limestone containing between 20 and 40 percent chert. Stylolites are common within this unit. Unlike the overlying weathered limestone, this unit has little Fe oxide staining, and unweathered pyrite has been identified on some fracture surfaces.

The contact between the unweathered limestone and the overlying weathered limestone is gradational. The weathered limestone ranges from about 9 to more than 50 ft thick (MK-Ferguson Company and Jacobs Engineering Group, 1990a), with the largest thickness adjacent to the north berm of raffinate pit 4 (fig. 5). It is a grayish-orange to yellow-gray, thinly bedded, silty, argillaceous limestone commonly containing as much as 60 percent chert.

Solution features, such as vugs, are common in the weathered limestone. Many of these are lined with calcite and drusy quartz. Loss of drilling fluid circulation and core loss were common during drilling of monitoring wells in this unit (MK-Ferguson Company and Jacobs Engineering Group, 1990a); however, the core loss generally was restricted to the northern part of the site, was concentrated in the top 20 to 30 ft of unweathered limestone, and usually was less than 5 ft per boring (MK-Ferguson Company and Jacobs Engineering Group, 1990a).

Overlying the weathered limestone are unconsolidated deposits (hereafter referred to as overburden) of residuum, till, clay, loess, and fill (fig. 4). The combined thickness of the overburden ranges

System	Series	Stratigraphic unit	Thickness[a] (in feet)	Geohydro-logic unit	Physical characteristics
QUATERNARY	HOLOCENE	Topsoil and fill	[b]0-30	OVERBURDEN	Black organic-rich clayey silt to silty clay topsoil (0-3.5 feet) and reworked overburden
	PLEISTOCENE	Loess	[b]0-11		Silt to clayey silt
		Ferrelview Formation	[b]0-20		Stiff, low to high plasticity clay and silty clay containing small quantities of sand
		Clay till	[b]0-30		Stiff, low to medium plasticity clayey silt to silty clay containing subrounded pebbles of chert, and igneous and metamorphic rock fragments
		Basal till	[b]0-11		Yellowish brown, sandy, clayey silt with angular chert and gravel cobbles
	--?--	Residuum	[b]0-26		Extremely heterogeneous gravelly clay to clayey gravel with abundant sand- to gravel-size chert nodules
MISSISSIPPIAN	OSAGEAN	Keokuk and Burlington Limestones (undifferentiated)	[c]105-122	SHALLOW AQUIFER	Weathered limestone--9-55 feet thick, grayish orange to yellow gray, highly permeable, thinly bedded, silty, argillaceous limestone with as much as 60 percent chert, abundant iron oxide staining; solution features and voids filled with variable quantities of clay are common[b]
					Unweathered limestone--gray to light gray, thinly to massively bedded, fine to coarsely crystalline, fossiliferous limestone containing 20 to 40 percent chert, styolites and unweathered pyrite[b]
		Fern Glen Limestone	[c]50-65		Thin to thickly bedded crystalline or argillaceous limestone
	KINDERHOOKIAN	Chouteau Group[d] (undifferentiated)	[c]20-43	CONFINING LAYER	Fine-grained, thinly to medium bedded, dolomitic limestone
--?--	--?--	Bushberg Sandstone	[e]5-22		Fine to medium-grained, medium to thickly bedded sandstone with abundant iron oxide nodules
--?--	--?-- UPPER	Lower part of Sulphur Springs Group (undifferentiated)	[e]0-2		Argillaceous, slightly calcareous to dolomitic, brown-grey siltstone
DEVONIAN ORDOVICIAN	UPPER	Maquoketa Shale	[e]8-12		Calcareous or dolomitic shale--typically thinly laminated, silty, with argillaceous limestone lenses

[a] Thickness indicates typical thickness in the vicinity of the Weldon Spring chemical plant site.

[b] MK-Ferguson Company and Jacobs Engineering Group (1991).

[c] C.E. Robertson (Missouri Department of Natural Resources, written commun., 1988).

[d] Thompson (1986).

[e] Gilbert (1991).

Figure 4. Thickness of overburden and upper bedrock units.
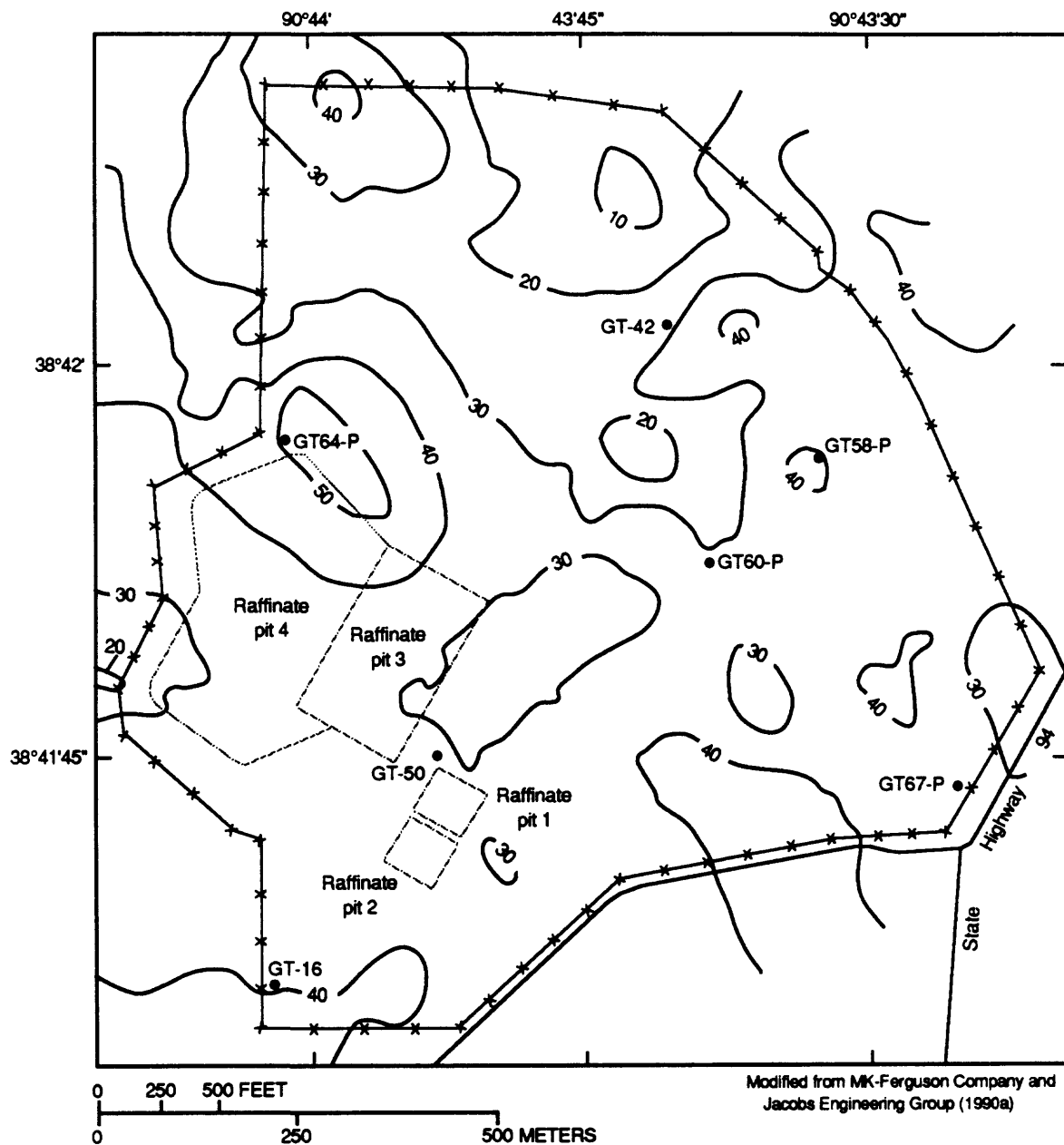
Figure 5. Thickness of the weathered limestone.

from 15 to 60 ft at the site with the smallest thickness along the northeastern border of the site in the vicinity of Frog pond (MK-Ferguson Company and Jacobs Engineering Group, 1990d). The overburden at the site can be subdivided into six units (fig. 4). From oldest to youngest, these are residuum, basal till, clay till, Ferrelview Formation (probable interglacial deposit), loess, and topsoil and fill.

The following descriptions of the overburden are derived from geotechnical investigations of the site by the USDOE. The residuum (0 to 26 ft thick) is a heterogeneous unit consisting of gravelly clay to clayey gravel with abundant sand- to gravel-size chert nodules. The coarse fraction is composed of angular to subangular fragments of chert and minor weathered limestone in a matrix of red, highly plastic clay. The mineralogic content is variable, with calcite contents ranging from 0 to 60 percent (average content of 20 percent) and quartz contents ranging from 36 to 98 percent (average content of 73 percent; Schumacher, 1990). This unit is thought to be derived from in-situ

weathering of the underlying cherty limestones. Bechtel National, Inc. (1984) reported variable drilling fluid loss (0 to 100 percent) in this unit during drilling at the site. Drilling by USDOE contractors (MK-Ferguson Company and Jacobs Engineering Group, 1990a) also indicated variable loss of drilling fluid in this permeable unit.

The basal till overlies the residuum at the site. This unit ranges from 0 to 11 ft thick and is restricted to the north-central and western parts of the site. The unit is a yellowish brown, sandy, clayey silt with angular chert gravel and cobbles (MK-Ferguson Company and Jacobs Engineering Group, 1990a). The unit contains lesser quantities of sand-size material (fig. 6) and smaller contents of calcite (fig. 7) than the underlying residuum (Schumacher, 1990).

The clay till is a stiff, clayey silt to silty clay with a low to medium plasticity (MK-Ferguson Company and Jacobs Engineering Group, 1990a). The unit is between 0 and 30 ft thick and was identified in all but two boreholes at the site. The largest thickness was in
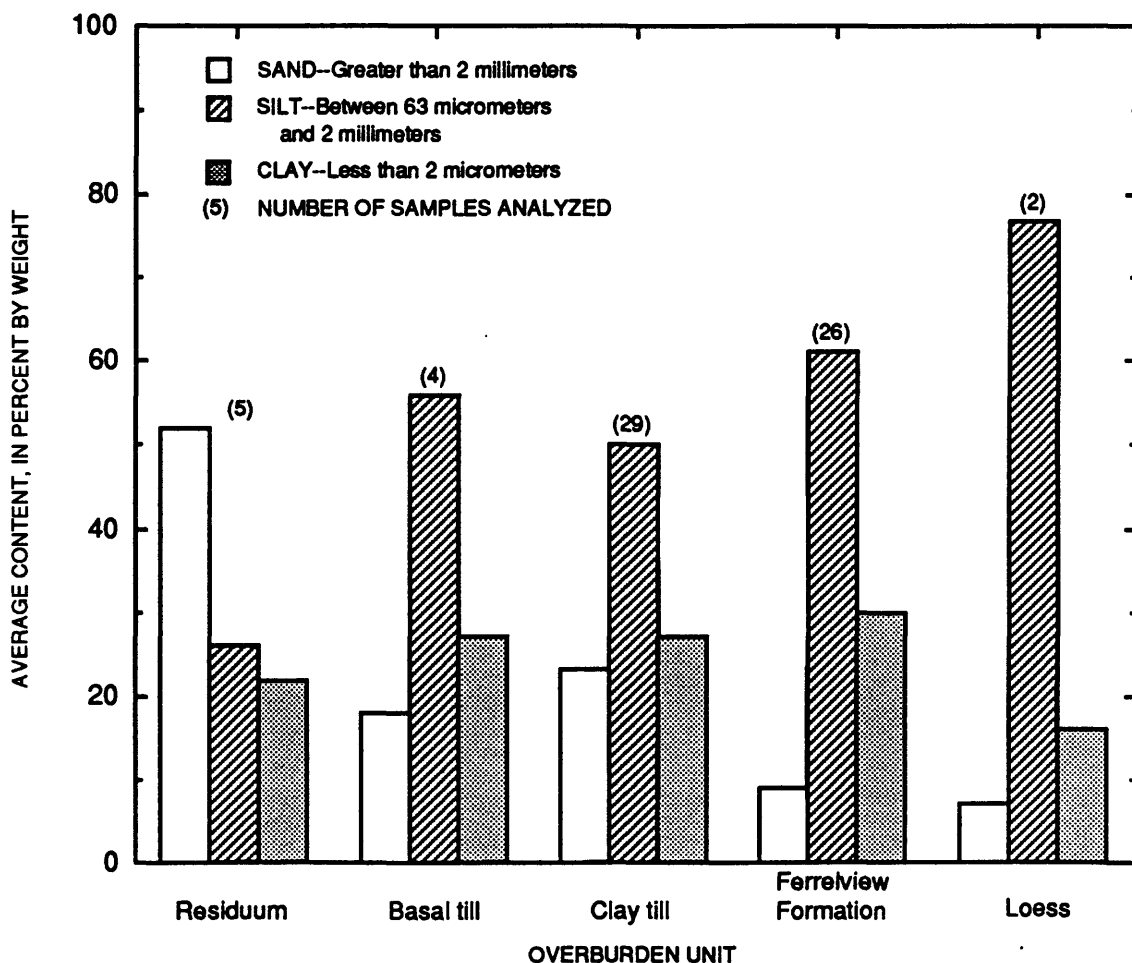
Figure 6. Average grain-size content of overburden units (Schumacher, 1990).
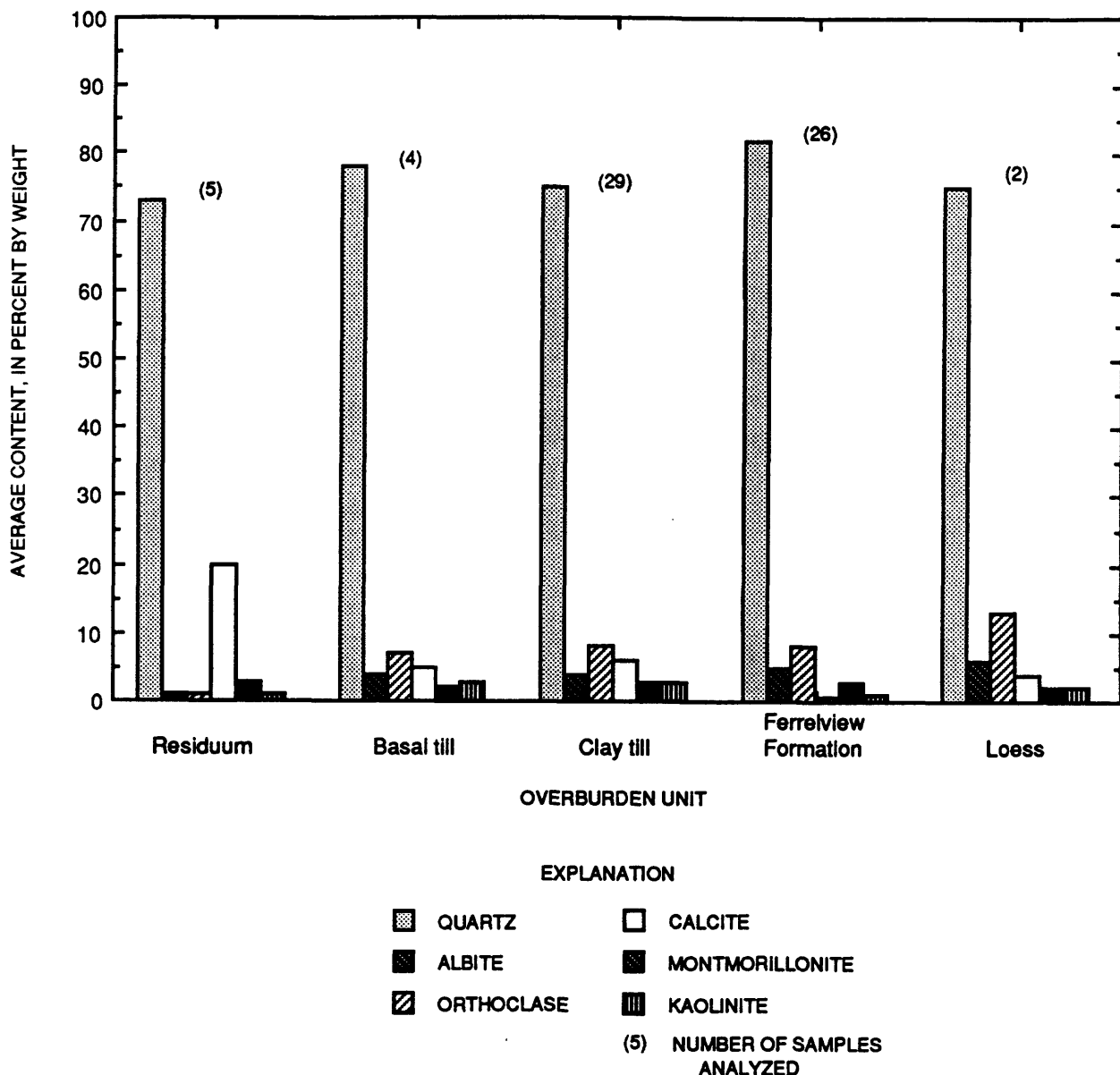
Figure 7. Average mineralogic content of overburden units.

the northernmost part of the site. Grain-size analyses (Schumacher, 1990) indicate the unit contains about 50 percent silt with subequal quantities of sand and clay (fig. 6). Although defined as a till, this unit has a nearly uniform distribution of grain size and probably has been reworked. The clay till contains about 75 percent quartz, 6 percent calcite, and about 9 percent total clay minerals (fig. 7). Detailed clay mineral analysis by X-ray diffraction indicated that about 70 percent of the clay minerals was montmorillonite (Schumacher, 1990). The unit contains numerous subrounded pebbles of chert and igneous and metamorphic rock fragments, in addition to Fe and manganese (Mn) oxide

nodules. Near vertical, blocky fractures filled with Mn oxide are common. The approximate thickness of the unit in the vicinity of the raffinate pits ranges from 5 to about 10 ft (MK-Ferguson Company and Jacobs Engineering Group, 1989e). Raffinate pit 4 probably is completed within this unit (Bechtel National, Inc., 1987).

Overlying the clay till is stiff, low to high plasticity clay and silty clay identified as the Ferrelview Formation (Howe and Heim, 1968). The unit is present throughout most of the site and ranges from 0 to 20 ft thick. Locally, the Ferrelview Formation is a dark yellowish orange to brown silty

clay with gray mottling. The unit contains lesser quantities of sand and slightly greater quantities of silt and clay than the underlying clay till (fig. 6). The Ferrelview Formation is thought to have been deposited as a distinct unit rather than derived from the underlying clay till. A distinctive mineralogic characteristic of the Ferrelview Formation reported by Howe and Heim (1968) is that, generally, plagioclase is present in slightly greater quantities than orthoclase. However, mineralogic analyses of 26 samples from the Ferrelview Formation at the site (Schumacher, 1990) indicate the inverse relation (fig. 7) in that orthoclase contents are slightly larger than albite (plagioclase). Unlike the underlying clay till, the Ferrelview Formation contains only trace quantities of calcite (less than 1 percent) and most of this occurs in the upper part of the unit (Schumacher, 1990). Several borings by Bechtel National, Inc. (1984) indicated the Ferrelview Formation has a blocky fracture pattern and that, where present, the fractures extend downward into the underlying clay till. Slickensided fracture surfaces were reported in several drill logs. The unit contains abundant Fe oxide nodules and, similar to the underlying clay till, contains Mn oxide filled fractures. One sample collected during this investigation contained an Fe-Mn oxide nodule larger than 1.5 cm (centimeters) in diameter. Similar to the underlying clay till, the Ferrelview Formation ranges from 5 to 10 ft thick in the vicinity of the raffinate pits. The bottom of raffinate pit 3 probably is completed within this unit.

Loess deposits range from 0 to 11 ft thick at the site (MK-Ferguson Company and Jacobs Engineering Group, 1990a). The thickness of the loess ranges from 2 to 4 ft in the vicinity of raffinate pits 3 and 4; however, this unit is not present beneath the raffinate pits. The loess contains a larger quantity of silt and a smaller quantity of sand and clay than the underlying deposits (fig. 6). This unit consists of silt-size particles (about 77 percent) and contains about 4 percent calcite (fig. 7).

A variable thickness of topsoil and fill material is present at the site. The topsoil generally is a black organic-rich clayey silt to silty clay ranging from 0 to 3.5 ft thick. The fill material is the result of earthmoving activities during decontamination of the former ordnance works and construction of the existing chemical plant and raffinate pits. This material ranges from 0 to 26.5 ft thick and comprises the raffinate pit dikes (MK-Ferguson Company and Jacobs Engineering Group, 1990a).

Surface-Water Hydrology

Surface-water drainage from most of the raffinate pit area and the northern part of the WSCP flows primarily to the north into unnamed tributaries to Schote Creek (fig. 8). Drainage from the western part of the raffinate pit area flows west onto the U.S. Army property into the middle fork of the west tributary of Schote Creek. During periods of low rainfall, the west tributary generally is dry. However, a small quantity of flow, less than 0.01 ft^3/s (cubic foot per second), leaves the site from a seep at the base of the west levee of raffinate pit 4 and flows into the middle fork of the west tributary but this water is soon lost to the subsurface.

Before 1989, runoff from most of the raffinate pit area flowed into a large shallow depression called Ash pond (fig. 8). The soils within this pond are radiologically contaminated (MK-Ferguson Company and Jacobs Engineering Group, 1989e), and during wet weather, the flow from this structure into the east fork of the west tributary of Schote Creek generally contained U concentrations greater than 1,000 µg/L (Kleeschulte and Emmett, 1987). In April 1989, the USDOE completed a diversion structure around Ash pond so that runoff from the raffinate pit area currently (1991) is held in a diversion pond immediately north of raffinate pit 3 and diverted around Ash pond (fig. 2). However, this drainage also flows into the east fork of the west tributary of Schote Creek. This tributary loses water to the ground-water system (Kleeschulte and Emmett, 1986). Recent dye traces conducted by the USDOE and Missouri Department of Natural Resources, Division of Geology and Land Survey (DGLS; 1991) traced a flow path from this tributary across the Schote Creek basin to Burgermeister spring approximately 1 mi to the northwest (fig. 8). The USGS has monitored Burgermeister spring since 1984 and has detected persistent increased values of specific conductance and concentrations of Na, Cl, NO$_2$ + NO$_3$, Li, and U (Kleeschulte and Emmett, 1987).

Surface drainage leaves the site along the northeastern boundary from what is locally called Frog pond (fig. 8). The pond receives runoff from the northernmost part of the chemical plant in addition to runoff from a road salt storage pile located at a highway department maintenance facility adjacent to the site. Runoff from this storage pile previously has contributed large concentrations of Na and Cl to Frog pond (Kleeschulte and Emmett, 1986). Uranium concentrations in the outflow from Frog pond ranged
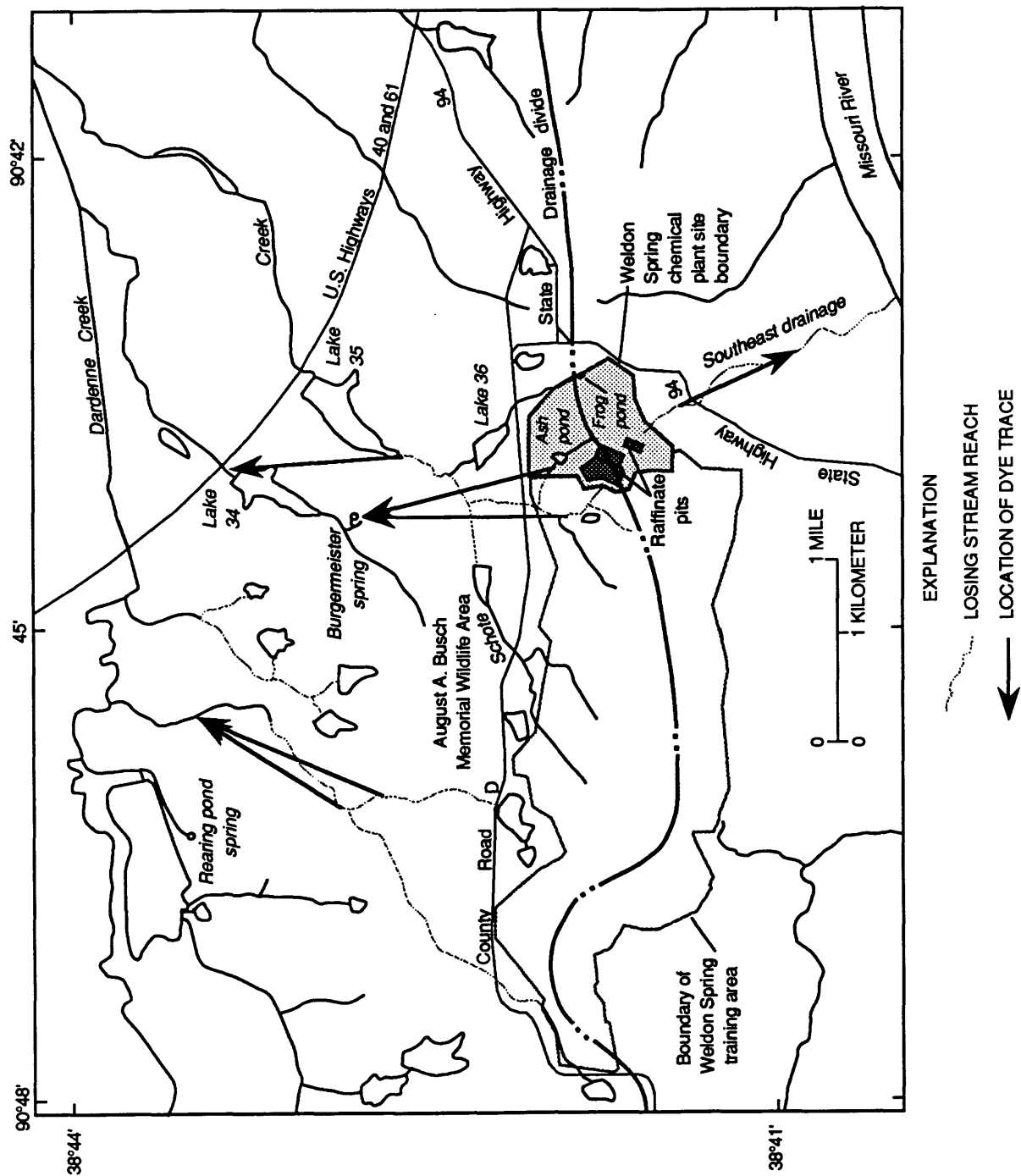
Figure 8. Surface-water features and dye traces in the vicinity of the Weldon Spring chemical plant site (modified from the Missouri Department of Natural Resources, 1991).

from 88 to 410 µg/L. In this report, aqueous concentrations of chemical constituents given are "dissolved", unless specified otherwise. The "dissolved" constituents are operationally defined as those that pass through a membrane filter with a pore size of 0.10 µm (micrometer). The outflow from Frog pond flows into the east tributary of Schote Creek, then into lake 36 on the August A. Busch Memorial Wildlife Area, and then into Schote Creek. The east tributary of Schote Creek was not identified as a losing stream (Kleeschulte and Emmett, 1986). However, the segment of Schote Creek downstream from the junction with the east tributary was identified as a losing stream (fig. 8).

Runoff from the southern part of the chemical plant, including the former plant process sewer system and a part of the area around raffinate pits 1 and 2, drains to the southeast into what is locally called the southeast drainage or sewage outfall tributary. This tributary flows approximately 1.5 mi through a steeply sloped valley before entering the Missouri River (fig. 8). A small wet weather seep (identified as the STP seep; Schumacher, 1990) emerging downslope from raffinate pits 1 and 2 enters this tributary immediately upstream from the former sewage treatment plant. When the seep flowed, it contained large concentrations of Ca, SO_4, $NO_2 + NO_3$, and U, possibly indicating seepage from raffinate pits 1 and 2. Uranium concentrations in this seep have been as large as 1,900 µg/L (Kleeschulte and Cross, 1990). Buried wastes possibly containing UF_4 have been discovered immediately upslope from this seep (D. Fleming, MK-Ferguson Company, written commun., 1990).

Ground-Water Hydrology

The weathered and unweathered units of the Burlington and Keokuk Limestones compose the uppermost part of the shallow aquifer at the site (fig. 4; Kleeschulte and Emmett, 1987). The water table generally is within the weathered limestone. In December 1989, the direction of ground-water flow beneath the site generally reflected that of surface drainage with a northeast trending ground-water divide located in the vicinity of raffinate pits 1 and 2 (fig. 9). The position of the ground-water divide does not change substantially with season, and water levels at the site generally fluctuate less than a few feet per year (Kleeschulte and Imes, in press). A map of the top of

the weathered limestone surface (fig. 10) beneath the site was constructed using borehole data (MK-Ferguson Company and Jacobs Engineering Group, 1989e).

The map depicts several linear depressions that could be buried stream courses (troughs; fig. 10). These troughs are oriented approximately parallel to the regional joint sets. The upper end of one of the troughs is near the south end of raffinate pits 3 and 4. Another trough is located north of raffinate pits 3 and 4 in the Ash pond area and a third trough is south of raffinate pit 4. Within parts of these troughs, the water table is above the weathered limestone and is within the residuum (fig. 10). Two of the troughs merge north of the site near County Road D to form a single trough that continues north towards Burgermeister spring (fig. 11). The location of these troughs coincides with depressions in the potentiometric surface of the shallow aquifer (fig. 12), indicating these areas are drains for the shallow aquifer and probably are areas of larger bedrock permeability in the bedrock.

Currently (1991), the USDOE has 59 active monitoring wells and 7 piezometers located on the WSCP and vicinity property (fig. 13). Monitoring wells installed by the USDOE use the prefix MW to indicate monitoring well. Depths of shallow monitoring wells are dependent on the depth to the weathered limestone and range from 29 to 150 ft (MK-Ferguson Company and Jacobs Engineering Group, 1989e). These wells have screen lengths ranging from 5 to 83 ft and are open to the weathered limestone or the weathered and the unweathered limestone. Depths of the deep monitoring wells range from 90 to 150 ft. These wells are screened only within the unweathered limestone. Twenty-two of the monitoring wells shown in figure 13 are nested pairs where one well is completed within the weathered limestone and the other is completed within the unweathered limestone. Two previously existing monitoring wells (MW-2016 and MW-3007) that were completed as open (uncased) holes have been plugged. The USGS has drilled additional monitoring wells on the August A. Busch Memorial Wildlife Area north of the site (fig. 11). These wells were completed as open holes from the top of the weathered limestone to the desired depth. The USGS also has collected water samples from an existing well (Army well) on the U.S. Army property (fig. 11). A description of the USDOE well installations is given in MK-Ferguson Company and Jacobs Engineering Group (1989e), and a description
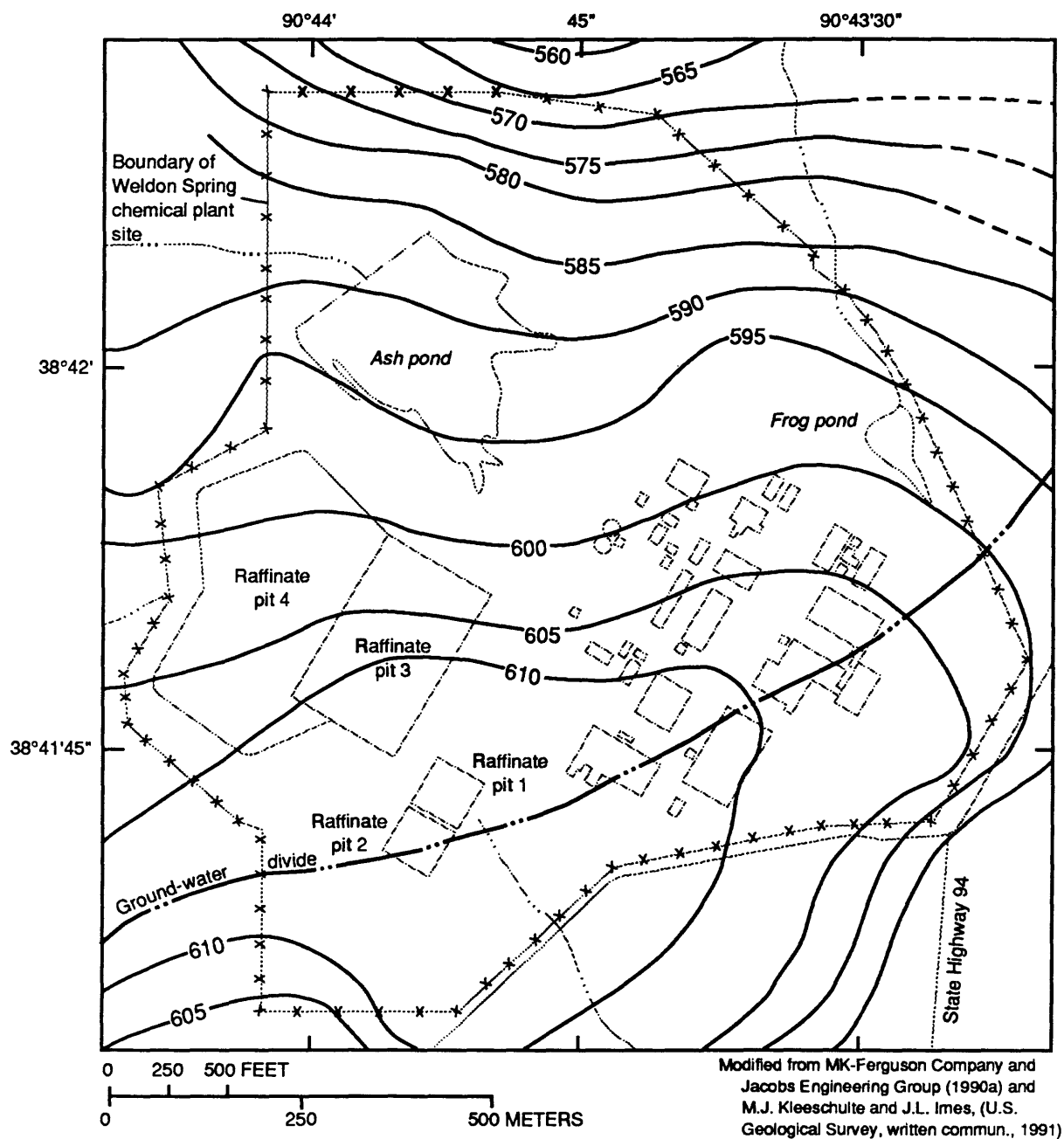
Figure 9. Altitude of the water table in the shallow aquifer, December 1989.
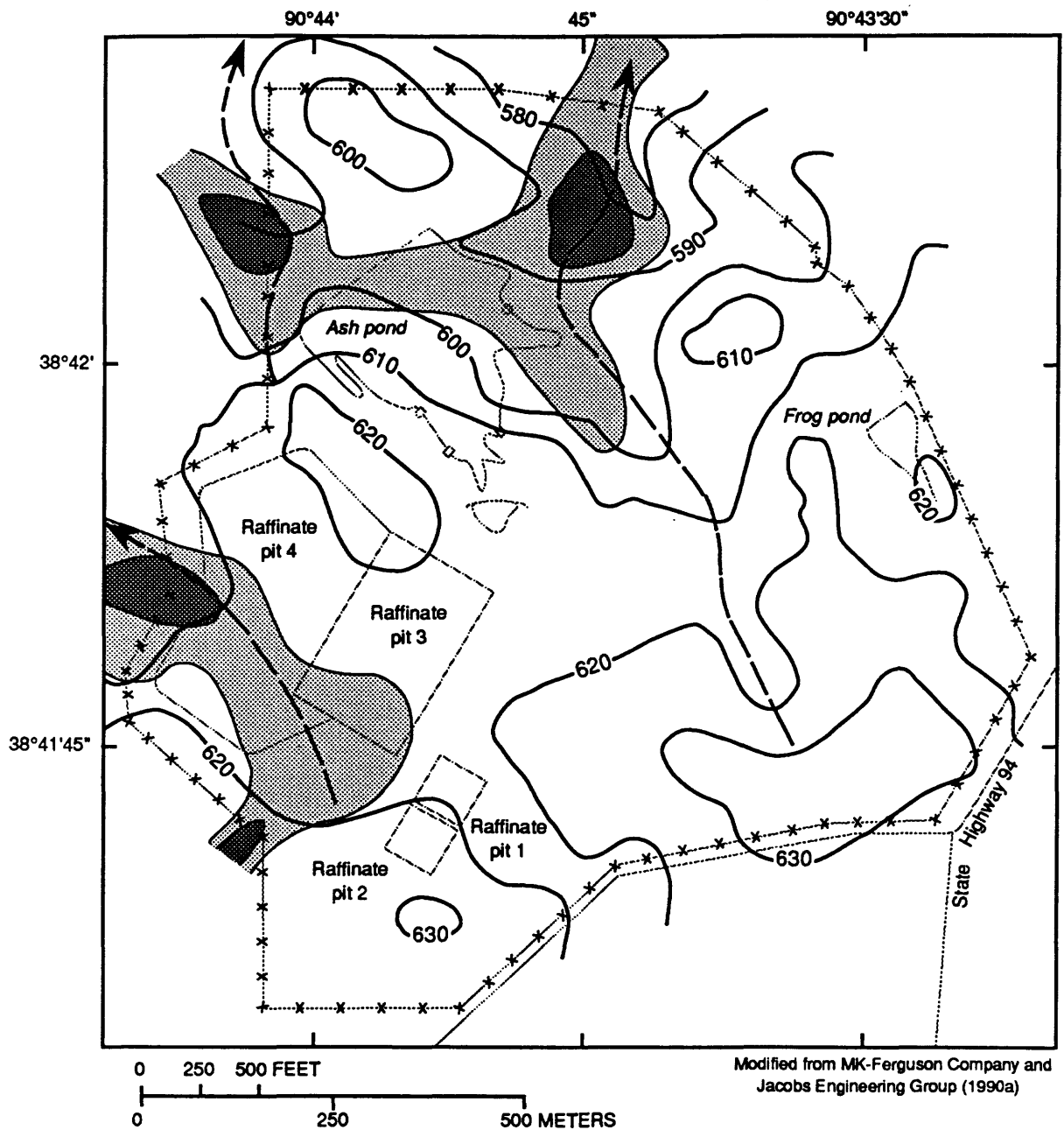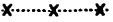
Figure 10. Relation between water table and top of the weathered limestone surface, December 1988.

Figure 11. Altitude of the weathered limestone surface in the vicinity of the Weldon Spring chemical plant site.

EXPLANATION

— 560 - - — BEDROCK CONTOUR--Shows altitude of the weathered limestone surface. Dashed where approximately located. Contour interval 20 feet. Datum is sea level

USGS-1 • MONITORING WELL AND NUMBER
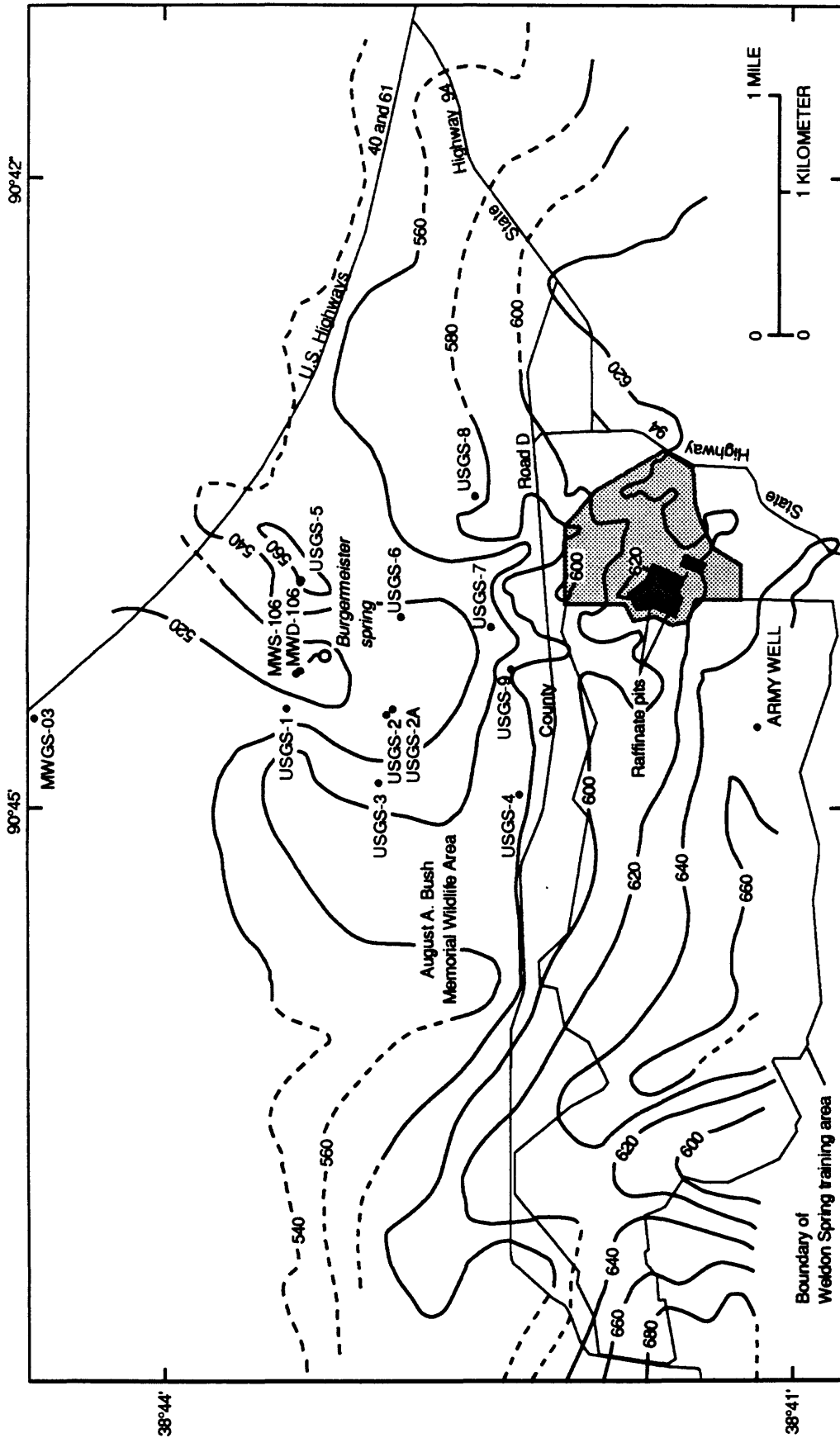
Modified from Kleeschulte and Emmett (1987) and MK-Ferguson Company and Jacobs Engineering Group (1990a)
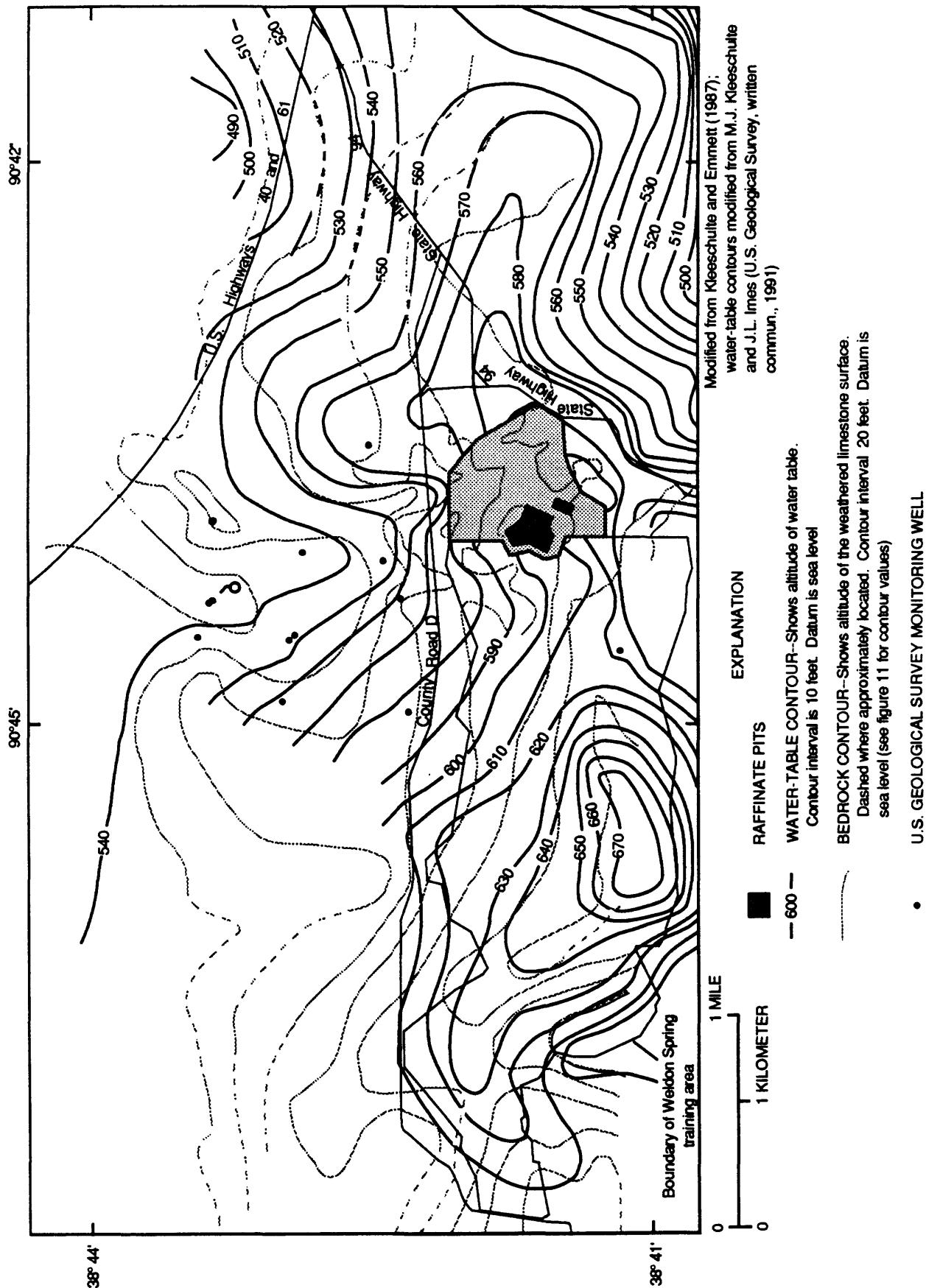
Figure 12. Water table in the shallow aquifer and altitude of the weathered limestone surface in the vicinity of the Weldon Spring chemical plant site, August 1989.

EXPLANATION

RAFFINATE PITS

— 600 — WATER-TABLE CONTOUR–Shows altitude of water table. Contour interval is 10 feet. Datum is sea level

BEDROCK CONTOUR–Shows altitude of the weathered limestone surface. Dashed where approximately located. Contour interval 20 feet. Datum is sea level (see figure 11 for contour values)

• U.S. GEOLOGICAL SURVEY MONITORING WELL

Modified from Kleeschulte and Emmett (1987); water-table contours modified from M.J. Kleeschulte and J.L. Imes (U.S. Geological Survey, written commun., 1991)

Figure 13. Location of monitoring wells completed in the shallow aquifer on and adjacent to the Weldon Spring chemical plant site.

of the USGS monitoring well installations is given in Kleeschulte and Cross (1990).

In addition to monitoring wells, three pump test arrays were located at the site (fig. 13). Each pump test array consists of a central pumping well surrounded by 9 or 10 observation wells. These sites were used by the USDOE to conduct aquifer and tracer tests and were removed during 1991. Results from these tests were interpreted to indicate primarily lateral anisotropy and generally poor vertical hydraulic connection between the shallow and deeper parts of the shallow aquifer (MK-Ferguson Company and Jacobs Engineering Group, 1990b). Results from slug tests performed on 69 monitoring wells at the site by USDOE contractors indicated an average hydraulic conductivity of the weathered and unweathered limestones of 1×10^{-4} cm/s (centimeter per second) using the Bouwer and Rice method (Carman, 1991). Most monitoring wells are open to the weathered and unweathered limestones; however, slug tests performed on one monitoring well and one piezometer (MW-4014 and GT58-P) completed only within weathered limestone indicated substantially larger hydraulic conductivities, 1.6×10^{-3} and 4.5×10^{-3} cm/s, using the Hvorslev Method (MK-Ferguson Company and Jacobs Engineering Group, 1990b). Monitoring wells with large hydraulic conductivity values are located in areas where ground water occurs in the weathered limestone or residuum. The large hydraulic conductivity values in the weathered limestone and the relatively constant water levels in the shallow aquifer, in addition to the core fracture data and drilling fluid losses in the residuum and upper weathered bedrock, indicate the water table may be controlled by a network of interconnected fractures, cobble zones, and solution features. Infiltration may be rapidly lost laterally through this network rather than being stored, resulting in stable water levels with time.

Seismic data and water levels in the overburden indicate the presence of ground-water mounding in the vicinity of raffinate pits 3 and 4. In the process of drilling several monitoring wells within the overburden (B-2, B-14, B-15, B-22, and B-24; fig. 14), water and debris were encountered (Bechtel National Inc., 1984). Geophysical surveys conducted at the site indicated that several large velocity zones in the overburden beneath and adjacent to raffinate pit 3 may be indicative of saturated conditions beneath, to the east, west, and to a limited extent, south of pit 3 (Bechtel National, Inc., 1984). Saturated conditions also were

indicated below raffinate pit 4; however, because of seismic inversion (the presence of a larger velocity layer above a smaller velocity layer), saturated conditions could not be determined to extend to bedrock. The presence of these large velocity zones indicated ground-water mounding in the vicinity of raffinate pits 3 and 4.

Permeability tests conducted by Bechtel National, Inc. (1984) indicated overburden permeabilities between 1.6×10^{-9} and 3.0×10^{-6} cm/s with the larger values corresponding to siltier materials. Falling head triaxial permeability tests were made under a range of confining pressures and indicate permeabilities in the Ferrelview Formation and clay till between 1.0×10^{-8} and 3.2×10^{-6} cm/s (MK-Ferguson Company and Jacobs Engineering Group, 1990a).

GEOCHEMISTRY OF THE SHALLOW AQUIFER

The USGS has collected more than 360 water-quality samples from 57 wells, 19 springs, 17 surface-water sites, and 10 special sources (raffinate pits and associated seeps; Kleeschulte and Cross, 1990) at and near the WSCP during various investigations since 1983. The upper limit of background concentrations for various constituents in wells, springs, and streams has been determined by Kleeschulte and Imes (in press). Monitoring wells, springs, and streams from which water samples contained constituent concentrations smaller than the upper limit of the background concentrations are identified as uncontaminated. Wells, springs, and streams from which water samples contained concentrations of constituents larger than background concentrations of constituents commonly detected in large concentrations in the raffinate (determined by Kleeschulte and Imes, in press) are referred to as contaminated. The discussion in this section is based on analyses of samples collected by the USGS from uncontaminated monitoring wells (table 2). This subjective determination also was based on other factors, such as the magnitude of the concentration, type of constituent, potential for other sources (natural and otherwise), geochemical properties, frequency of occurrence, number of samples from the well or piezometer, and the presence of other constituents larger than background concentrations. Water-quality analyses of samples from these monitoring wells are

Figure 14. Location of overburden monitoring wells and trenches encountering water or debris in the vicinity of the raffinate pits.

Table 2. Uncontaminated monitoring wells in the shallow aquifer

[Wells sampled by the U.S. Geological Survey; WSCP, Weldon Spring chemical plant]

Wells at or near the WSCP site (fig. 13)	Wells north of the WSCP site (fig. 11)
MW-2004	[a]MWD-106
MW-2011	MWS-106
MW-2016	MWGS-03
MW-2019	USGS-1
[a]MW-2021	USGS-2
[a]MW-2022	USGS-2A
[a]MW-2024	USGS-3
[a]MW-2025	USGS-4
[a]MW-2026	USGS-7
[a]MW-2029	
[a]MW-3002	
MW-3010	
MW-4002	
MW-4003	

[a] Monitoring well completed in the unweathered limestone unit of the shallow aquifer.

given in Kleeschulte and Cross (1990) and Schumacher (1990).

Samples from uncontaminated wells (table 2) within the shallow aquifer have near-neutral pH values, specific conductance values generally less than 651 μS/cm (microsiemens per centimeter at 25 degrees Celsius), and Ca, Mg, and bicarbonate (HCO_3) as the predominate ions. These samples plot within a narrow field on a trilinear diagram near the Ca plus Mg-CO_3 plus HCO_3 vertex (fig. 15), reflecting the carbonate lithology of the shallow aquifer. These samples also had concentrations of $NO_2 + NO_3$ less than 1.60 mg/L (milligrams per liter) as N and small concentrations of trace elements (Schumacher, 1990). Because samples

collected from shallow uncontaminated monitoring wells contain measurable quantities of dissolved oxygen (greater than 1 mg/L), an abundance of oxidized forms of N as compared to reduced forms, and small concentrations of dissolved Fe and ferrous iron (Fe^{2+}), moderately oxidizing conditions are thought to exist within the weathered limestone of the shallow aquifer. This is collaborated by the presence of Fe oxide staining on core samples of the weathered limestone, as described by the USDOE (MK-Ferguson Company and Jacobs Engineering Group, 1990b). The availability of dissolved oxygen in the shallow aquifer may decrease with depth as shown in wells completed within the unweathered limestone, such as in the
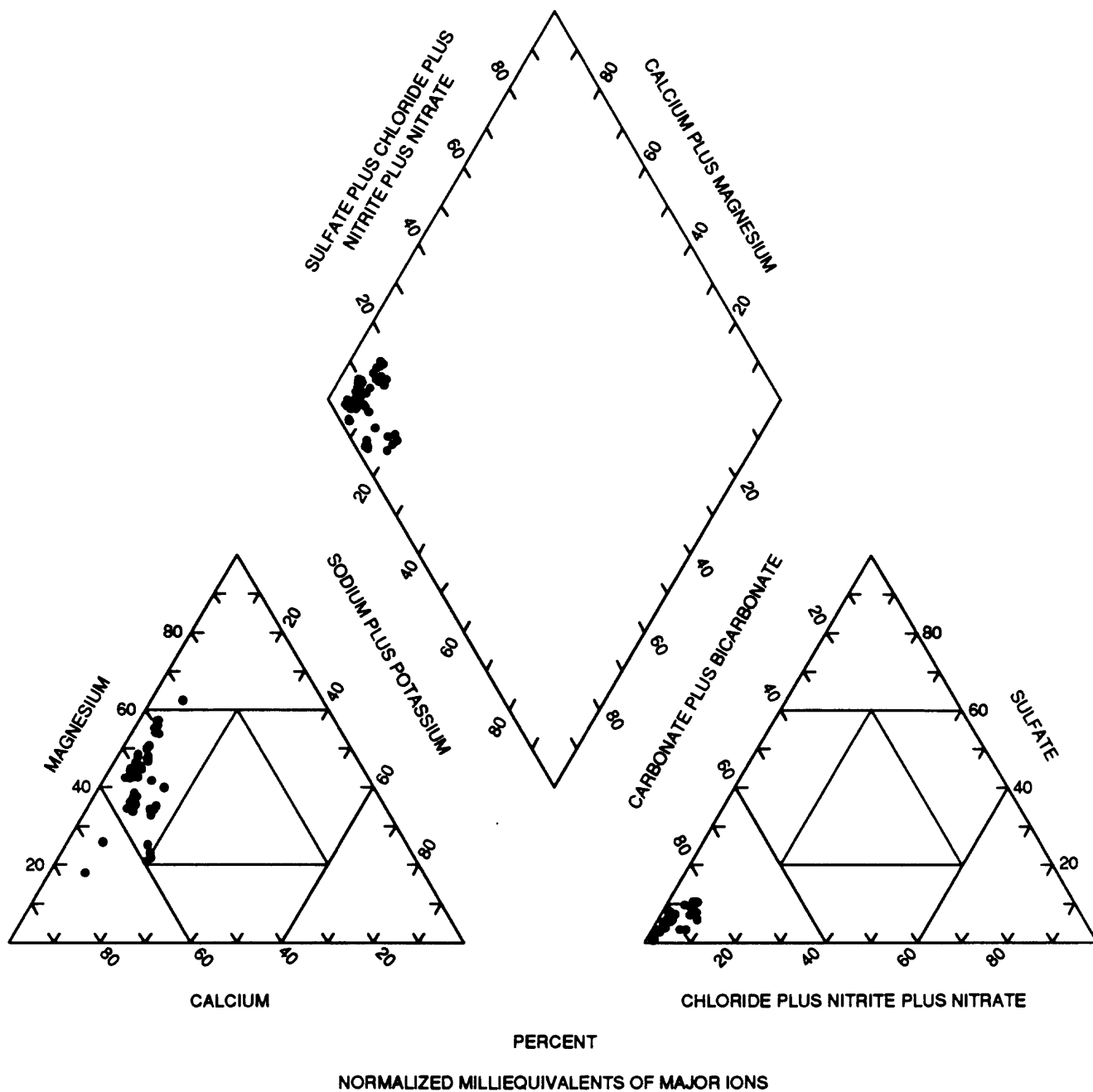
Figure 15. Trilinear diagram of major constituents in water samples from uncontaminated monitoring wells at the Weldon Spring chemical plant site and vicinity property.

sample from monitoring well MW-2022, which had a small concentration of dissolved oxygen (0.7 mg/L; Schumacher, 1990). The sample from the well also had a moderate concentration of dissolved Fe (120 µg/L), indicative of more reducing conditions. The existence of more reducing conditions is confirmed by the presence of unweathered pyrite observed on fracture faces in core samples from the unweathered limestone of the shallow aquifer (MK-Ferguson Company and Jacobs Engineering Group, 1990b).

Tritium analyses were made on samples from 11 monitoring wells at or near the site (MW-2003, MW-2005, MW-2006, MW-3002, MW-3006, MW-3008, MW-3009, MW-3010, MW-4002, MW-4006, and MW-4013; fig. 13) and 3 downgradient monitoring wells (USGS-2, USGS-7, and MWGS-03) north of the site (fig. 11) to determine if substantial quantities of recent (post-1953) atmospheric recharge has entered the shallow aquifer. Tritium concentrations larger than 5.7 pCi/L (picocuries per liter) indicate effects of atmospheric testing of nuclear weapons during the 1950's and 1960's (Carlston, 1964; Hendry, 1988).

Eight of the monitoring wells sampled were screened primarily within the weathered limestone and three (MW-3002, MW-3006, and MW-3009) were screened within the unweathered limestone of the shallow aquifer. The three downgradient monitoring wells north of the site (USGS-2, USGS-7, and MWGS-03) are open holes from the top of the unweathered limestone. All but one of the shallow monitoring wells (MW-4006) in the weathered limestone at or near the site contained tritium values larger than 5.7 pCi/L. None of the deeper monitoring wells in the unweathered limestone at the site or the three downgradient monitoring wells north of the site contained tritium values larger than 5.7 pCi/L. The data indicate longer residence times for water in the deeper part of the shallow aquifer at the site and older water within the upper part of the shallow aquifer downgradient of the site. The tritium data combined with the larger hydraulic conductivities and relatively stable water levels in the weathered limestone indicate much of the recharge at the site is moving laterally above the unweathered limestone to vicinity springs and streams.

To investigate thermodynamic controls on water composition, equilibrium-speciation calculations were made using the geochemical codes WATEQ4F (Ball and others, 1987), SOLMINEQ.88 (Kharaka and others, 1988), and PHREEQE (Parkhurst and others, 1980). These calculations provide the probable speciation of aqueous constituents based on thermodynamic association constants and saturation index (SI) of mineral phases that may be reacting in the system. Values of the SI larger than 0 indicate supersaturation with respect to a given mineral phase and that precipitation may occur, whereas SI values less than 0 indicate undersaturation with a given mineral phase and dissolution may occur. Because of uncertainty in the thermodynamic and analytical data, an accepted range of error in the SI values for common minerals is about ± (plus or minus) 0.5. The error for many uncommon minerals, such as U minerals, may be much larger. A major limitation in the use of thermodynamic equilibrium calculations is that reaction kinetics are not considered and generally are poorly understood for most mineral phases.

Samples from uncontaminated monitoring wells generally are at equilibrium with calcite and supersaturated with respect to dolomite (fig. 16). Samples from these monitoring wells contain nearly equal molar concentrations of Ca and Mg and molar ratios of Ca to Mg range from 0.49 to 2.80 (fig. 17). Ground water in equilibrium with limestone (predominately calcite) would be expected to contain molar concentrations of Ca much larger than Mg. These relatively small Ca/Mg ratios probably are caused by dissolution of limestone (that contains appreciable quantities of Mg) and small quantities of dolomite and subsequent precipitation of calcite. Hem (1985) postulated that small Ca/Mg ratios in ground water from limestone aquifers are caused by dissolution of the rock, which brings Mg into solution. The process generally is not readily reversible because the precipitate that forms is nearly pure calcite. Variable quantities of dolomite occur within the Burlington Limestone and the lower part of the unit may be dolomite in some areas (T.L. Thompson, Missouri Department of Natural Resources, written commun., 1990). Ratios of Ca to Mg in 36 whole-rock samples of the Burlington and Keokuk Limestones from St. Charles County (Rueff, 1977) ranged from 1.4 to 110, indicating the presence of some dolomite within the units.

Water samples from the deep uncontaminated monitoring wells have smaller Ca/Mg ratios (median of 0.79) than the shallow uncontaminated monitoring wells (median of 0.98), USGS monitoring wells (median of 1.14), or uncontaminated springs (median of 3.10). The smaller Ca/Mg ratios in samples from the
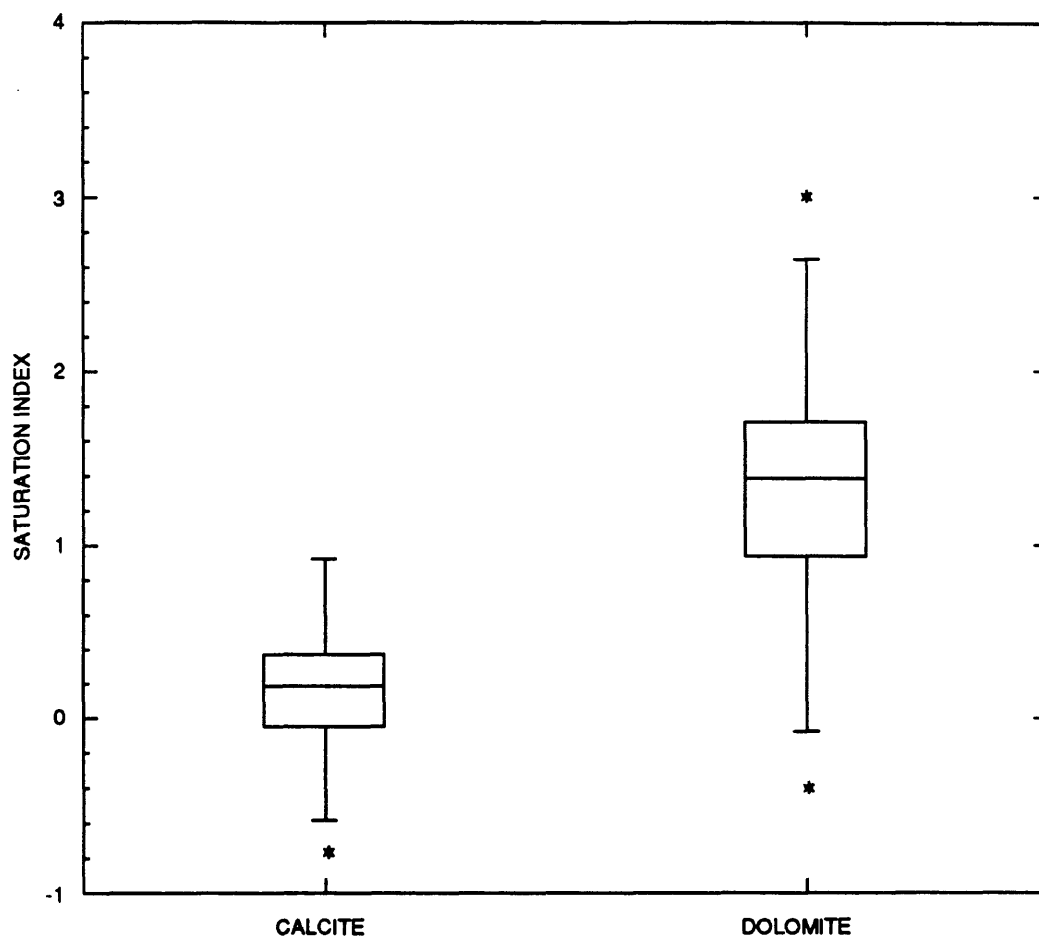
Figure 16. Boxplots of calcite and dolomite saturation indices in samples from uncontaminated monitoring wells in the shallow aquifer at the Weldon Spring chemical plant site and vicinity property.
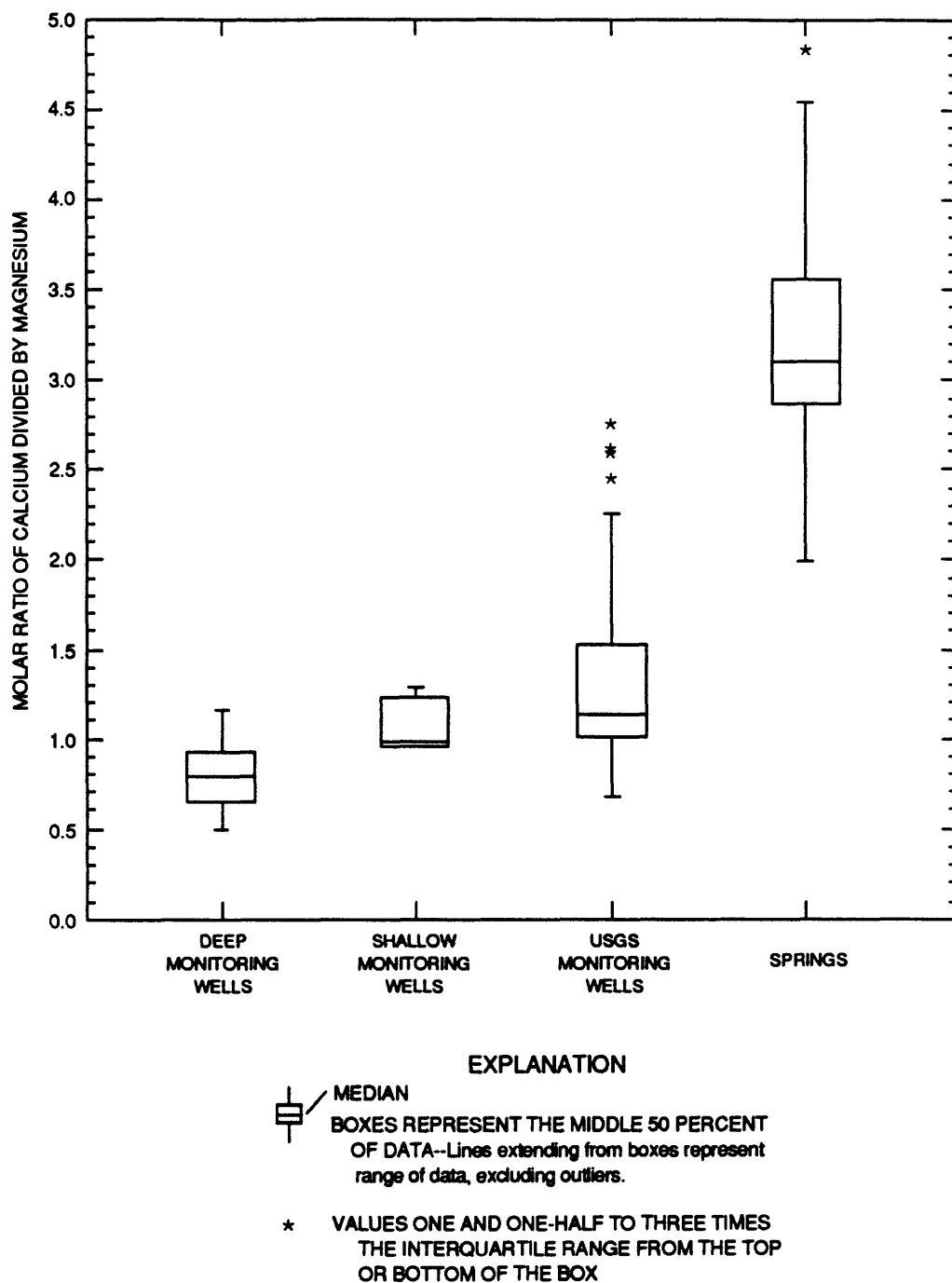
Figure 17. Boxplots of the molar ratio of calcium to magnesium in samples from uncontaminated monitoring wells and springs in the shallow aquifer at the Weldon Spring chemical plant site and vicinity property.

deep uncontaminated monitoring wells probably are related to the longer residence time (samples from these wells generally have tritium concentrations less than the detection limit) of water in the deeper unweathered limestone. Longer residence times would enable the dissolution-precipitation reaction to proceed more completely. Dissolution of small quantities of dolomite also would contribute to the small Ca/Mg ratios. The larger Ca/Mg ratios in the shallow uncontaminated monitoring wells can be explained by the shorter residence time of water within the upper, generally weathered, part of the shallow aquifer (many samples from these wells contained detectable concentrations of tritium) and dissolution of calcitic material within the upper bedrock and lower part of the overburden.

Because the USGS wells are open holes from the top of the unweathered limestone, they may be affected by conditions within the shallow and deep parts of the shallow aquifer. Tritium concentrations were less than the detection limit in samples from two of the USGS wells sampled (USGS-2 and USGS-7; Kleeschulte and Cross, 1990) and the Ca/Mg ratios in these two wells averaged 1.50 (USGS-2) and 0.70. The small tritium concentrations reflect the downgradient position of these wells; however, the Ca/Mg ratio of 1.50 in USGS-2 may indicate some mixing of water from the shallow part of the aquifer. The larger Ca/Mg ratios in the uncontaminated springs were expected because of the relatively short residence time of water in the spring system. Also, solution pathways, such as springs, may tend to develop within the more soluble or calcite-rich parts of the aquifer.

Analyses of ground-water samples from uncontaminated monitoring wells sampled by the USGS plot along the line for weathering of carbonate material by carbonic acid (fig. 18), according to the following reaction

$$CO_2 + H_2O + (Ca, Mg, Sr)\,CO_3 = (Ca, Mg, Sr)^{2+} + 2HCO_3^-, \qquad (3)$$
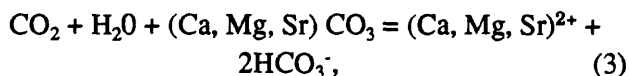
rather than mineral acid dissolution or hydrolysis. The slope of the regression line is 0.538 compared to the theoretical slope of 0.5 from reaction 3, indicating weathering of the carbonate material by carbonic acid. Those samples that plot substantially above the regression line in figure 18 are from contaminated monitoring wells and were not used to calculate the regression line. The plotting position of these contaminated wells indicates that a substantial quantity of the Ca in sam-

ples from these wells may be derived from the action of mineral acids on carbonate material, such as the neutralization of acidic raffinate with lime or spillage of acids during ordnance production rather than by carbonic acid weathering. The action of mineral acids, such as hydrochloric acid (HCl) or H_2SO_4, on carbonate material results in large concentrations of Ca and relatively small concentrations of HCO_3 because much of the carbon is lost as CO_2 gas. The chemistry of these wells is further discussed in the section titled "Migration of Constituents Within the Shallow Aquifer."

Results of stable carbon and oxygen isotope analyses from composite overburden samples, bedrock drill cores, and water samples from several shallow aquifer wells are listed in table 3. Isotopic composition is expressed in the delta notation (δ) as per thousand (per mil) differences between isotopic ratios of carbon ($^{13}C/^{12}C$) in the sample relative to PDB (Pedee Belemnite) standard according to the relation

$$\delta^{13}C = \frac{(^{13}C/^{12}C)\,\text{sample} - (^{13}C/^{12}C)\,PDB}{(^{13}C/^{12}C)\,PDB} \times$$
$$1,000. \qquad (4)$$

The average $\delta^{13}C$ of the four overburden samples was -1.4 per mil and the average of the eight bedrock samples was +1.9 per mil. The average $\delta^{13}C$ of the two water samples was -6.0 per mil. No differences were detected in the $\delta^{18}O$ contents of the overburden and bedrock. If dissolution of carbonate material by carbonic acid occurs as is indicated in figure 18, then 50 percent of the carbon should be derived from the solid phase and 50 percent from carbonic acid. Assuming an average $\delta^{13}C$ of -6.0 per mil for the ground water and either -1.4 or 1.9 for the solid phase based on reaction 4, the theoretical $\delta^{13}C$ of carbonic acid should be between -10.6 and -13.9. Carbonic acid generally is produced in the soil zone by the reaction of CO_2 (produced by the decomposition of organic matter) and water. The $\delta^{13}C$ of the carbon in the carbonic acid produced will closely approximate that of the original organic matter (W.W. Wood, U.S. Geological Survey, written commun., 1990). The theoretical $\delta^{13}C$ of the carbonic acid computed above (-10.6 to -13.9) is larger than that generated from the decomposition of C3 plants more characteristic of the area (-22 to -33) but within the range of C4 plants, about -9.0 to -16.0 (Deines, 1980). The theoretical values are not unusual because before the construction
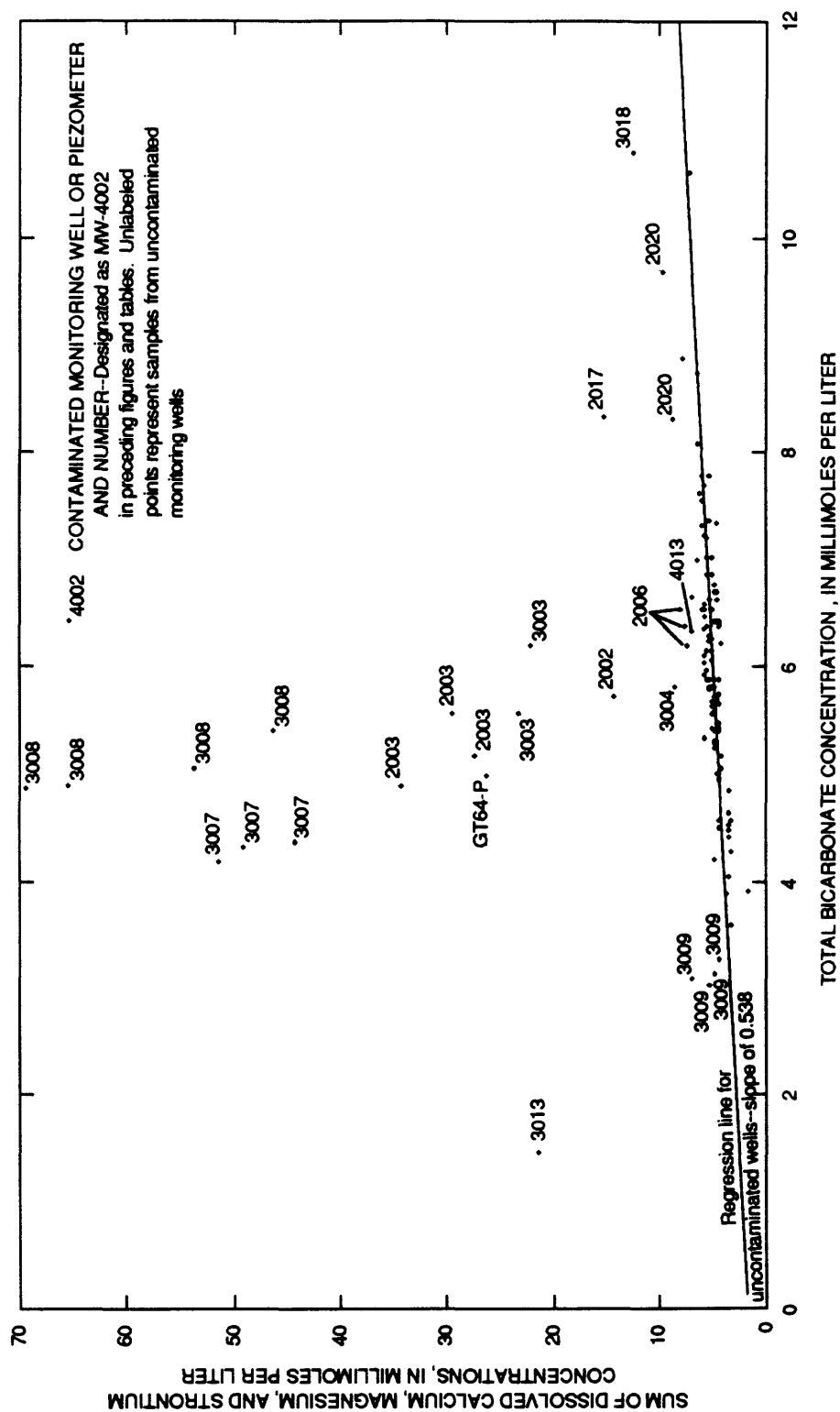
Figure 18. Sum of calcium, magnesium, and strontium concentrations and bicarbonate concentrations in samples from monitoring wells in the shallow aquifer at the Weldon Spring chemical plant site and vicinity property.

Table 3. Stable carbon and oxygen isotope contents of rock samples from the overburden and shallow aquifer and water samples from the shallow aquifer

[δ^{13}C, Delta carbon-13 (per mil); δ^{18}O, delta oxygen-18 (per mil); --, no data]

Sample	δ^{13}C	δ^{18}O
Overburden		
Loess	-0.4	26.0
Ferrelview Formation[a]	--	--
Clay till	-3.0	26.5
Basal till	-2.8	25.8
Residuum	.8	26.1
Shallow aquifer (figs. 5 and 13)		
GT-16 unweathered limestone	3.2	25.4
GT-16 weathered limestone	1.8	30.2
GT-42	- .5	25.4
GT-50	2.2	25.8
GT58-P	1.4	25.5
GT64-P	2.0	26.0
GT67-P	2.4	26.6
MW-2006	3.0	26.1
Water from shallow aquifer (fig. 13)		
MW-2005	-5.0	--
MW-2025	-7.0	--

[a] Carbonate content too small for isotope analysis.

of the chemical plant and ordnance works, the area was heavily farmed with crops, such as corn, a known C4 plant (Lowdon and Dyck, 1974). The $\delta^{13}C$ values of the three water samples from the shallow aquifer are consistent with the proposed weathering by carbonic acid (fig. 18), assuming the acid was produced from oxidation of C4 plant matter. Additional isotopic data, such as soil gas and soil organic matter determinations, are required to distinguish between carbonate dissolution of the overburden and the shallow aquifer.

GEOCHEMISTRY OF THE RAFFINATE PITS

The largest concentrations of inorganic constituents detected in water samples at the WSCP site were in the raffinate pits. A summary of surface-water-quality data from the raffinate pits collected since 1979 by various agencies is given in table 4. Samples from the raffinate pits contained large concentrations of Ca (11 to 1,400 mg/L), Mg (21 to 480 mg/L), Na (120 to 1,500 mg/L), K (13 to 181 mg/L), SO_4 (70 to 990 mg/L), $NO_2 + NO_3$ (less than 10 to more than 1,800 mg/L as N), Li (10 to 6,240 µg/L), Mo (670 to 7,100 µg/L), Sr (122 to 5,460 µg/L), V (70 to 3,200 µg/L), and U (less than 10 to more than 4,000 µg/L). Water in raffinate pit 4 generally contained the smallest concentrations of all constituents except HCO_3 and U, where concentrations were the largest. The raffinate pits have been determined to be leaking (Kleeschulte and Emmett, 1987) and are the most likely sources of increased concentrations of several constituents in ground water at the site. A previous investigation (Kleeschulte and others, 1986) and data collected during this study (Schumacher, 1990) indicate increased concentrations of Ca, Mg, Na, SO_4, Cl, $NO_2 + NO_3$, Li, Se, Sr, and U in ground water at the site, particularly in the vicinity of the raffinate pits.

The migration of constituents from the raffinate pits and their effect on the shallow aquifer was a primary focus of this investigation. Any effort to characterize the migration of contaminants from the raffinate pits requires an understanding of the nature of the contaminants within the pits, including the solid and aqueous phases. The USGS has collected surface-water samples from the raffinate pits since 1984. A trilinear plot of these data is given in figure 19. This plot shows the relative normalized milliequivalents of the major ions in the raffinate pits and other sites

relative to the uncontaminated wells. The surface-water chemistry was slightly different in each raffinate pit. Surface water in raffinate pit 1 had Ca plus Mg slightly greater than Na plus K and the predominate anion was NO_3 (table 4). Water in raffinate pit 2 contained Ca plus Mg greater than Na plus K, and large SO_4 relative to other anions. Water in raffinate pit 3 contained the largest concentrations of most ions, and had nearly equal equivalents of Ca plus Mg and Na plus K. The predominate anion was NO_3 (table 4). Water in raffinate pit 4 contained Na plus K greater than Ca plus Mg, and variable quantities of CO_3 plus HCO_3 and Cl plus NO_3, and SO_4 contributed generally less than 20 percent of the negative charge in samples from this pit.

Subtle differences in the distribution of ions within the pits probably are related to differences in the quantity and composition of the sludge, dilution effects from rainfall, and biologic processes. The distribution of major constituents in raffinate pits 1, 2, and 3 have changed little, probably because of the large quantity of sludge within these pits (table 1). However, the combined effects of dilution and biologic activity on water chemistry in raffinate pit 4 are evident in figure 19. Since 1984, the plotting position of samples from this pit has gradually shifted from a Na-NO3 type water to a Na-HCO3 type water. Concentrations of most constituents have decreased during this time (table 4). Based on data collected in September 1984 (Kleeschulte and others, 1986) and in September 1989 (Schumacher, 1990), concentrations of Ca decreased 35 percent, Mg decreased 29 percent, Na did not decrease, SO_4 decreased 27 percent, Cl decreased 16 percent, $NO_2 + NO_3$ decreased 92 percent, Li decreased 21 percent, and U decreased 20 percent. The decreases in most constituent concentrations probably are related in part to dilution from rainfall because water levels generally have increased in the raffinate pits; however, the excessively large decrease in concentration of $NO_2 + NO_3$ probably is related in part to biologic uptake because large quantities of algae have been observed and large concentrations of dissolved oxygen have been measured in raffinate pit 4 during the summer months.

Equilibrium-speciation calculations were made on the most complete water-quality analysis from each raffinate pit using WATEQ4F and PHREEQE (table 5). These calculations indicate surface water in the raffinate pits generally is supersaturated with calcite and aragonite and approaching saturation with gypsum,

Table 4. Historical water-quality data from the raffinate pits

[BCHT, Bechtel National, Inc., (1984); USGS, U.S. Geological Survey, Kleeschulte and Cross (1990), Schumacher (1990); W&B, Weidner and Boback (1982); ORNL, Taylor and others (1979); year indicates date of sample collection; μS/cm, microsiemens per centimeter at 25 degrees Celsius; mg/L, milligrams per liter; μg/L, micrograms per liter; pCi/L, picocuries per liter; --, no data available; <, less than; all concentrations are dissolved unless noted otherwise]

Physical property or chemical constituent	Raffinate pit 1			Raffinate pit 2		
	BCHT 1983	USGS 1984	USGS 1986	BCHT 1983	USGS 1984	USGS 1986
Specific conductance, μS/cm	--	--	--	--	--	--
pH, standard units	--	--	--	--	--	--
Dissolved oxygen, mg/L	--	--	--	--	--	--
Calcium, mg/L	--	560	340	--	380	140
Magnesium, mg/L	--	26	21	--	66	47
Sodium, mg/L	--	520	390	--	180	120
Potassium, mg/L	--	48	29	--	33	17
Alkalinity, mg/L	--	34	40	--	37	41
Sulfate, mg/L	100	400	280	460	990	580
Chloride, mg/L	15	17	13	6	5.7	4.4
Fluoride, mg/L	1.1	2.5	2.0	1	2.7	2.2
Silica, mg/L	--	5.4	5.4	--	2.2	2.8
Nitrite, dissolved as nitrogen, mg/L	--	32	3.8	--	5.4	2.9
Nitrite plus nitrate, dissolved as nitrogen, mg/L	[a]710	668	416	[a].1	205	50
Aluminum, μg/L	--	30	--	--	40	--
Arsenic, μg/L	100	6	--	90	15	--
Barium, μg/L	<100	90	--	<100	72	--
Beryllium, μg/L	<1	12	--	1	8	--
Boron, μg/L	<100	--	--	<100	--	--
Cadmium, μg/L	.4	<3	--	.2	<3	--

Table 4. Historical water-quality data from the raffinate pits--Continued

Physical property or chemical constituent	Raffinate pit 3						Raffinate pit 4					
	W&B 1979-80	ORNL average 1979	BCHT 1983	USGS 1984	USGS 1986	USGS 1989	W&B 1979-80	ORNL average 1979	BCHT 1983	USGS 1984	USGS 1986	USGS 1989
Specific conductance, μS/cm	--	--	--	--	--	12,000	--	--	--	--	--	1,120
pH, standard units	--	--	--	--	--	8.51	--	--	--	--	--	8.92
Dissolved oxygen, mg/L	--	--	--	--	--	10.4	--	--	--	--	--	--
Calcium, mg/L	1,400	1,396	--	880	510	490	--	14.9	--	17	18	11
Magnesium, mg/L	440	480	--	320	290	370	--	34.1	--	52	49	37
Sodium, mg/L	1,460	1,187	--	1,500	970	1,300	--	122	--	190	190	190
Potassium, mg/L	--	181	--	150	80	87	--	17.8	--	23	18	13
Alkalinity, mg/L	--	--	--	37	52	48	--	--	--	240	259	432
Sulfate, mg/L	--	[b]625	260	640	410	630	--	140	70	150	130	110
Chloride, mg/L	29.3	37	20	25	22	23	12	10	7	7.7	7.4	6.5
Fluoride, mg/L	7.4	6	2.7	8.9	6.9	6.9	8.7	13	5.8	7.8	6.3	6.0
Silica, mg/L	--	--	--	2.8	2.9	1.1	--	--	--	1.7	.4	1.4
Nitrite, dissolved as nitrogen, mg/L	--	[a]40	--	15	6.7	1.1	--	[a]<5	--	3.4	.6	<.01
Nitrite plus nitrate, dissolved as nitrogen, mg/L	[a]13,300	[a]13,000	[a]1,500	1,880	1,190	1,500	[a]55	[a]56	[a]100	91.6	78.4	7.4
Aluminum, μg/L	--	31	--	30	--	10	--	27	--	10	--	10
Arsenic, μg/L	--	--	140	4	--	3	--	--	20	2	--	6
Barium, μg/L	--	186	<100	170	--	100	--	125	100	100	--	150
Beryllium, μg/L	--	<1	1	<5	--	<10	--	<4	<1	--	--	<1
Boron, μg/L	--	183	<100	--	--	100	--	91	<100	--	--	40
Cadmium, μg/L	--	--	<.1	<10	--	<1	--	--	3	<1	--	<1

Table 4. Historical water-quality data from the raffinate pits--Continued

Physical property or chemical constituent	Raffinate pit 1			Raffinate pit 2		
	BCHT 1983	USGS 1984	USGS 1986	BCHT 1983	USGS 1984	USGS 1986
Chromium, µg/L	<1	<1	--	<1	<1	--
Cobalt, µg/L	28	<9	--	32	<9	--
Copper, µg/L	111	4	--	5	4	--
Iron, µg/L	12	15	--	5	<9	--
Lead, µg/L	<1	<1	--	2	<1	--
Lithium, µg/L	--	140	10	--	140	26
Manganese, µg/L	28	9	--	33	9	--
Mercury, µg/L	<1	<.1	--	<1	<.1	--
Molybdenum, µg/L	--	3,000	--	--	7,100	--
Nickel, µg/L	<10	<1	--	20	<1	--
Selenium, µg/L	10	<1	--	<10	<1	--
Silver, µg/L	<1	<1	--	<1	<1	--
Strontium, µg/L	--	1,400	1,000	--	780	380
Vanadium, µg/L	--	3,200	--	--	2,000	--
Zinc, µg/L	70	45	--	40	25	--
Radium-226, pCi/L	500	290	--	480	120	--
Uranium, µg/L	°6	26	46	°43	28	180
Cyanide, µg/L	<20	--	--	30	--	--

Table 4. Historical water-quality data from the raffinate pits--Continued

Physical property or chemical constituent	Raffinate pit 3						Raffinate pit 4					
	W&B	ORNL average 1979-80	BCHT 1979	USGS 1983	USGS 1984	USGS 1986	W&B 1989	ORNL average 1979-80	BCHT 1979	USGS 1983	USGS 1984	USGS 19861989
Chromium, μg/L	--	<4	<1	<1	--	2	--	<4	<1	<1	--	<1
Cobalt, μg/L	--	<8	40	<30	--	<1	--	<4	13	<3	--	<3
Copper, μg/L	<1	27	11	7	--	3	<1	<4	<1	1	--	3
Iron, μg/L	--	56	11	<30	--	40	--	<4	74	<3	--	3
Lead, μg/L	--	--	2	11	--	<1	--	--	4	17	--	<5
Lithium, μg/L	--	6,240	--	460	2,700	3,600	--	689	--	660	590	520
Manganese, μg/L	--	93	9	35	--	10	--	<4	7	7	--	1
Mercury, μg/L	--	--	<1	<.1	--	--	--	--	<1	<.1	--	--
Molybdenum, μg/L	--	3,940	--	3,600	--	4,700	--	1,040	--	670	--	740
Nickel, μg/L	--	7	<10	<1	--	1	--	<4	<10	<1	--	<1
Selenium, μg/L	--	--	80	<1	--	<1	--	--	<10	<1	--	7
Silver, μg/L	--	3	<1	<1	--	<1	--	<3	<1	<1	--	2
Strontium, μg/L	--	5,460	--	2,800	1,600	2,100	--	122	--	190	180	140
Vanadium, μg/L	--	484	--	810	--	520	--	181	--	79	--	70
Zinc, μg/L	--	--	50	66	--	10	--	--	10	5	--	<3
Radium-226, pCi/L	--	195	200	180	--	--	--	10	14	8.4	--	--
Uranium, μg/L	150	[b,c]219	[c]89	350	170	320	4,000	[b,c]5,580	[c]1,670	3,500	2,400	2,800
Cyanide, μg/L	--	--	50	--	--	--	--	--	<20	--	--	--

Note: A gamma spectrometer scan on water from each of the four raffinate pits by the USGS detected no artificial isotopes present in the water.

[a] Reported as nitrate. No determination if total or dissolved nitrate, or if reported as milliequivalents of nitrate or nitrogen.

[b] Value reported in the text and a table in Taylor and others (1979) does not agree.

[c] Value in picocuries per liter. A general conversion is to multiply picocuries per liter by 1.5 to obtain micrograms per liter.
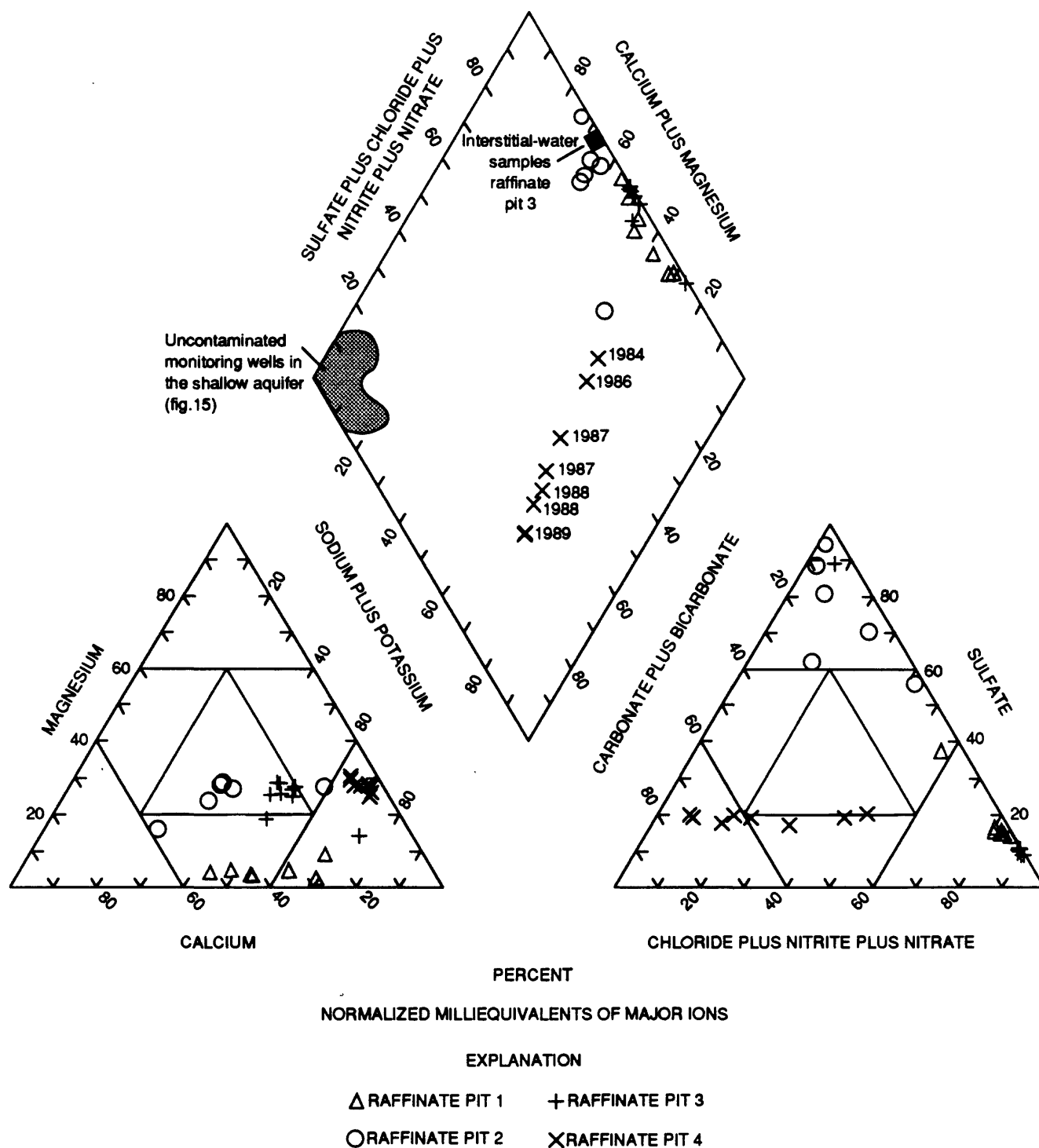
Figure 19. Trilinear diagram of major constituents in surface-water samples from the raffinate pits, uncontaminated wells in the shallow aquifer, and interstitial-water samples from raffinate pit 3.

Table 5. Saturation indices for selected mineral phases in surface water from the raffinate pits

[--, no data available]

Mineral phase	Chemical formula	Raffinate pit 1 (9-05-84)	Raffinate pit 2 (9-05-84)	Raffinate pit 3 (6-08-89)	Raffinate pit 4 (3-14-89)
Calcite	$CaCO_3$	1.26	1.36	0.96	0.82
Aragonite	$CaCO_3$	1.11	1.20	.82	.67
Gypsum	$CaSO_4 \cdot 2H_2O$	- .56	- .32	- .65	-2.47
Strontianite	$SrCO_3$	.88	- .86	- .95	- .50
Celestite	$SrSO_4$	-1.45	-1.29	-1.30	-2.62
Barite	$BaSO_4$	.48	.71	.44	.77
Fluorite	CaF_2	.41	.26	.84	- .23
Fluorapatite	$Ca_5(PO_4)_3F$	--	--	4.40	.83
Hydroxyapatite	$Ca_5(PO_4)_3(OH)$	--	--	2.49	-1.44
Quartz	SiO_2	- .07	- .53	- .78	- .47
Carnotite	$K_2(UO_2)_2(VO_4)_2 \cdot 3H_2O$	2.11	.72	1.97	-2.60
Tyuyamunite	$Ca(UO_2)_2(VO_4)_2 \cdot 5\text{-}8H_2O$	2.63	1.31	2.03	-3.23
Schoepite	$UO_3 \cdot 2H_2O$	-2.67	-2.69	-2.12	-4.32
Rutherfordine	UO_2CO_3	-3.49	-3.97	-2.43	-3.56

indicating probable solubility controls on aqueous concentrations of Ca, HCO_3, and possibly SO_4. Samples from raffinate pits 1, 2, and 3 contained large concentrations of Ca and consequently had small concentrations of alkalinity. Because of the small volume of sludge within the pit, the sample from raffinate pit 4 had small concentrations of Ca (less than 20 mg/L) and other major cations and large concentrations of alkalinity (more than 430 mg/L as $CaCO_3$). Surface water in raffinate pits 3 and 4 is saturated to supersaturated with respect to fluorapatite and near saturation with respect to fluorite (table 5). The sample from raffinate pit 3 is supersaturated with respect to hydroxyapatite. Gypsum is at saturation in raffinate pit 2, slightly undersaturated in raffinate pits 1 and 3, and appreciably undersaturated in raffinate pit 4.

Calculations using PHREEQE indicated that the predominate aqueous species of U in samples from raffinate pit 4 is uranyl tricarbonate, $UO_2(CO_3)_3^{4-}$. The predominate U species in samples from raffinate pits 1, 2, and 3 is uranyl dicarbonate, $UO_2(CO_3)_2^{2-}$, because the concentrations of carbonate were smaller. Saturation indices of selected U minerals (table 5) indicate that raffinate pits 1, 2, and 3 are supersaturated with respect to carnotite [$K_2(UO_2)_2(VO_4)_2 \cdot 3H_2O$] and tyuyamunite [Ca $(UO_2)_2(VO_4)_2 \cdot 5-8H_2O)$] and undersaturated with respect to schoepite ($UO_3 \cdot 2H_2O$) and rutherfordine (UO_2CO_3). Surface water in raffinate pit 4 is undersaturated with respect to these U minerals. Uraninite (UO_2) solubility was not computed because of the oxidizing conditions at the surface of the pits. The large U concentrations in raffinate pit 4 probably are related to U-contaminated material flushed from process lines and placed into pit 4 during decommissioning of the Weldon Spring uranium feed materials plant.

Geochemistry of Interstitial Water in Raffinate Pit 3

Numerous water-quality samples have been collected from the surface of the raffinate pits [Taylor and others (1979); Weidner and Boback (1982); Bechtel National, Inc. (1984); MK-Ferguson Company and Jacobs Engineering Group (1989c); Kleeschulte and Cross (1990)]; however, prior to this investigation no attempt had been made to determine the chemistry of the interstitial water or the mineralogic content of the raffinate sludge. Knowledge of the interstitial-

water chemistry is necessary in assessing the migration of U and other contaminants from the raffinate pits because the interstitial water best approximates the chemistry of solutions migrating from the bottom of the raffinate pits. Relatively insoluble U minerals may precipitate in a reducing environment, thereby limiting migration of U from the raffinate pits. To determine the chemistry and redox state of the raffinate sludges and the geochemical controls on U solubility within the raffinate sludge, in-situ interstitial-water samples were collected from the sludge at various depths below the water-sediment interface in raffinate pit 3 using a dialysis technique. A pilot study was conducted during 1989 to test the feasibility of the technique (Schumacher, 1990). Results from the pilot study were favorable and additional studies were conducted in raffinate pit 3. Raffinate pit 3 was selected because it contains the largest quantity of sludge and the largest constituent concentrations in the surface water.

Interstitial-water samples were collected between 1 and 9 ft below the water-sediment interface near the middle of raffinate pit 3 in August 1990. Dissolved oxygen measurements were made immediately after the samplers were retrieved from the sludge. The samplers were then wrapped in aluminum foil and immediately transported to shore where the remaining onsite measurements (specific conductance, pH, temperature, and alkalinity) were made. Because samples may have warmed during transport to shore, the temperature values could be biased high. The increased temperature may cause the pH values to increase slightly due to outgassing of CO_2; however, the total carbonate concentrations were small and this probably is not a major concern. Specific conductance values increased and pH values and dissolved oxygen concentrations decreased with increasing depth below the water-sediment interface (table 6). Small quantities of dissolved oxygen (between 0.1 and 1.0 mg/L) were detected in all interstitial-water samples.

Concentrations of Ca and Na increased from 490 and 1,300 mg/L in the surface water to 6,200 and 5,200 mg/L at 9 ft below the water-sediment interface (table 6). Although concentrations of Mg and SO_4 tended to increase with increasing depth, they were more variable and ranged from 340 to 1,400 mg/L and 910 to 3,300 mg/L in three samples collected from 9 ft deep. Alkalinity generally decreased with increasing depth to a minimum of 16 mg/L (as $CaCO_3$) in a sample from a depth of 9 ft. Concentrations of nitrite (NO_2), ammonia (NH_3), Mn, and selenium (Se) increased more than two

ABBREVIATIONS AND SYMBOLS USED IN TABLE 6

Depth	Depth below the water-sediment interface, in feet
Temp	Temperature, in degrees Celsius
SC	Specific conductance, in microsiemens per centimeter at 25 degrees Celsius
pH	In standard units
DO	Dissolved oxygen, in milligrams per liter
Ca	Calcium, dissolved, in milligrams per liter
Mg	Magnesium, dissolved, in milligrams per liter
Na	Sodium, dissolved, in milligrams per liter
K	Potassium, incremental titration, dissolved, in milligrams per liter
HCO_3 (IT)	Bicarbonate, incremental titration, in milligrams per liter
Alk (IT)	Alkalinity, incremental titration, total as $CaCO_3$, in milligrams per liter
SO_4	Sulfate, dissolved, in milligrams per liter
Cl	Chloride, dissolved, in milligrams per liter
F	Fluoride, dissolved, in milligrams per liter
SiO_2	Silica, dissolved, in milligrams per liter
NO_3	Nitrate, dissolved, in milligrams per liter as NO_3
NO_2	Nitrite, dissolved, in milligrams per liter as NO_2
NH_3	Ammonia, dissolved as nitrogen, in milligrams per liter as NH_3
P	Phosphorus, dissolved, in milligrams per liter
Al	Aluminum, dissolved, in micrograms per liter

As	Arsenic, dissolved, in micrograms per liter
Ba	Barium, dissolved, in micrograms per liter
Be	Beryllium, dissolved, in micrograms per liter
B	Boron, dissolved, in micrograms per liter
Cd	Cadmium, dissolved, in micrograms per liter
Cr	Chromium, dissolved, in micrograms per liter
Co	Cobalt, dissolved, in micrograms per liter
Cu	Copper, dissolved, in micrograms per liter
Fe	Iron, dissolved, in micrograms per liter
Pb	Lead, dissolved, in micrograms per liter
Li	Lithium, dissolved, in micrograms per liter
Mn	Manganese, dissolved, in micrograms per liter
Mo	Molybdenum, dissolved, in micrograms per liter
Ni	Nickel, dissolved, in micrograms per liter
Se	Selenium, dissolved, in micrograms per liter
Ag	Silver, dissolved, in micrograms per liter
Sr	Strontium, dissolved, in micrograms per liter
V	Vanadium, dissolved, in micrograms per liter
U	Uranium, dissolved, in micrograms per liter
Zn	Zinc, dissolved, in micrograms per liter
pE	In standard units
--	No data available
<	Less than

Table 6. Water-quality data and saturation indices of selected mineral phases of interstitial-water samples from raffinate pit 3

Sample	Depth	Temp	SC	pH	DO	Ca	Mg	Na	K	HCO₃ (IT)
Surface water	--	25.5	12,000	8.51	10.4	490	370	1,300	87	30
15	1.0	a27.9	14,630	7.16	1.0	1,000	540	1,700	130	77
12	1.0	a28.7	17,540	7.22	.15	1,400	650	2,000	150	134
14	1.0	a27.4	23,000	7.22	.10	2,300	760	2,500	190	59
4	3.0	a30.5	32,300	7.19	.20	3,800	830	3,300	200	34
13	6.0	a26.9	39,400	7.67	.40	4,900	1,000	4,500	320	36
8	8.0	a26.8	39,000	7.22	.30	5,100	610	4,900	240	27
7	9.0	a26.8	38,700	7.44	.20	5,400	340	5,000	240	44
6	9.0	a29.0	42,200	6.97	.20	5,200	1,400	4,600	250	24
5	9.0	a30.5	43,900	6.84	.25	6,200	970	5,200	290	20

Sample	Depth	Alk (IT)	SO₄	Cl	F	SiO₂	NO₃	NO₂	NH₃	P	Al
Surface water	--	44	630	23	6.9	--	1,499	1	0.32	0.01	20
15	1.0	64	1,100	7.8	4.1	5.7	1,890	12	.02	.37	300
12	1.0	112	770	14	4.4	7.7	2,190	13	.02	.11	540
14	1.0	49	980	--	2.9	8.5	3,070	31	6.50	1.1	740
4	3.0	28	1,700	--	2.4	7.5	5,020	83	22	.04	240
13	6.0	30	2,800	--	4.3	10	6,080	120	33	.48	1,400
8	8.0	22	3,100	--	2.9	6.6	6,160	140	39	.83	220
7	9.0	36	3,300	--	2.3	5.8	6,050	150	37	.01	280
6	9.0	20	2,600	--	3.1	8.3	6,670	130	30	.50	200
5	9.0	16	910	30	1.4	8.4	8,020	180	46	1.1	560

Table 6. Water quality and saturation indices of selected mineral phases of interstitial-water samples from raffinate pit 3--Continued

Sample	Depth	As	Ba	Be	B	Cd	Cr	Co	Cu	Fe	Pb
Surface water	--	3	100	10	100	--	2	1	3	40	1
15	1.0	7	110	10	260	20	20	60	200	290	--
12	1.0	14	140	10	330	20	20	60	200	800	--
14	1.0	11	150	10	330	20	20	60	200	1,200	--
4	3.0	7	210	10	460	20	20	60	200	98	--
13	6.0	37	250	10	420	20	30	60	200	1,800	40
8	8.0	17	240	10	470	20	40	60	200	70	--
7	9.0	6	300	10	610	20	30	60	200	130	--
6	9.0	13	260	10	480	20	20	60	200	120	--
5	9.0	14	360	10	420	26	30	60	200	580	20

Sample	Depth	Li	Mn	Mo	Ni	Se	Ag	Sr	V	U	Zn
Surface water	--	3,600	10	4,700	1	1	20	2,100	520	320	10
15	1.0	4,400	160	6,000	--	410	20	3,200	410	240	86
12	1.0	5,700	190	6,800	--	550	20	4,100	590	610	60
14	1.0	6,600	320	6,800	--	710	20	6,000	420	530	99
4	3.0	2,600	2,400	3,100	--	1,700	21	11,000	340	53	80
13	6.0	3,400	2,600	4,700	40	1,800	20	14,000	1,000	320	94
8	8.0	610	4,100	2,300	--	1,600	27	13,000	300	70	69
7	9.0	800	2,000	2,900	--	4,200	20	13,000	230	120	96
6	9.0	1,900	11,000	3,400	40	2,800	20	16,000	200	72	90
5	9.0	1,000	8,300	2,600	40	2,300	24	17,000	170	41	60

Table 6. Water quality and saturation indices of selected mineral phases of interstitial-water samples from raffinate pit 3--Continued

Sample	Depth	Temp	pH	pE[b]	Saturation Indices				
					Calcite[c]	Aragonite[c]	Gypsum[c]	Fluorapatite[b,c]	Hydroxyapatite[b,c]
Surface water	--	--	--	--	--	--	--	--	--
15	1.0	[a]27.9	7.16	1.4	0.61	0.47	-0.37	--	2.55
12	1.0	[a]28.7	7.22	1.4	.60	.45	-.38	--	2.48
14	1.0	[a]27.4	7.22	.8	.49	.35	-.17	--	6.80
4	3.0	[a]30.5	7.19	2.5	.24	.10	.15	--	2.52
13	6.0	[a]26.9	7.67	-.2	.65	.51	.40	--	7.74
8	8.0	[a]26.8	7.22	2.7	.15	.01	.48	--	6.85
7	9.0	[a]26.8	7.44	2.1	.66	.52	.54	4.63	2.18
6	9.0	[a]29.0	6.97	3.2	-.12	-.26	.34	--	5.00
5	9.0	[a]30.5	6.84	2.8	-.32	-.46	-.04	--	6.03

Sample	Depth	Saturation Indices							Predominate U species[b]
		Fluorite[c]	Ferrihydrite[c]	Carnotite[c]	Schoepite[c]	Rutherfordine[c]	Uraninite[c]	Uraninite (amorphous)[b,c]	
Surface water	--	--	--	--	--	--	--	--	--
15	1.0	0.60	0.00	2.40	-2.66	-1.33	-0.93	-6.63	$UO_2(CO_3)_3^{4-}$
12	1.0	.58	.00	2.29	-2.65	-1.30	-1.03	-6.77	$UO_2(CO_3)_3^{4-}$
14	1.0	.36	.00	.69	-3.50	-2.71	-.85	-6.51	$UO_2(HPO_4)_2^{2-}$
4	3.0	.26	.00	2.25	-2.38	-1.73	-2.90	-8.70	$UO_2(CO_3)_3^{4-}$
13	6.0	.84	.00	4.02	-2.25	-2.16	1.80	-3.86	$UO_2(HPO_4)_2^{2-}$
8	8.0	.63	.00	-1.10	-4.40	-3.84	-5.18	-10.84	$UO_2(HPO_4)_2^{2-}$
7	9.0	.55	.00	2.14	-2.59	-1.96	-1.88	-7.53	$UO_2(CO_3)_3^{4-}$
6	9.0	.41	.00	-1.10	-4.10	-3.39	-5.47	-11.23	$UO_2(HPO_4)_2^{2-}$
5	9.0	-.14	.00	-3.41	-5.18	-4.55	-5.64	-11.44	$UO_2(HPO_4)_2^{2-}$

[a] Value may be biased high because of time interval between sample collection and temperature measurement.

[b] pE values, saturation indices, and speciation calculated by assuming all dissolved iron is ferrous (Fe^{2+}) and in equilibrium with ferrihydrite [$Fe(OH)_3$] at the measured temperature and pH.

[c] Calculated using the geochemical code PHREEQE (Parkhurst and others, 1980).

orders of magnitude from the surface to 9 ft deep (fig. 20). Concentrations of most other constituents also increased with increasing depth below the water-sediment interface. However, concentrations of U reached a maximum of 610 µg/L at 1 ft below the interface and tended to decrease with depth (fig. 20).

The concentrations of N species in the interstitial water in relation to depth below the water-sediment interface are shown in figure 20. The predominate N species detected was nitrate (NO_3). Converting the concentrations to molar ratios indicated that more than 97 percent of the N was present in the oxidized form (NO_3). The ratio of NO_3 to NO_2 plus NH_3, as N, decreased from a maximum of 168 at 1 ft below the water-sediment interface to a minimum of 32.4 at 9 ft below the interface. This indicates that although large quantities of NO_2 and NH_3 were measured in many of the interstitial-water samples, only small quantities of the available NO_3 are being, or have been, reduced within the sludge. A lack of substantial microbial colonization of the dialysis membranes may indicate that the reduction of NO_3 could be an abiotic process affected by slow reaction kinetics. Large concentrations of NO_2 and NH_3, or trace elements, such as Cr, copper (Cu), Mo, and Se, may inhibit biologic activity within the sludge.

Equilibrium-speciation calculations using PHREEQE indicated that all interstitial-water samples were at saturation or were slightly supersaturated with respect to calcite, aragonite, and gypsum. This indicates plausible mineralogic controls on the concentrations of Ca, alkalinity, and SO_4, (table 6). The SI values for an apatite phase (hydroxyapatite) ranged from 2.18 to 7.74 in the interstitial-water samples, indicating supersaturation with respect to this phase. Most interstitial-water samples, except for the sample from 8 ft and two samples from 9 ft deep, were at saturation or were supersaturated with respect to carnotite. The pE values were calculated by assuming the dissolved Fe was Fe^{2+} and in equilibrium with ferrihydrite [$Fe(OH)_3$] at the measured temperature and pH. Using the calculated pE values, all but one of the samples were undersaturated with respect to UO_2. Because of the potential for warming of samples during transport to shore, calculations were made on several samples at temperatures as much as 10 °C (degrees Celsius) lower than those measured onsite. The SI values for calcite, aragonite, gypsum, fluorite, schoepite, and UO_2 varied by less than 0.3. Values for hydroxyapatite and carnotite generally increased by

about 1.0 and 2.5, indicating SI values listed for these phases could be biased low.

Determination of a unique pE in a system with multiple redox couples often is not possible (Lindburgh and Runnells, 1984); however, limits on possible pE values for the system can be established by considering the individual redox couples involved. Stumm and Morgan (1981) indicate that microbial denitrification of NO_3 to NO_2 occurs at a pE of about 7 and that at less than a pE of about 6, ammonium (NH_4^+) becomes the stable species. The distribution of N species in the interstitial-water samples indicated an equilibrium pE value of about 7 or larger. Concentrations of Fe in the interstitial-water samples ranged from 70 to 1,800 µg/L and indicated no relation to depth (table 6). At pH values less than 6, large concentrations of dissolved Fe indicated reduction of Fe to the more soluble Fe^{2+} species, which occurs at lower equilibrium pE values than those indicated by N speciation. Equilibrium speciation calculations on data from the interstitial-water samples indicate that reduction of ferric iron (Fe^{3+}) to Fe^{2+} requires pE values less than about 3.2. However, concentrations of Fe^{2+} determined onsite using the phenanthroline method were less than the detection limit, indicating that the Fe in the interstitial-water samples may be Fe^{3+} or Fe(III) complexes. Large concentrations of Fe^{3+} in a NO_3-rich solution possibly can be stabilized by ligands, such as nitrous oxide (Cotton and Wilkinson, 1972). Other ligands, such as F, also could complex and stabilize Fe^{3+} against reduction (Stumm and Morgan, 1981). Another possibility is that the large Fe concentrations are caused by the presence of Fe(III) oxide colloids, such as $Fe(OH)_3$, or Fe-Mn oxide colloids, which are smaller than the pore size (0.22 µm) of the membranes used in the interstitial-water samplers. The large concentrations of Mn (table 6) in the interstitial water may indicate reduction of Mn(IV) to the more soluble Mn(II) species. This reduction occurs at about the same pE value as NO_3 reduction (Stumm and Morgan, 1981). If the dissolved Fe in solution is Fe^{3+}, Fe(III) complexes, or Fe(III) colloids, the distribution of N and Mn species indicates a pE value of about 6 to 7. An alternative is that the phenanthroline method was unreliable and Fe in solution is actually Fe^{2+}, indicating a possible disequilibrium between the redox species. The pE values in this system would be non-unique and could range from larger than those for NO_3 reduction (about 6 to 7) to Fe reduction (about 3.2) or possibly lower.
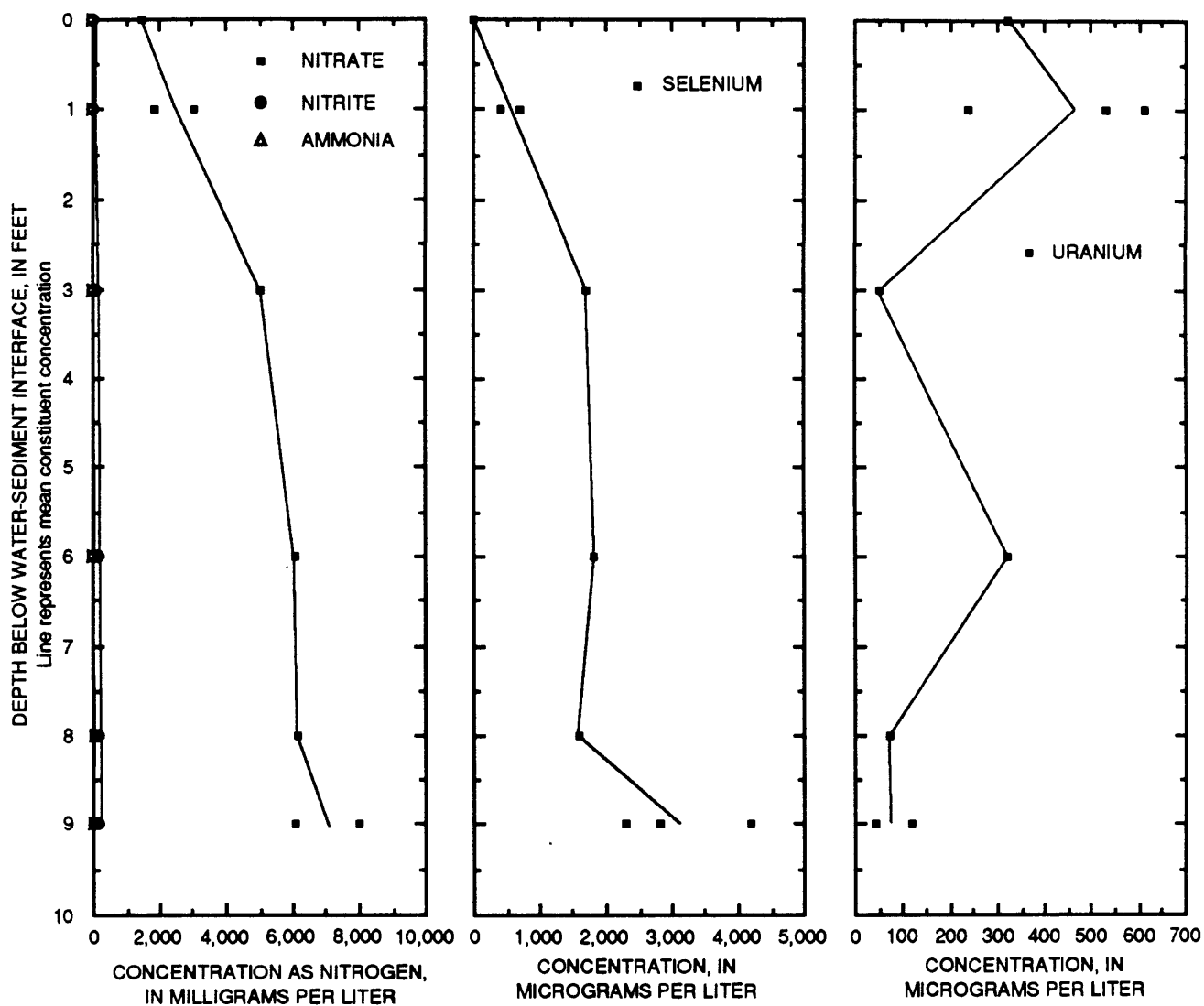
Figure 20. Concentrations of nitrogen species, selenium, and uranium in interstitial-water samples at various depths from raffinate pit 3.

Because the speciation and solubility of U is dependent on pE, a range of pE values for the interstitial water were calculated using the geochemical code PHREEQE. Three scenarios were evaluated: (1) assume reduction of U(VI) occurs and the pE required to achieve equilibrium with crystalline and amorphous UO_2 is determined; (2) a pE is calculated for the system and U is speciated, assuming dissolved Fe is Fe^{2+} and in equilibrium with $Fe(OH)_3$; and (3) a pE is calculated for the system based on the distribution of N species and U is speciated accordingly.

A summary of the results of equilibrium speciation calculations for the three scenarios is given in table 7. These calculations were made for a sample 9 ft below the sediment-water interface (sample 7, table 6) during the August 1990 sampling. Calculated pE values ranged from 0.80, assuming equilibrium between dissolved U and crystalline UO_2, to 12, assuming equilibrium between NO_3 and NO_2. Attempts to achieve equilibrium between amorphous UO_2 and the measured dissolved U concentrations were unsuccessful because this would require pE values less than the stability of water. The calculations indicate the predominance of aqueous uranyl carbonate complexes and the persistent supersaturation with respect to carnotite and tyuyamunite and undersaturation with respect to amorphous UO_2. Langmuir (1978) indicated that under anoxic conditions, equilibrium with UO_2 would limit concentrations of U in solution to less than 1 $\mu g/L$; however, the solubility of UO_2 at intermediate pE values greatly is enhanced by the formation of highly stable aqueous uranyl carbonate and phosphate complexes.

Calculations based on the three scenarios indicate that determination of a unique pE for the interstitial-water system is difficult. These data could equally be explained by an oxidizing environment at a high pE with dissolved Fe(III) stabilized by complex ligand formation or present as Fe(III) colloids, as well as a low pE environment in which limited NO_3 reduction occurs because of a lack of microbial activity. However, in all scenarios the calculations indicate reduction of U(VI) to U(IV) and precipitation of U(IV) minerals, such as UO_2, is unlikely because of the formation of stable aqueous uranyl carbonate and phosphate complexes.

Mineralogy and Chemistry of Sludge In Raffinate Pit 3

Raffinate pit 3 contains about 13 ft of sludge. The sludge generally is a reddish-orange, fine-grained silt that contains between 70 and 75 percent water (MK-Ferguson Company and Jacobs Engineering Group, 1989c). Several sludge samples were collected during the removal of the interstitial-water samplers to characterize the chemical and mineralogic composition of the sludge and to verify the results of equilibrium-speciation calculations.

Mineralogic analyses (using X-ray diffraction) of a composite sample from the upper 4.5 ft of the sludge identified large quantities of a Ca phosphate phase (predominantly apatite) and small quantities of quartz, hornblende, amorphous and poorly crystalline Fe oxides, and trace quantities of graphite (Schumacher, 1990). The apatite lattice was distorted and probably contained substantial quantities of F and CO_3 (S.J. Sutley, U.S. Geological Survey, written commun., 1990). Chemical analyses substantiate the X-ray diffraction data because the molar ratio of Ca to P (phosphorus) in the sludge was about 5 to 3, as would be expected in apatite. The quantities of Ca and P in the sludge, however, were smaller than expected, if the predominant mineral was apatite. The sludge should contain about 40 percent by weight Ca and 20 percent by weight P, if predominately apatite. The smaller than expected quantities of Ca and P were because of the presence of substantial quantities of amorphous material (possibly up to several tens of percent) within the sludge that were "invisible" to the X-ray. Thorium was detected at 1,290 mg/kg (milligrams per kilogram). No U specific minerals were identified using X-ray diffraction; however, detailed SEM (scanning electron microscope) analyses using energy dispersive X-ray (EDS) of a shallow sludge sample identified small scattered grains of carnotite (fig. 21). Carnotite is a common secondary ore mineral of U that forms in oxidizing environments (Langmuir and Chatham, 1980). Because equilibrium-speciation calculations indicated supersaturation with respect to carnotite in the interstitial water, the carnotite may be authigenic. The U content (table 8) in this sludge sample was 1,700 mg/kg with most of the U associated with the apatite phase.

Large differences in the mineralogic content concentration of the sludge with depth were detected. Three deep composite samples collected from raffinate

Table 7. Variation of ionic species for selected mineral phases with pE in an interstitial-water sample from raffinate pit 3

[Calculations were made using data from sample number 7, table 6; --, not applicable]

Element or mineral phase	Chemical formula	pE determined by assuming equilibrium between dissolved uranium and uraninite	pE determined by assuming equilibrium between dissolved iron and ferrihydrite	pE determined by assuming equilibrium between concentrations of dissolved nitrate and nitrite
pE, millivolts	--	0.80	1.75	12
Predominate species				
Sulfur	S	SO_4^{2-}	SO_4^{2-}	SO_4^{2-}
Nitrogen	N	NH_3	NH_3	NO_3^-
Iron	Fe	Fe^{2+}	Fe^{2+}	$Fe(OH)_3^0$
Uranium	U	$UO_2(CO_3)_3^{4-}$	$UO_2(CO_3)_3^{4-}$	$UO_2(CO_3)_3^{4-}$
Saturation indices				
Calcite	$CaCO_3$	0.66	0.66	0.61
Aragonite	$CaCO_3$	.52	.52	.47
Gypsum	$CaSO_4 \cdot 2H_2O$	.54	.54	.51
Fluorite	CaF_2	.54	.55	.51
Fluorapatite	$Ca_5(PO_4)_3F$	4.63	4.63	4.63
Hydroxyapatite	$Ca_5(PO_4)_3(OH)$	2.18	2.18	2.02
Ferrihydrite	$Fe(OH)_3$	- .95	.00	1.85
Carnotite	$K_2(UO_2)_2(VO_4)_2 \cdot 3H_2O$	2.14	2.14	1.30
Tyuyamunite	$Ca(UO_2)_2(VO_4)_2 \cdot 5-8H_2O$	2.37	2.37	1.55
Rutherfordine	UO_2CO_3	-1.96	-1.96	-2.41
Schoepite	UO_3	-2.59	-2.59	-3.03
Uraninite	UO_2	.03	-1.88	-22.8
Uraninite (amorphous)	UO_2	-5.65	-7.53	-28.4

Carnotite

0   1 MICROMETER

Figure 21. Scanning electron microscope photomicrograph showing scattered grains of carnotite on apatite in a shallow sludge sample from raffinate pit 3.

pit 3 (0 to 9 ft) contained large quantities of gypsum (40 to 75 percent), and MgF_2 (which was used in the production of U metal, 10 to 40 percent), and lesser quantities of apatite (5 to 15 percent), quartz (5 to 10 percent), and Fe oxides (primarily goethite, about 5 percent). The deep samples (0 to 9 ft) contained larger quantities (up to a few percent by weight) of Fe oxides (probably goethite) than the shallow sample (0 to 4 ft). The identification of goethite in the deeper sludge samples indicates an increase in the degree of crystallinity of the Fe oxides in the deeper samples. Concentrations of Ca and P were smaller in the deep samples as expected because of the smaller apatite concentrations (table 8). Concentrations of most trace elements, including U and Th, were larger in the deep sludge samples than in the shallow sludge sample (table 8). The U concentrations were uniform and

ranged from 3,300 to 3,680 mg/kg, and Th concentrations ranged from 4,740 to 8,010 mg/kg in the deep samples. Small quantities of rare earth elements also were detected in the deep samples.

Slurry mounts of deeper sludge samples were analyzed by fission-track radiography to examine the distribution of U within the solid phase. In this technique, a small quantity of sludge is placed between a glass slide and a thin sheet of muscovite. This assembly then is irradiated in a reactor to induce fission of the ^{235}U. As the atomic fragments from this fission move through the muscovite, they destroy part of the crystal lattice, producing the tracks observed in the center of figure 22 (bottom photograph). The density of the tracks is proportional to the U concentration. This analysis indicates most of the U was uniformly distributed within the sludge with a few tiny grains of

49

Table 8. Mineralogic and chemical analyses of sludge samples from raffinate pit 3

[SEM, scanning electron microscope; mg/kg, milligrams per kilogram; --, no data; <, less than]

Mineralogic analysis[a]		
Shallow (0-4.5 feet)		**Deep (0-9 feet composite samples, 1990)**
X-ray diffraction—Predominately apatite (semiquantitative) with minor quartz, hornblende, amorphous iron oxides, and trace flakes of graphite		Gypsum 40-75 percent; sellaite (MgF₂, 10-40 percent); apatite 5-15 percent; quartz 5-10 percent; goethite and other iron oxides (about 5 percent)
SEM—————————Scattered grains of carnotite		Carnotite, undetermined U-rich phase

Chemical Analysis					
		Shallow	**Deep (0-9 feet composite samples, 1990)**		
Element	**Unit**	**(0-4.5 feet, 1989)**	**Sample 1**	**Sample 2**	**Sample 3**
Calcium	weight percent	20	16	16	17
Phosphorus	weight percent	10	3.2	3.8	4.0
Iron	weight percent	8.9	5.2	5.5	5.8
Magnesium	weight percent	3.5	4.3	2.5	2.6
Aluminum	weight percent	1.5	2.7	2.5	2.6
Sodium	weight percent	.90	1.8	1.7	1.8
Potassium	weight percent	.11	.19	.19	.19
Titanium	weight percent	.05	.14	.14	.15
Arsenic	mg/kg	360	1,490	1,260	1,330
Barium	mg/kg	230	130	207	221
Beryllium	mg/kg	--	8.7	8.1	8.3
Cadmium	mg/kg	2.5	3.8	3.2	3.5
Cesium	mg/kg	4.3	--	--	--
Chromium	mg/kg	104	181	217	219
Cobalt	mg/kg	11	37	61	63
Copper	mg/kg	850	1,430	1,310	1,380
Lead	mg/kg	205	889	1,770	1,840
Lithium	mg/kg	177	133	95.1	100
Manganese	mg/kg	520	4,060	3,190	3,350
Molybdenum	mg/kg	388	1,410	1,250	1,310
Nickel	mg/kg	120	758	175	185
Scandium	mg/kg	17	72	78	81
Silver	mg/kg	1	--	--	--
Strontium	mg/kg	127	278	302	318
Thorium	mg/kg	1,290	4,740	7,750	8,010
Tin	mg/kg	166	37	5	<1
Uranium	mg/kg	1,700	3,680	3,300	3,470
Vanadium	mg/kg	1,300	7,740	6,970	7,330
Yttrium	mg/kg	22	350	551	569
Zinc	mg/kg	127	410	392	409
Zirconium	mg/kg	530	--	--	--
Neodymium	mg/kg	--	94	122	126
Cerium	mg/kg	--	174	217	222
Europium	mg/kg	--	6.2	7.4	7.6
Gallium	mg/kg	--	53	82	86
Holmium	mg/kg	--	18	29	30.9
Lanthanum	mg/kg	--	77	99	103
Ytterbium	mg/kg	--	54	76	79

[a] Mineral percentages, if reported, are expressed as percentage of the crystalline matter, and all samples contained an appreciable quantity (possibly up to a few tens of percent) amorphous material.
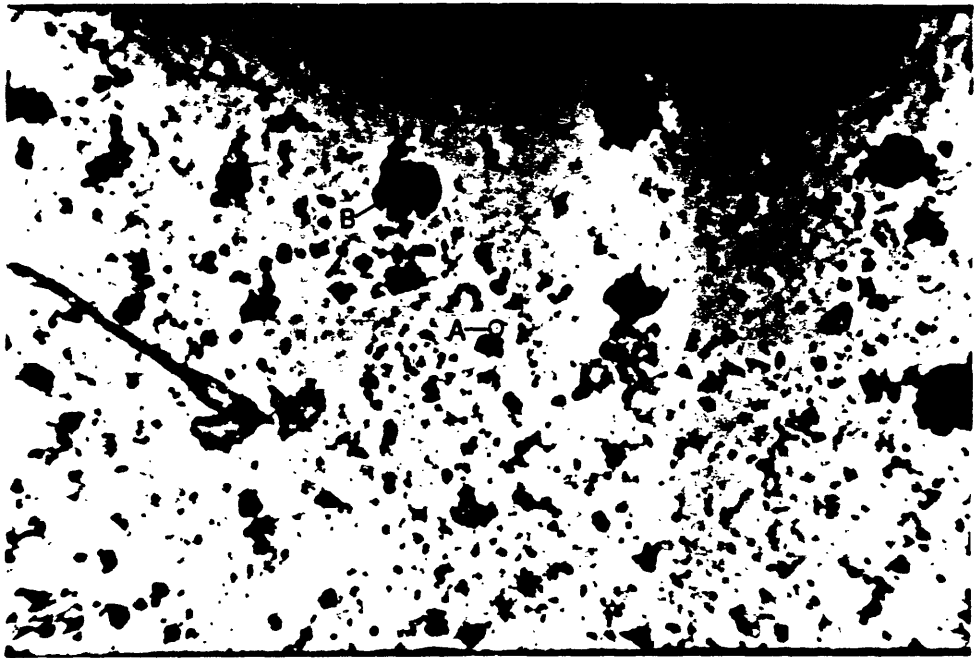
Photograph of sludge grains from raffinate pit 3.
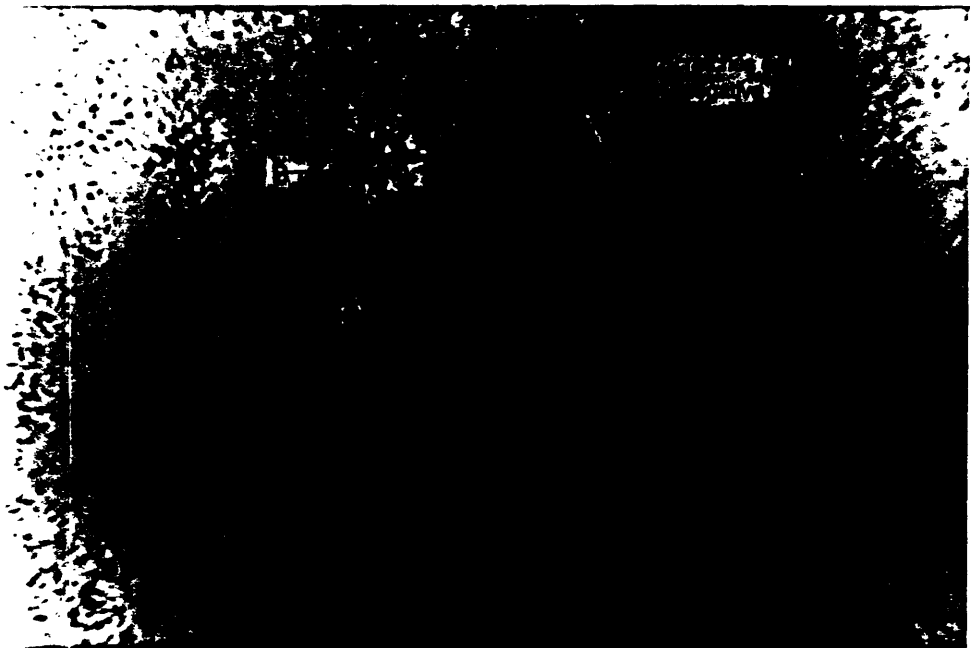
Image of fission tracks in muscovite produced by irradiation induced fission of ^{235}U in the sample. Note the large track density produced from the small opaque grain (labeled A). This grain is a uranium mineral containing approximately 76 percent by weight uranium. The larger grain (labeled B) contains a much smaller uranium concentration.

0   100 MICROMETERS

Figure 22. Fission-track photograph of a oeep sludge sample from raffinate pit 3.

larger U concentration. Analysis of the grain labeled A in figure 22 by SEM and EDS (fig. 23) indicated that this grain contained about 75 percent by weight U with small quantities of Fe, Ni, and SiO_2. The theoretical U concentration in UO_2 is about 88 percent by weight U and it is uncertain whether this grain is UO_2 that contains impurities or another U-rich phase. Other grains of high-track density were identified by the SEM as carnotite, which collaborated the equilibrium-speciation calculations, and a Th-rich phase (fig. 24), probably thorianite (R.A. Zielinski, U.S. Geological Survey, written commun., 1991).

Mineralogic analyses generally confirm the results of equilibrium-speciation calculations as no reduced U(IV) minerals were positively identified. Substantial quantities of U were detected in the Ca phosphate phase. Because U commonly is associated with phosphate minerals (Cathcart, 1978), much of the U within the sludge probably is bound in the apatite phase. Cathcart (1978) indicated U(VI) can be absorbed on the apatite crystal structure and is readily removed during weathering; however, additional leaching studies on the sludge to determine the potential for mobilization of U during remedial activities would be more reliable. Uranium within the mineral lattice probably would not be readily leached because of the small solubility of apatite.

Analyses of interstitial water and sludge in raffinate pit 3 indicate that concentrations of U in solution are stabilized by the formation of aqueous U(VI) carbonate and to a lesser extent phosphate complexes (Schumacher and Stollenwerk, 1991). Concentrations of U in the interstitial water probably are controlled by the formation of aqueous uranyl carbonate and uranyl phosphate complexes, the availability of U in the solid phase, and a combination of sorption reactions involving Fe oxides, incorporation into apatite, and precipitation of carnotite. Redox process involving the precipitation of U(IV) minerals, such as UO_2, are unlikely. Uranium will not be completely removed from solution within the raffinate pit sludges and is expected to migrate along with other constituents into the overburden where sorption reactions may affect its distribution (Schumacher and Stollenwerk, 1991).

MIGRATION OF CONTAMINANTS WITHIN THE OVERBURDEN

Transport of contaminants from the raffinate pits is controlled by a number of hydrologic and geochemical factors, including flow path, flow rate, dilution, dispersion, sorption, biologic activity, precipitation/dissolution reactions, oxidation/reduction reactions, and exchange reactions. In this section, results of laboratory sorption experiments between a simulated raffinate pit leachate and the overburden are given, and onsite evidence for migration of raffinate pit constituents within the overburden is presented. The laboratory experiments were designed to evaluate the effect of pH value and equilibration time on the interaction between various raffinate constituents and the Ferrelview Formation and the clay till. These two units comprise the largest thickness of overburden beneath raffinate pits 3 and 4 and could be used in future remediation activities at the site (MK-Ferguson Company and Jacobs Engineering Group, 1990a). The second part of this discussion presents onsite evidence for contaminant migration within the overburden. In this section several conceptual models for contaminant migration from the raffinate pits are presented based on water-quality data collected from overburden lysimeters adjacent to the raffinate pits, results of laboratory experiments, and equilibrium and mass-balance calculations using the geochemical model PHREEQE (Parkhurst and others, 1980).

Laboratory Investigation of Constituent Attenuation

Investigations of interstitial water and sludge from raffinate pit 3 indicate that chemical reduction (and complete removal from solution) of U probably does not occur within the raffinate pit sludges. To investigate the possible sorption controls on the migration of U and other raffinate constituents within the overburden, a series of laboratory experiments were conducted. These experiments were designed to investigate the interaction between a simulated raffinate pit leachate and the Ferrelview Formation and the clay till. The laboratory experiments were designed to evaluate the sorption of contaminants from a simulated raffinate pit leachate by the Ferrelview Formation and the clay till at three fixed values of pH (4.5, 7.0, and 9.0) and under unadjusted pH conditions

0 2 MICROMETERS

Figure 23. Scanning electron microscope photomicrograph of a uranium-rich grain (labeled A in figure 22) from a deep sludge sample from raffinate pit 3.
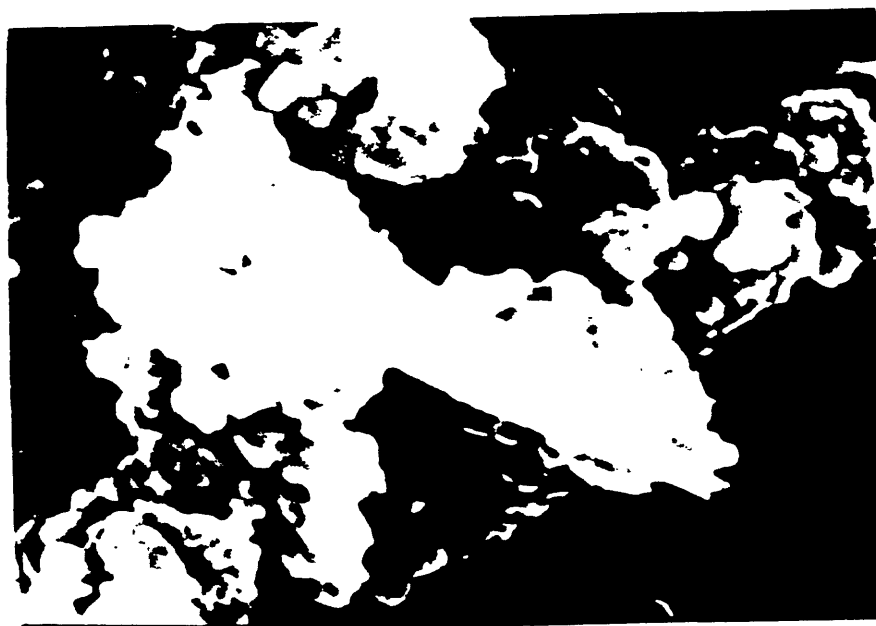
0 2 MICROMETERS

Figure 24. Scanning electron microscope photomicrograph of thorianite (ThO_2, elongated crystal) from a deep sludge sample from raffinate pit 3..

(Schumacher and Stollenwerk, 1991). The range of pH values was selected to bracket the natural variability expected to occur in the raffinate pit-overburden system. Equilibration times ranged from 24 to 480 hours. The simulated leachate was constructed using surface water from raffinate pit 3 that had been spiked with various concentrations of aluminum (Al), Cr, Pb, Ni, and U. The initial U concentrations in the solutions ranged from 3,100 to 3,400 μg/L and were similar to concentrations detected in raffinate pit 4. The pH value of each solution was maintained by the addition of dilute HCl or sodium hydroxide (NaOH). The experimental procedures and results are discussed in Schumacher (1990). At the conclusion of each experiment the solutions were centrifuged and filtered, and the filtrate was analyzed for the various constituents of interest. The difference between the initial and the final concentration was the quantity sorbed by the overburden material. In this report, the term "sorption" is used to describe the general removal of a solute from solution by a sorbent (solid phase). Unless specified, no mechanistic process is inferred.

Selected results from the laboratory sorption experiments are given in table 9. A complete listing of the experimental results is given in Schumacher (1990). During the experiments, small fluctuations in pH value were detected in solutions in contact with the Ferrelview Formation. The Ferrelview Formation buffered the pH of the solutions to between 4.5 and 7.0; however, this buffering capacity was small, which required the addition of 5.082×10^{-4} equivalents of acid per 22 g (grams) of sample. Assuming the consumption of hydrogen ions was because of the dissolution of calcite, 0.0508 g of calcite per 22 g of sample, or about 0.2 percent by weight of sample, was removed. This indicated much of the carbonate material in the Ferrelview Formation sample was dissolved in the low pH value experiments. In similar experiments using low ionic strength solutions (deionized water and rainwater), solutions in contact with the Ferrelview Formation were buffered to pH values near 8.0. The buffering action indicated other processes affected the pH in the Ferrelview Formation experiments, such as exchange reactions involving hydrogen on the edges of clay minerals. Large fluctuations in pH values were observed in the clay till experiments, especially at low pH values. The clay till buffered the pH of the solution to between 7.0 and 9.0. The magnitude of this capacity was large when compared to the capacity of the Ferrelview Formation

because of the larger initial calcite content. In these experiments a total of 1.056×10^{-2} equivalent of acid was added in the low pH experiments, which corresponds to dissolution of 1.057 g of calcite per 22 g, or about 4.8 percent by weight of the sample. Therefore, most of the carbonate material in the clay till sample was removed in the low pH experiments. The geochemical model PHREEQE (Parkhurst and others, 1980) was used to evaluate the changes in pH value and concentrations of Ca, Mg, Na, HCO_3, and Cl in the experiments. Results of these simulations indicate that the detected changes in pH value and major constituent concentrations in the experiments can be explained by the addition of dilute HCl or NaOH, dissolution of calcite and dolomite or precipitation of calcite, and exchange of Ca for Mg (Schumacher and Stollenwerk, 1991).

A common expression used to describe the quantity of a solute sorbed to a solid phase is the distribution coefficient (K_d). The K_d value is used to describe the degree of interaction of a solute with a solid phase and is used to simulate solute-solid interactions in many solute transport codes. The K_d generally is defined as:

$$K_d = \frac{C_s}{C_w}, \tag{5}$$

where C_s is the mass of solute sorbed per unit dry mass of solid phase and C_w is the concentration of the solute in solution at equilibrium. The K_d values in this study were calculated according to the following expression:

$$K_d = \frac{(C_i - C_f) \times 0.22L/22g}{C_f} \times (1,000mL/L). \tag{6}$$

The mass of solute sorbed is expressed as the difference between the initial solution concentration of the solute (C_i) and the final (equilibrium) solution concentration (C_f) of the solute. The quotient in the numerator expresses the quantities of solute sorbed in liters of solution per gram of solid. The units of K_d in this paper are milliliters per gram. The K_d value for reactive solutes ranges from near 0 to more than 1,000 (Freeze and Cherry, 1979). The K_d values larger than 0 indicate sorption of the solute by the solid and K_d values near 0 indicate little or no sorption of the solute by the solid. The calculated K_d values for sorption of

Table 9. Composition of initial solutions and filtrate from laboratory batch experiments

[mg/L, milligrams per liter; µg/L, micrograms per liter; pH, pH in standard units; Ca, calcium; Mg, magnesium; Na, sodium; Alk, alkalinity, total as CaCO3; SO4, sulfate; Cl, chloride; F, fluoride; NO3, nitrate as nitrogen; Cr, Chromium; Li, lithium; Pb, lead; Mo, molybdenum; Sr, strontium; V, vanadium; U, uranium; --, no data; <, less than]

| | pH | Concentration, in mg/L | | | | | | | | Concentration, in µg/L | | | | | | |
		Ca	Mg	Na	Alk	SO4	Cl	F	NO3	Cr	Li	Pb	Mo	Sr	V	U
Ferrelview Formation																
pH 4.5																
Initial solution	4.50	540	380	1,300	--	610	70	7.0	1,300	52	3,900	105	4,400	2,000	480	3,400
Filtrate	4.60	640	360	1,300	--	630	150	1.7	1,400	11	3,600	<2	0	2,400	<12	160
pH 7.0																
Initial solution	7.00	540	390	1,300	30	620	24	7.0	1,300	54	4,000	115	4,400	2,000	480	3,400
Filtrate	6.96	610	340	1,400	23	650	23	2.1	1,300	--	3,400	<5	2,600	2,400	<12	100
pH 9.0																
Initial solution	9.00	540	380	1,300	49	610	22	7.2	1,300	60	4,100	<10	4,200	2,100	480	3,400
Filtrate	8.93	570	280	1,600	53	630	67	6.4	1,300	--	2,900	--	4,000	1,900	<12	520
Unadjusted pH																
Filtrate[a]	6.28	620	350	1,300	10	--	--	--	--	40	3,500	--	1,700	2,400	--	17
Filtrate[b]	6.60	590	340	1,300	26	--	--	--	--	20	3,500	--	2,100	2,700	--	76
Filtrate[c]	6.87	610	350	1,300	32	--	--	--	--	30	3,500	--	2,200	3,000	--	167
Clay till																
pH 4.5																
Initial solution	4.50	530	370	1,400	--	660	47	7.0	1,400	60	3,900	96	4,000	2,300	440	3,100
Filtrate	5.00	1,400	440	1,300	--	570	1,900	2.8	1,500	<10	3,300	<1	0	2,200	<60	75
pH 7.0																
Initial solution	7.00	540	370	1,400	32	650	22	7.0	1,400	60	3,800	96	4,000	2,000	460	3,100
Filtrate	6.98	700	360	1,300	90	590	130	2.6	1,500	<10	3,300	<1	3,100	2,200	<60	1,500
pH 9.0																
Initial solution	9.00	530	370	1,400	55	650	22	7.0	1,400	50	3,900	100	4,000	2,000	520	3,100
Filtrate	8.60	590	320	1,400	25	600	25	4.7	1,500	<10	2,900	<1	4,400	2,100	<60	240
Unadjusted pH																
Filtrate[a]	7.42	660	350	1,300	34	640	48	3.7	--	70	3,600	<6	3,300	2,100	71	670
Filtrate[b]	7.43	640	350	1,300	44	640	22	3.8	--	50	3,600	<6	3,300	1,400	71	860
Filtrate[c]	7.58	630	340	1,300	43	640	22	3.9	--	70	3,600	<6	3,400	--	73	730

[a] Solution pH adjusted to 4.5 immediately before interaction with solid phase, unadjusted throughout experiment.
[b] Solution pH adjusted to 7.0 immediately before interaction with solid phase, unadjusted throughout experiment.
[c] Solution pH adjusted to 9.0 immediately before interaction with solid phase, unadjusted throughout experiment.

several raffinate pit constituents in fixed and unadjusted pH experiments are given in table 10. The K_d values for several constituents (Ca, Mg, Na, SO_4, NO_3, and Sr) in table 10 were less than 0 because relation 6 does not account for the mass of solute occurring naturally in the solid. A negative K_d value computed by relation 6 indicates that some of the solute of interest actually was leached from the solid phase. Slightly negative K_d values for constituents not usually detected in large quantities in the mineral phases, such as NO_3, are attributed to analytical error in the laboratory analysis.

Substantial quantities of Ca, Mg, Na, SO_4, NO_3, and Sr were not removed from solution in contact with either unit at any pH value evaluated (table 9). In most cases the equilibrium concentrations of Ca and Mg were larger than the initial concentrations and, as a result, the K_d values for these constituents were negative. Simulations made using PHREEQE indicated that the variations in the concentrations of Ca and Mg in the low and neutral pH solutions in contact with the Ferrelview Formation or the clay till were most likely caused by the dissolution of calcite and dolomite approximated by assuming a single reactive carbonate phase of $(Ca_{0.8} Mg_{0.2})CO_3$ and the exchange of Mg for Ca. Only Mg for Ca exchange was required to simulate the Ca and Mg concentrations in solutions in contact with the Ferrelview Formation at pH 7.0 and the clay till at pH 9.0. Precipitation of a small quantity of calcite (3.37×10^{-7} mole per liter) and exchange of Mg for Ca was required to simulate the Ca and Mg concentrations in the high pH solution in contact with the Ferrelview Formation. Concentrations of Sr generally increased in the sorption experiments because of the dissolution of carbonate minerals containing Sr. Because the increase in solution concentrations of these constituents and the resulting negative K_d values involved mineral dissolution, and not exchange or partitioning processes, the behavior of these constituents is best described through the use of equilibrium-speciation calculations. However, because most solute-transport codes cannot accept the equilibrium-speciation calculations, the negative K_d values were calculated. Concentrations of Na, SO_4, and NO_3 generally remained unchanged in the experiments, indicating these constituents probably will behave in a conservative manner.

Sorption of F, Cr, Pb, Li, and V were indicated in the experiments. Substantial sorption of F occurred in solutions in contact with either unit at pH less than

7.0. The sorption decreased with increasing pH value probably because of competition with hydroxyl ions for mineral surfaces. Hem (1985) has shown that substitution of F for hydroxyl ions at mineral surfaces is likely because of their similar charge and ionic radius. Small quantities of Li were sorbed (K_d values less than about 4.1 mL/g) from solutions in contact with either unit, and the sorption generally increased with increasing pH value. Lithium may substitute for Mg in some minerals (Heir and Billings, 1970); however, Li sorbs less strongly to ion-exchange minerals than do other common elements (Kelly, 1948). Hem (1985) indicates that once in solution, Li should tend to remain in the dissolved state, and substantial sorption and attenuation of Li within the overburden is unlikely (Schumacher and Stollenwerk, 1991). Because Cr analyses were made using different analytical methods (atomic adsorption and inductively coupled plasma), a direct comparison between the sorption of Cr by the Ferrelview Formation and the clay till cannot be made. The data indicate, however, that Cr probably is sorbed to a greater extent than Li. Lead and V were completely removed from solutions in contact with either unit at all pH values (Schumacher, 1990), indicating substantial attenuation of both of these constituents within the overburden is likely. Although Pb is not present in large concentrations in the raffinate pits, its sorption was investigated because of possible sources from soils contaminated by the production of military ordnance at the site before 1946. Because no Pb remained in any solutions at the end of the sorption experiment, the K_d values reported are minimum values.

The sorption experiments indicated that substantial sorption of both Mo and U occurs from solutions in contact with either overburden unit; however, the magnitude is dependent on the pH value of the solution. Under oxidizing conditions of these experiments, both Mo and U occurred in the hexavalent [Mo(VI), U(VI)] state. Sorption of Mo(VI) was inversely proportional to pH value and Mo(VI) was essentially completely removed from solutions in contact with either unit at pH less than about 5.0 (K_d values of 390 and 430 mL/g, table 10). Sorption of U(VI) is more complex than that of Mo(VI) because of the formation of weakly sorbed aqueous U(VI) di- and tri-carbonate complexes (Schumacher and Stollenwerk, 1991). This effect was most pronounced in the clay till experiments where dissolution of carbonate minerals resulted in larger concentrations of

Table 10. Calculated distribution coefficient (K_d) values for sorption of various constituents by the Ferrelview Formation and the clay till

[Ca, calcium; Mg, magnesium; Na, sodium; SO$_4$, sulfate; F, fluoride; NO$_3$, nitrate as nitrogen; Cr, chromium; Pb, lead; Li, lithium; Mo, molybdenum; Sr, strontium; V, vanadium; U, uranium; --, no data; >, greater than; all coefficients in milliliters per gram]

	Ca	Mg	Na	SO$_4$	F	NO$_3$	Cr	Pb	Li	Mo	Sr	V	U
							Ferrelview Formation						
pH 4.5													
Fixed	-1.6	0.6	-0.8	-0.3	31.0	-0.7	37.3	>515	0.8	430	-1.7	390	202
Unadjusted	-1.3	.9	-.8	--	--	--	3.0	--	1.1	15.9	-1.7	--	1,990
pH 7.0													
Fixed	-1.1	1.5	-.7	-.5	23.0	-1.9	--	>220	1.8	6.9	-1.7	390	330
Unadjusted	-.8	1.5	0	--	--	--	17.0	--	1.4	11	-2.6	--	437
pH 9.0													
Fixed	-.5	3.6	-1.9	-.3	1.3	--	--	--	4.1	.5	1.1	390	55
Unadjusted	-1.1	.9	0	--	--	--	10.0	--	1.7	9.1	-.3	--	194
							Clay till						
pH 4.5													
Fixed	-6.2	-1.6	.8	-1.6	15.0	-.7	50.0	>950	1.8	390	-2.1	63.3	403
Unadjusted	-2.0	.6	.8	.3	8.9	--	-1.4	>150	.8	2.1	1.0	52.0	36.3
pH 7.0													
Fixed	-2.3	.3	.8	1.0	16.9	-.7	50.0	>950	1.5	2.9	-.9	66.7	10.7
Unadjusted	-1.6	.6	.8	.2	8.4	--	2.0	>150	.6	2.1	4.3	55.0	26
pH 9.0													
Fixed	-1.0	1.6	0	.8	4.9	-.7	40.0	>990	3.4	0	-.5	76.7	119
Unadjusted	-1.6	.9	.8	.2	7.9	--	-2.9	>157	.8	1.8	--	61.2	32.5

57

carbonate in solution. In the fixed pH experiments with the Ferrelview Formation, the maximum sorption of U(VI) occurred at pH 7.0 (K_d value of 330 mL/g). Smaller quantities of U(VI) were removed at pH less than 5.0 (K_d value of 202 mL/g), and the minimum sorption occurred at pH 9.0 (K_d value of 55.0 mL/g). Sorption of U(VI) by the clay till in the fixed pH experiments was markedly different. The maximum sorption was at pH less than 5.0 (K_d value of 403 mL/g) and the minimum sorption was at pH 7.0 (K_d value of 10.7 mL/g). In the unadjusted pH experiments, larger quantities of U(VI) were sorbed by the Ferrelview Formation at near-neutral pH (K_d value of 437 mL/g) than by the clay till (K_d value of 26 mL/g). The K_d values for U(VI) sorption in this study, as compared to those reported by Langmuir (1978) and Hsi (1981), indicate that the sorption of U(VI) by the Ferrelview Formation and clay till is larger than expected for sorption by clay minerals, but smaller than the sorption indicated by the Kd values reported for several other pure substances, including Fe(III) oxides (fig. 25). This indicates that the small quantities of Fe and Mn oxides within the Ferrelview Formation and clay till most likely control the sorption of U(VI).

A particular deficiency in using K_d values to describe sorption of solutes is the dependence of the K_d values on solution parameters, such as pH values. The variation in the K_d values with pH values for the sorption of both Mo(VI) and U(VI) indicate the inability of the simple K_d model to accurately describe the sorption of these constituents. Schumacher and Stollenwerk (1991) concluded that the sorption of Mo(VI) and U(VI) could not be simulated by the simple K_d model, but could be simulated using a diffuse-layer surface-complexation approach. In their simulations, $Fe(OH)_3$ was assumed to control the sorption of both Mo(VI) and U(VI). The weight percent of $Fe(OH)_3$ in the Ferrelview Formation and the clay till in the simulations was estimated at 4.7 percent and 2.8 percent. The surface complexation reactions and equilibrium constants (K^{int}) from Dzombak and Morel (1990) were used to describe the sorption of Mo(VI) and U(VI) by Fe oxide were:

$$s\text{-}FeOH^\circ + H^+ = s\,FeOH_2^+ \qquad \log K^{int} = 7.27; \qquad (7)$$

$$s\text{-}FeOH^\circ = FeO^- + H^+ \qquad \log K^{int} = 8.93; \qquad (8)$$

$$s\text{-}FeOH^\circ + UO_2^{2+} + H^+ =$$
$$s\text{-}FeUO_2^{3+} + H_2O \qquad \log K^{int} = 15.65; \qquad (9)$$

$$s\text{-}FeOH^\circ + UO_2^{2+} + H_2O =$$
$$s\text{-}FeOUO_2OH + 2H^+ \qquad \log K^{int} = -5.7; \text{ and}(10)$$

$$s\text{-}FeOH^\circ + MoO_4^{2-} + H^+ =$$
$$s\text{-}FeMoO_4^- + H_2O \qquad \log K^{int} = 8.57. \qquad (11)$$
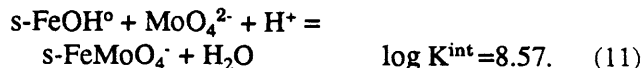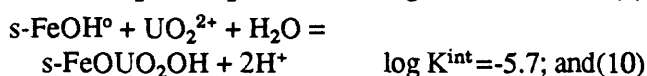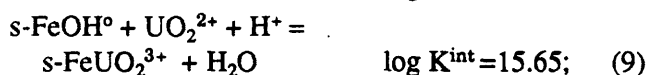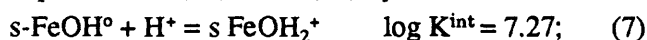
Based on the experimental data and results of the diffuse-layer surface-complexation model, Schumacher and Stollenwerk (1991) concluded that the sorption of Mo(VI) was controlled only by solution pH, but sorption of U(VI) was controlled by solution pH values and carbonate concentration. Diffuse-layer model simulations indicated that in the absence of carbonate, essentially all of the U(VI) should have been sorbed at pH values greater than 5.5. Uranium remaining in solution above pH 5.5 was due to complexation with carbonate, which formed aqueous $UO_2(CO_3)_2^{2-}$ and $UO_2(CO_3)_3^{4-}$. The importance of carbonate in increasing U(VI) mobility is evident in a comparison of the experimental results at pH 7.0. About 97 percent of the U(VI) was sorbed by the Ferrelview Formation (HCO_3 plus CO_3 equals 23 mg/L as $CaCO_3$), whereas only 52 percent was sorbed by the clay till (HCO_3 plus CO_3 equals 90 mg/L as $CaCO_3$). Schumacher and Stollenwerk (1991) also indicated that the presence of Fe and Mn oxyhydroxides within the overburden at the site is important in the sorption and attenuation of U, and that ion-exchange with clay minerals probably is of minimal importance. The experimental data and simulations indicate that the Ferrelview Formation is more effective in sorbing U(VI) than the clay till and that Mo(VI) and U(VI) should be completely removed from solutions within the overburden provided carbonate concentrations are small. However, U(VI) could be relatively mobile within the overburden or within the underlying bedrock if solution pH values are near neutral and alkalinity values (such as those within raffinate pit 4 and the shallow aquifer) are large.

Geochemistry and Distribution of Constituents Within the Overburden

Water samples from lysimeters near the raffinate pits reflect the interaction between leachate migrating from the raffinate pits and the overburden. Some of these interactions were evaluated by the laboratory sorption experiments; however, the most accurate data on contaminant interaction within the overburden can be obtained from the analysis of water samples collected from overburden lysimeters installed adjacent to raffinate pits 1, 3, and 4.
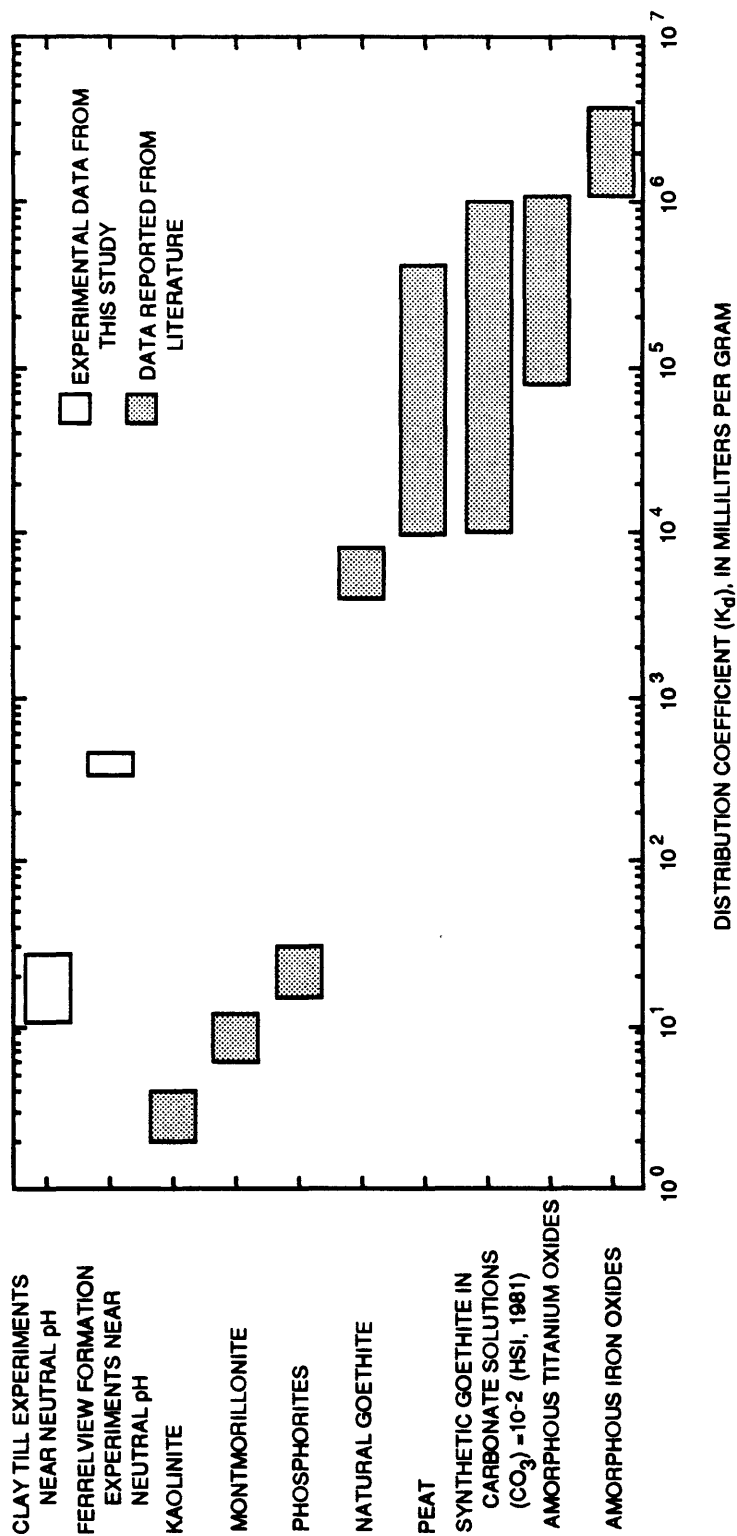
Figure 25. Uranium distribution coefficient (K_d) values determined in this study and K_d values from Langmuir (1978) and Hsi (1981).

Lysimeters LY 3601, LY 3602, and LY 3603 are located at various depths in a single borehole at the base of the west levee of raffinate pit 4 (fig. 26). This is a low, wet area containing cattails and a small seep thought to be related to a pore-pressure relief drain at the base of the levee (MK-Ferguson Company and Jacobs Engineering Group, 1989e). The lysimeters in this location were installed with a 3- to 4-ft thick sand pack at the following depths below land surface; LY 3601 (8 to 11 ft), LY 3602 (16.5 to 20.8 ft), and LY 3603 (23 to 26 ft). A comparison of driller's logs to general descriptions of the overburden (MK-Ferguson Company and Jacobs Engineering Group, 1990a) indicate that LY 3601 probably is completed within the Ferrelview Formation, LY 3602 within the lower clay till, and LY 3603 within a cherty-clay material possibly indicating the residuum. This location is within a bedrock trough (fig. 10) and water levels in a nearby monitoring well (B-2, fig. 14) have been approximately 23 ft below land surface (Bechtel National, Inc., 1984), indicating lysimeter LY 3603 probably is within saturated residuum.

Samples from the lysimeters adjacent to raffinate pit 4 contained increased concentrations of various constituents detected in the raffinate pits. The largest values of specific conductance (3,050 and 3,130 μS/cm), and the largest concentrations of Ca (280 and 290 mg/L), Mg (75 to 78 mg/L), Na (250 mg/L), Cl (18 to 21 mg/L), $NO_2 + NO_3$ (330 mg/L as N), and Sr (620 to 650 μg/L), and the smallest concentrations of HCO_3 (295 mg/L) were detected in samples from the deepest lysimeter, LY 3603 (table 11). Samples from the shallowest lysimeter (LY 3601) generally contained the largest concentrations of SO_4 (250 and 290 mg/L), F (0.4 and 0.7 mg/L), Fe (7 and 810 μg/L), Li (47 and 110 μg/L), Mn (620 and 660 μg/L), V (less than 6 and 14 μg/L), and U (21 and 46 μg/L). Samples from the intermediate depth lysimeter (LY 3602) generally contained the smallest constituent concentrations, except for HCO_3 and Ba, where the concentrations were the largest.

Because concentrations of Ca, Mg, Na, NO_2 + NO_3, and Sr in samples from lysimeter LY 3603 were larger than those detected in the nearby raffinate pit 4 or the shallower lysimeters, it is unlikely that raffinate pit 4 or downward percolation of these constituents from contaminated soils is the source. Molar ratios of $NO_2 + NO_3$ (as N)/Li (2,975 to 3,805) and $NO_2 + NO_3$ (as N)/SO_4 (19.7 to 20.7) in samples from this lysimeter compare favorably with those ratios in interstitial-

water samples from the bottom of raffinate pit 3 of 1,774 to 4,065 and 12.9 to 61.8. This indicates the migration of constituents from raffinate pit 3 westward beneath raffinate pit 4. The conceptual model for contamination in this lysimeter (fig. 27) is the downward percolation of water from raffinate pit 3 through preferential pathways, such as fractures, in the underlying unsaturated Ferrelview Formation and clay till into the highly permeable residuum where mixing with uncontaminated ground water and lateral migration occurs. The horizontal transport of contaminants from raffinate pit 3 beneath raffinate pit 4 may be through perched saturated zones within the overburden or migration along the top of the water table near the residuum-weathered limestone contact.

Schumacher and Stollenwerk (1991) indicated that it is possible to generate a water chemistry similar to that of samples collected from LY 3603 in March 1990 by the mixing of water from raffinate pits 3 and 4 with an uncontaminated ground-water component (table 12). Solid-phase controls on the migration of raffinate constituents in the simulation were Mg for Ca exchange, as indicated by laboratory experiments, and equilibrium with calcite. Sorption of Mo and U were not required to simulate the measured concentrations, mainly because of the large quantity of dilution indicated. The pE in the simulation (12.6) was calculated by assuming NO_3 was not reduced, because little reduced N species were detected in the sample from this lysimeter. However, additional simulations using a pE value of about 3.6, calculated by assuming equilibrium between dissolved Fe and $Fe(OH)_3$, indicated no substantial reduction of U, which implies UO_2 equilibrium probably is not a control on U concentrations. The component from raffinate pit 3 was approximated by the water-quality data from interstitial-water sample 5 (9 ft below the water-sediment interface) and the component from raffinate pit 4 was approximated by water-quality data collected from the surface (Schumacher, 1990). The uncontaminated component was approximated by water-quality data from a shallow uncontaminated bedrock monitoring well (MWGS-03). Results of the simulation (table 12) indicate that the water in lysimeter LY 3603 can be generated by mixing small quantities of water from raffinate pits 3 and 4 with an uncontaminated ground-water component and precipitating of a small quantity of calcite, according to the equation on page 70:
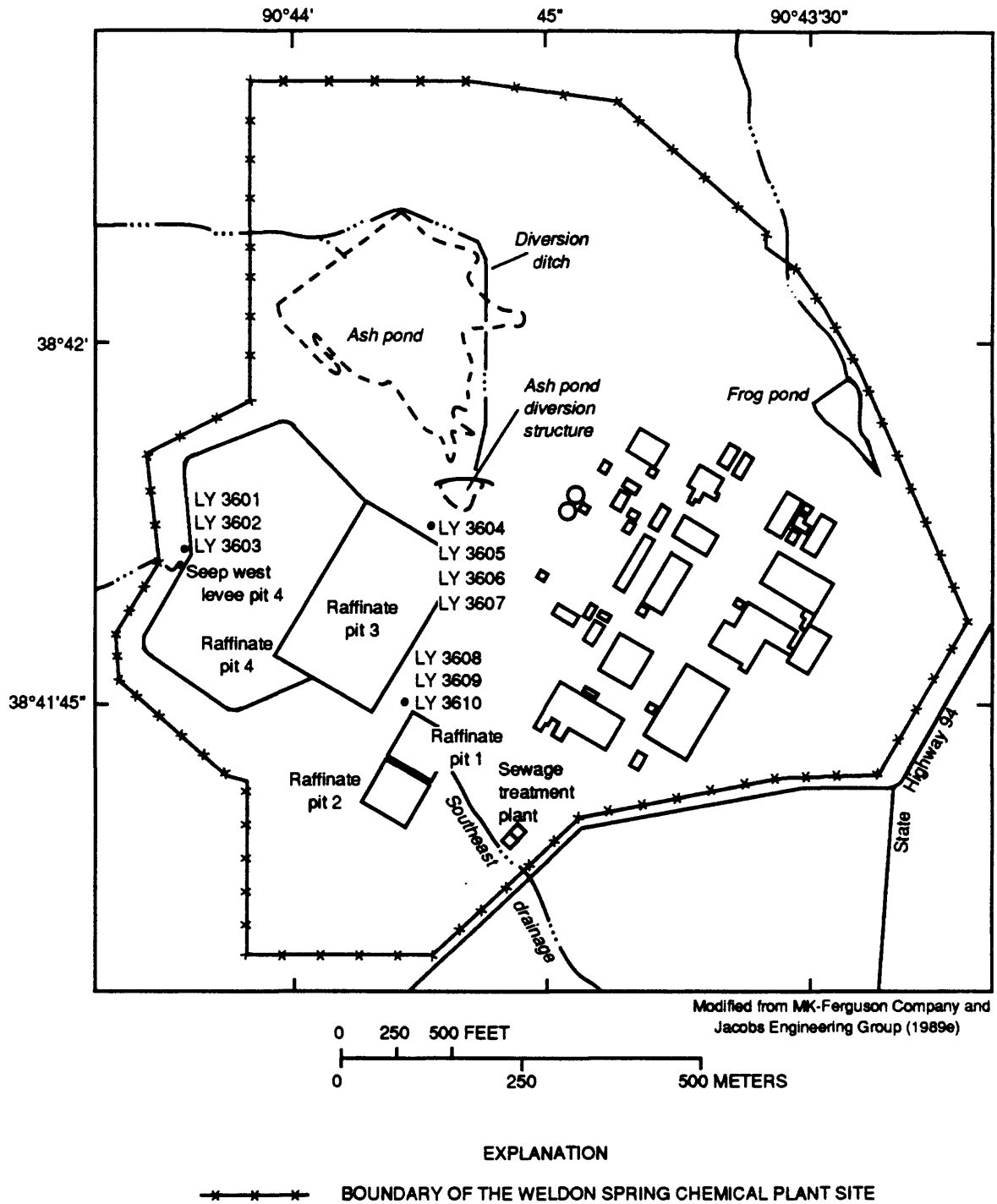
Figure 26. Location of lysimeters and seep in the vicinity of the raffinate pits.

ABBREVIATIONS AND SYMBOLS USED IN TABLE 11

Symbol	Definition
Q	Discharge, instantaneous, in cubic feet per second
SC	Specific conductance, in microsiemens per centimeter at 25 degrees Celsius
pH	In standard units
Temp	Temperature, in degrees Celsius
DO	Dissolved oxygen, in milligrams per liter
Ca	Calcium, dissolved, in milligrams per liter
Mg	Magnesium, dissolved, in milligrams per liter
Na	Sodium, dissolved, in milligrams per liter
K	Potassium, dissolved, in milligrams per liter
HCO_3 (IT)	Bicarbonate, incremental titration, in milligrams per liter
Alk (IT)	Alkalinity, incremental titration, total as $CaCO_3$, in milligrams per liter
SO_4	Sulfate, dissolved, in milligrams per liter
Cl	Chloride, dissolved, in milligrams per liter
F	Fluoride, dissolved, in milligrams per liter
SiO_2	Silica, dissolved, in milligrams per liter
NO_2+NO_3	Nitrite plus nitrate, dissolved as nitrogen, in milligrams per liter
NO_2	Nitrite, dissolved as nitrogen, in milligrams per liter
NH_3	Ammonia, dissolved as nitrogen, in milligrams per liter
P	Phosphorus, dissolved, in milligrams per liter
Al	Aluminum, dissolved, in micrograms per liter
As	Arsenic, dissolved, in micrograms per liter
Ba	Barium, dissolved, in micrograms per liter
Be	Beryllium, dissolved, in micrograms per liter
B	Boron, dissolved, in micrograms per liter
Cd	Cadmium, dissolved, in micrograms per liter
Cr	Chromium, dissolved, in micrograms per liter
Co	Cobalt, dissolved, in micrograms per liter
Cu	Copper, dissolved, in micrograms per liter
Fe	Iron, dissolved, in micrograms per liter
Fe^{2+}	Iron, ferrous, dissolved, in micrograms per liter
Pb	Lead, dissolved, in micrograms per liter
Li	Lithium, dissolved, in micrograms per liter
Mn	Manganese, dissolved, in micrograms per liter
Mo	Molybdenum, dissolved, in micrograms per liter
Ni	Nickel, dissolved, in micrograms per liter
Se	Selenium, dissolved, in micrograms per liter
Ag	Silver, dissolved, in micrograms per liter
Sr	Strontium, dissolved, in micrograms per liter
V	Vanadium, dissolved, in micrograms per liter
Zn	Zinc, dissolved, in micrograms per liter
Ra-226	Radium-226, dissolved, planchet count, in picocuries per liter
U	Uranium, dissolved, in micrograms per liter
TOC	Total organic carbon, in milligrams per liter
DOC	Dissolved organic carbon, in milligrams per liter
pE	In millivolts
--	No data available
>	Greater than
<	Less than

Table 11. Water-quality data and saturation indices for selected mineral phases in samples from lysimeters, seep from the west levee of raffinate pit 4, and raffinate pit 4

Sample location (fig. 26)	Sample Interval (feet)	Date	Time	Q	SC	pH	Temp	DO	Ca	Mg	Na	K	HCO$_3$(IT)	Alk(IT)
LY 3601	8-11	8-03-89	1140	--	--	7.0	23.0	--	91	19	170	2.3	--	--
		3-09-90	0940	--	1,400	6.9	13.5	0.1	90	21	210	2.0	523	429
LY 3602	16.5-20.8	8-03-89	1145	--	--	7.1	21.0	--	--	--	--	--	--	--
		3-09-90	0933	--	1,140	7.2	15.0	.1	84	24	150	1.0	581	476
LY 3603	23-26	8-03-89	1155	--	--	6.9	22.0	--	290	76	250	1.1	--	--
		3-09-90	0950	--	3,130	6.9	13.5	.1	280	75	250	1.1	295	242
		8-10-90	1045	--	3,050	6.4	--	>1.0	280	78	250	1.1	295	242
LY 3604	4-8	7-17-90	1215	--	953	6.4	22.0	>1.0	89	27	55	6.3	597	489
LY 3605	9.9-13.9	7-17-90	1210	--	1,020	6.7	24.0	.7	43	17	180	.9	698	572
LY 3606	14-18	7-17-90	1205	--	817	6.2	20.0	>1.0	35	9.9	130	.4	286	234
LY 3607	20-25	7-17-90	1200	--	1,330	6.6	22.5	>1.0	100	24	170	1.6	456	374
LY 3608	2.5-6.5	3-09-90	0850	--	12,700	5.6	15.0	.1	--	--	--	--	40	33
Seep west levee pit 4	--	4-11-89	1030	0.07	785	7.2	7.0	--	110	39	12	1.0	190	154
		6-08-89	0815	--	713	7.6	20.5	6.6	97	36	9.1	.6	150	124
Raffinate pit 4	--	3-14-89	--	--	1,120	8.9	--	--	11	37	190	13	400	432

Table 11. Water-quality data and saturation indices for selected mineral phases in samples from lysimeters, seep from the west levee of raffinate pit 4, and raffinate pit 4--Continued

Sample location (fig. 26)	Sample interval (feet)	Date	Time	SO$_4$	Cl	F	SiO$_2$	NO$_2$+NO$_3$	NO$_2$	NH$_3$	P	Al	As	Ba
LY 3601	8-11	8-03-89	1140	250	--	0.7	73	--	--	--	--	<170	5	140
		3-09-90	0940	290	14	.4	15	<0.10	0.01	0.12	<0.01	--	--	97
LY 3602	16.5-20.8	8-03-89	1145	--	--	--	--	--	--	--	--	--	--	--
		3-09-90	0933	80	14	.3	13	.32	.03	.02	<.01	--	--	230
LY 3603	23-26	8-03-89	1155	160	19	.3	78	--	--	--	--	<100	1	150
		3-09-90	0950	110	18	.2	17	330	1.4	.17	.03	--	--	150
		8-10-90	1045	130	21	.4	79	330	.41	.06	.02	--	1	150
LY 3604	4-8	7-17-90	1215	59	7.9	.3	51	14	.02	.06	<.01	--	<1	520
LY 3605	9.9-13.9	7-17-90	1210	31	16	.2	49	16	<.01	.02	<.01	--	<1	270
LY 3606	14-18	7-17-90	1205	150	25	<.1	56	31	<.01	.02	.02	--	<1	57
LY 3607	20-25	7-17-90	1200	180	19	<.1	58	6.8	.03	.02	.02	--	1	45
LY 3608	2.5-6.5	3-09-90	0850	--	--	--	--	--	--	--	--	--	--	--
Seep west levee pit 4	--	4-11-89	1030	270	1.9	.5	4.4	.48	<.01	--	--	20	<1	34
		6-08-89	0815	250	3.1	.5	6.7	1.2	<.01	.02	<.01	<10	<1	21
Raffinate pit 4	--	3-14-89	--	110	6.5	6.0	1.4	7.4	<.01	<.01	.02	10	6	150

Table 11. Water-quality data and saturation indices for selected mineral phases in samples from lysimeters, seep from the west levee of raffinate pit 4, and raffinate pit 4--Continued

Sample location (fig. 26)	Sample interval (feet)	Date	Time	Be	B	Cd	Cr	Co	Cu	Fe	Fe²⁺	Pb	Li	Mn
LY 3601	8-11	8-03-89	1140	<8	70	2.0	3	4	5	810	880	1	110	660
		3-09-90	0940	<.5	--	2.0	<5	6	<10	7	200	<10	47	620
LY 3602	16.5-20.8	8-03-89	1145	--	--	--	--	--	--	--	<10	--	--	--
		3-09-90	0933	<.5	--	<1.0	<5	3	<10	3	<10	<10	21	230
LY 3603	23-26	8-03-89	1155	<5	30	1.0	4	5	2	80	20	4	52	600
		3-09-90	0950	<.5	--	<1.0	<5	5	<10	4	<10	<10	43	540
		8-10-90	1045	<2	20	5.0	<20	<9	<30	25	--	<30	55	520
LY 3604	4-8	7-17-90	1215	<.5	40	2.0	<5	40	<10	1,400	--	<10	9	8,000
LY 3605	9.9-13.9	7-17-90	1210	<.5	30	<1.0	<5	90	<10	2,600	--	<10	9	14,000
LY 3606	14-18	7-17-90	1205	<.5	20	1.0	<5	<3	<10	940	--	<10	16	430
LY 3607	20-25	7-17-90	1200	<.5	20	2.0	<5	<3	<10	29	<0	<10	13	12
LY 3608	2.5-6.5	3-09-90	0850	--	--	--	--	--	--	--	--	--	--	--
Seep west levee pit 4	--	4-11-89	1030	<.5	40	1.0	<1	<3	<1	110	--	<5	8	590
		6-08-89	0815	<.5	30	<1.0	<1	<3	1	4	0	<1	8	4
Raffinate pit 4	--	3-14-89	--	<1	40	<1	<1	<3	2	3	--	<5	520	1

65

Table 11. Water-quality data and saturation indices for selected mineral phases in samples from lysimeters, seep from the west levee of raffinate pit 4, and raffinate pit 4--Continued

Sample location (fig. 26)	Sample Interval (feet)	Date	Time	Mo	Ni	Se	Ag	Sr	V	Zn	Ra-226	U	TOC	DOC
LY 3601	8-11	8-03-89	1140	<170	47	<33	--	560	14	--	--	46	--	--
		3-09-90	0940	70	40	--	2.0	490	<6	56	--	21	--	--
LY 3602	16.5-20.8	8-03-89	1145	--	--	--	--	--	--	--	--	--	--	--
		3-09-90	0933	30	10	--	2.0	280	8	29	--	17	--	--
LY 3603	23-26	8-03-89	1155	<100	33	<3	--	630	6	--	--	21	--	--
		3-09-90	0950	20	20	--	<1.0	620	<6	39	--	13	--	--
		8-10-90	1045	<30	<30	--	<3.0	650	<18	49	--	--	--	--
LY 3604	4-8	7-17-90	1215	<10	30	<1	2.0	440	<6	36	--	9.3	--	--
LY 3605	9.9-13.9	7-17-90	1210	<10	50	1	3.0	340	<6	13	--	3.1	--	--
LY 3606	14-18	7-17-90	1205	<10	30	6	<1.0	160	6	34	--	1.2	--	--
LY 3607	20-25	7-17-90	1200	<10	<10	5	<1.0	260	<6	42	--	2.9	--	--
LY 3608	2.5-6.5	3-09-90	0850	--	--	--	--	--	--	--	--	--	--	--
Seep west levee pit 4	--	4-11-89	1030	50	20	11	<1.0	250	<6	53	<0.4	--	1.7	--
		6-08-89	0815	80	22	<1	<1.0	190	<6	12	--	13	2.6	1.8
Raffinate pit 4	--	3-14-89	--	740	<1	7	2.0	140	70	<3	4.9	2,800	--	11.0

Table 11. Water-quality data and saturation indices for selected-mineral phases in samples from lysimeters, seep from the west levee of raffinate pit 4, and raffinate pit 4--Continued

Sample location (fig. 26)	Sample Interval (feet)	Date	Time	pE[a]	Saturation Indices					
					Calcite	Gypsum	Siderite	Carnotite	Uraninite	Tyuyamunite
LY 3601	8-11	8-03-89	1140	--	--	--	--	--	--	--
		3-09-90	0940	4.8	-0.18	-1.19	-2.18	-6.30	-8.35	-4.25
LY 3602	16.5-20.8	8-03-89	1145	--	--	--	--	--	--	--
		3-09-90	0933	4.3	.11	-1.70	-2.29	-7.11	-8.07	-4.36
LY 3603	23-26	8-03-89	1155	3.5	.15	-1.11	-1.22	-7.73	-5.86	-4.21
		3-09-90	0950	--	.03	--	-2.70	-6.48	-8.72	-3.39
		8-10-90	1045	--	--	--	--	--	--	--
LY 3604	4-8	7-17-90	1215	3.8	-.46	-1.82	-.16	-7.70	-6.24	-6.19
LY 3605	9.9-13.9	7-17-90	1210	2.6	-.37	-2.39	.48	-11.2	-5.26	-8.18
LY 3606	14-18	7-17-90	1205	4.5	-1.40	-1.75	-.79	-4.17	-4.45	-.76
LY 3607	20-25	7-17-90	1200	4.9	-.36	-1.34	-1.80	-3.58	-6.16	-.82
LY 3608	2.5-6.5	3-09-90	0850	--	--	--	--	--	--	3.50
Seep west levee pit 4	--	4-11-89	1030	2.8	-.32	-1.07	-1.12	--	--	--
		6-08-89	0815	2.7	.17	-1.18	-2.11	-7.33	-5.13	-3.82
Raffinate pit 4	--	3-14-89	--	--	.72	-2.44	-12.4	-1.86	-25.5	-2.47

[a] pE value was calculated by assuming dissolved iron was Fe^{2+} and in equilibrium with $Fe(OH)_3$ at the measured pH and temperature.
[b] Alkalinity was not determined in this sample. The alkalinity value used was the average alkalinity value of other samples from this lysimeter.

Arrows indicate generalized direction of contaminant migration
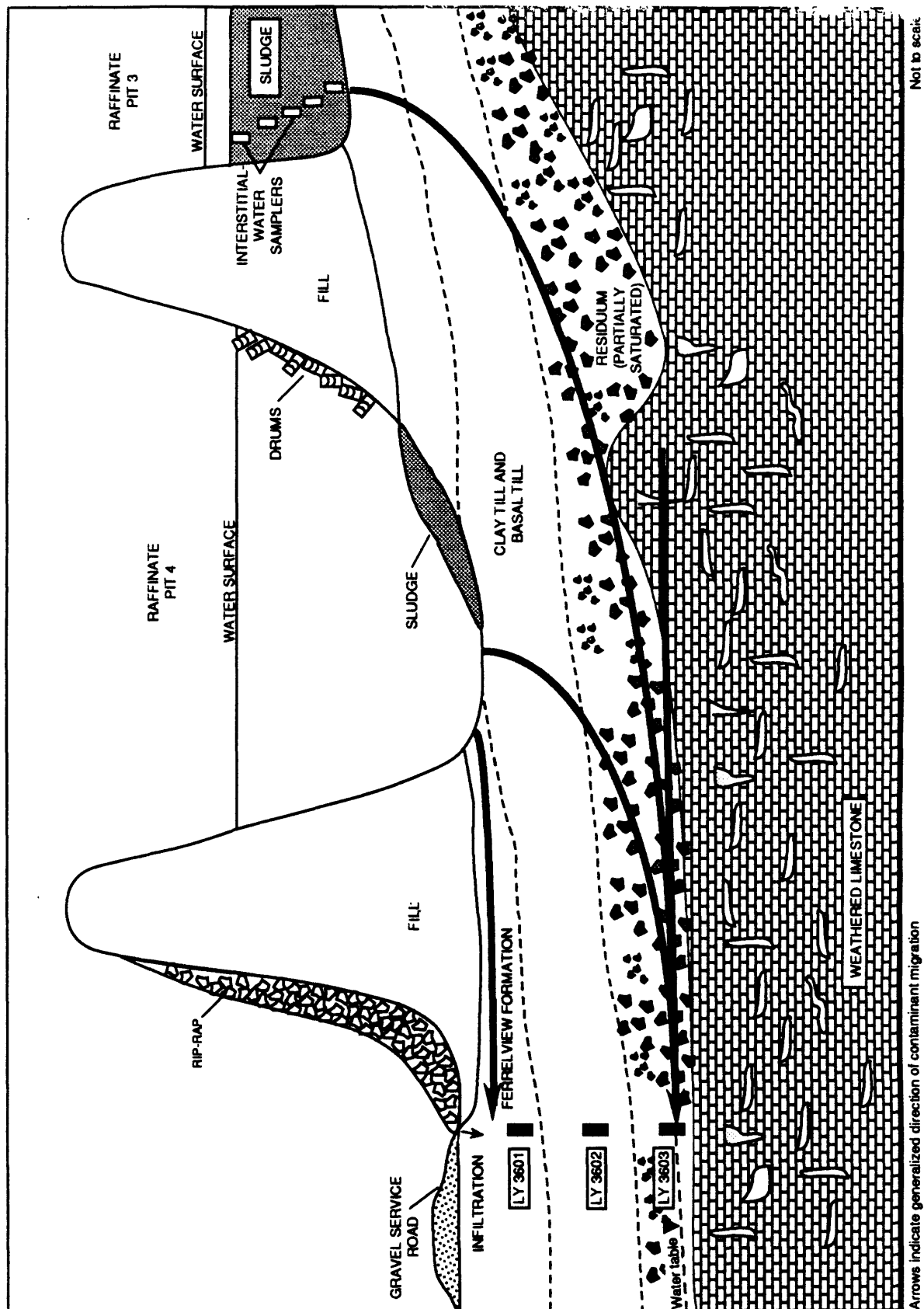
Figure 27. Conceptual model for contaminant migration from the raffinate pits to lysimeters west of raffinate pit 4.

Table 12. Measured and simulated water quality in lysimeters west of raffinate pit 4 and values used to approximate background ground-water quality in the simulations

[--, no data; mg/L, milligrams per liter; µg/L, micrograms per liter; <, less than; SI, saturation index; mmol, millimole; Ca, calcium; Mg, magnesium; U, uranium]

Physical property or constituent	Uncontaminated component[a]	[b]LY 3601		[c]LY 3603		
		Measured (3-09-90)	Simulated	Measured (3-09-90)	Simulation A[d]	Simulation B[e]
pH, standard units	7.5	6.9-7.0	7.4	6.9	7.02	7.02
pE, standard units	12	--	1.4	--	12.6	3.62
Calcium, mg/L	59	90-91	75	280	296	295
Magnesium, mg/L	41	19-21	20	75	80	80
Sodium, mg/L	8	170-210	45	250	226	226
Potassium, mg/L	1.2	1.0-2.3	4	1.1	13	13
Sulfate, mg/L	23	80-290	40	110	60	60
Chloride, mg/L	1.9	14	3	18	3	3
Bicarbonate, mg/L	360	523	382	295	338	338
Fluoride, mg/L	1.0	.4-.7	2.0	--	--	--
Nitrate, mg/L	1.8	.4	<1	330	337	[f]<1
Lithium, µg/L	6	47-110	109	52	47	47
Strontium, µg/L	220	490-560	204	630	962	962
Vanadium, µg/L	<6	<6-14	8	<6	<6	<6
Uranium, µg/L	1	21-46	17	21	17	17
Calcite SI	--	-.18	.07	.03	.18	.18
Carnotite SI	--	-6.30	-5.23	-6.48	-3.46	-3.43
Uraninite SI	--	-8.35	-2.28	-8.47	-24.7	-5.88

[a] Average constituent concentrations from monitoring well MWGS-03, data from Kleeschulte and Cross (1990).

[b] LY 3601 simulation--20 percent raffinate pit 4 water + 80 percent uncontaminated ground water + 0.14 mmol organic carbon + 0.82 mmol Ca -> Mg exchange + 0.002 mmol U sorption = water in LY 3601 + 0.304 mmol calcite.

[c] LY 3603 simulation--3.98 percent interstitial water, raffinate pit 3 + 0.52 percent raffinate pit 4 water + 95.5 percent uncontaminated ground water = water in LY 3603 + 0.518 mmol calcite. Sorption of U was not considered.

[d] pE calculated by assuming equilibrium between dissolved nitrate and nitrite.

[e] pE calculated by assuming dissolved iron is ferrous (Fe II) and in equilibrium with ferrihydrite.

[f] Nearly all nitrate reduced.

3.98 percent interstitial water, raffinate pit 3 + 0.52 percent raffinate pit 4 water + 95.5 percent uncontaminated ground water = water in LY 3603 + 0.518 mmol (millimole) of calcite. (12)

Small quantities of water from raffinate pit 4 were required to generate the U concentrations detected in lysimeter LY 3603. No Mg for Ca exchange was indicated, but large quantities of dilution of the raffinate components were indicated. Sorption of U was not required in the simulation because the large quantity of dilution used. Also, the lack of U sorption in the model could indicate minimal contact with the Ferrelview Formation, preferred flow paths, or saturation of the available sorption sites. Because no sorption of U was used in the simulation, the raffinate pit 4 component may be biased low. The excess Sr predicted could easily be removed by coprecipitation with calcite or aragonite. The Cl concentration was underestimated because the small Cl concentration (1.9 mg/L) in the uncontaminated component is smaller than the average background Cl concentration of 8.4 mg/L determined by Kleeschulte and Imes (in press). The detection of contaminants from raffinate pit 3 in lysimeter LY 3603 is somewhat unusual because the contaminants have migrated perpendicular to the direction of ground-water flow shown on figure 9. Water levels in bedrock monitoring wells, however, probably are not representative of localized perched or mounding conditions within the overburden near the raffinate pits that could move contaminants from the raffinate pit to the west.

Similar simulations were used to investigate the source of increased constituents in the shallower lysimeter LY 3601 and seep in the area near raffinate pit 4. The SO_4 and U concentrations in samples from lysimeter LY 3601 were larger than concentrations in samples from LY 3603; however, concentrations of most other constituents were smaller (table 11). The best simulation of the water in LY 3601 was obtained by mixing water from raffinate pit 4 with an uncontaminated ground-water component. Water from raffinate pit 4 may be migrating horizontally along the base of the dike (fig. 27). Because substantial quantities of reduced N species and Fe^{2+} were detected in samples from this lysimeter, the pE (1.4) was calculated by oxidizing organic matter until equilibrium with calcite, $Fe(OH)_3$, and dissolved Fe was achieved. Additional solid-phase constraints were Ca for Mg exchange and U sorption. No component from raffinate pit 3 was required; however, additional

sources of Na, SO_4, and Cl were indicated (table 12). Large concentrations of SO_4, NO_3, Cd, Ni, and antimony (Sb) have been detected in fill material from this area (MK-Ferguson Company and Jacobs Engineering Group, 1989b). The source for these increased concentrations is thought to be contaminated soils moved from the WSOW process areas (MK-Ferguson Company and Jacobs Engineering Group, 1989b) and used to construct part of the raffinate pit levee. Calcite equilibrium also was maintained and, because of the small Ca/Mg ratios (0.18) in water from raffinate pit 4, Mg for Ca exchange was added. Calcium for Mg exchange was detected in the laboratory sorption experiments at Ca/Mg ratios less than about 0.86. The simulation indicates that at a pE value of 1.4 and U concentration of 17 μg/L, UO_2 is undersaturated and U concentrations would have to approach 560 μg/L before equilibrium with UO_2 is achieved. Additional controls on U concentrations, such as sorption, are indicated because the measured U concentrations were much smaller (21 and 46 μg/L) than concentrations allowed by solution equilibrium with UO_2. The conceptual model for contamination in this lysimeter is the movement of contaminated water from raffinate pit 4 mixing with precipitation percolating through WSOW-contaminated soils.

The increased concentrations of Na and SO_4, but small concentrations of Ca, Mg, $NO_2 + NO_3$, Li, and Sr in samples from lysimeter LY 3602 probably indicate sources from WSOW-contaminated soils rather than raffinate pit 3. The slightly increased concentration of U (17 μg/L) indicates a small component of water from raffinate pit 4 in this lysimeter as compared to water from lysimeters LY 3601 and LY 3603; however, water quality in this lysimeter was not simulated.

The nature of the seep in the area along the toe of the raffinate pit 4 levee (fig. 26) has been uncertain. The concentration of U in this seep (13 μg/L) approximated the concentrations in samples from LY 3601 (21 and 46 μg/L); however, the concentrations of Na (9.1 and 12 mg/L) and Li (8 μg/L) were much smaller (table 11). It is unlikely that this seepage can be generated by a simple dilution of water from raffinate pit 4 as in the simulation of LY 3601. Movement of water from raffinate pit 4 to this seep may be following the contact between the base of the levee and underlying undisturbed soils and may not flow through the same materials that seepage to LY 3601 does. Laboratory experiments indicated Li behaved in a conservative manner; therefore, dilution

of this constituent would indicate a component of water from raffinate pit 4 about 3 to 10 times smaller than the component in water from LY 3601. Because concentrations of SO_4 in this seep were similar to those detected in water from lysimeter LY 3601, both probably are affected by WSOW-contaminated soils. The small molar ratio of Na/SO_4 in this seep (0.2) compared to LY 3601 (2.8 to 3.0) indicates the source of Na in this seep may not be related to the source of SO_4.

A second group of lysimeters is located near the northeast corner of raffinate pit 3 (fig. 26). Geologic descriptions from the installation of these lysimeters indicate a minimum of 7 ft of fill material in this area. Lysimeter LY 3604 is completed within the fill material and LY 3605 probably is completed within the loess. The location of the remaining two lysimeters (LY 3606 and LY 3607) near raffinate pit 3 is uncertain because detailed geologic descriptions are lacking; however, it seems the deepest lysimeter, LY 3607, probably is completed within the residuum. Interpretation of the water quality in these lysimeters is complicated by previous landfill activities in this area. Two overburden monitoring wells (B-22 and B-24; fig. 14) and overburden trench excavations (TR-11 and TR-12) immediately north of raffinate pits 3 and 4 reached water, in addition to disturbed material, including pipes, wood posts, drums and other debris of unknown origin, indicating that the area (Bechtel National Inc., 1984) was used as a landfill sometime after the construction of raffinate pits 3 and 4. Because of this, the water quality in these lysimeters probably represents a mixture of constituents from both the raffinate pits and the nearby landfilled area. Vegetation in this area is a deeper green and more lush than in other areas, presumably from root uptake of NO_3-rich water migrating from raffinate pit 3. One region of lush vegetation extended to a small area about 15 ft above the base of the north levee of raffinate pit 3.

Chemical analyses of samples from these lysimeters near raffinate pit 3 indicated generally increasing concentrations of Ca, Na, SO_4, Cl, Li, and smaller concentrations of Ba and U with depth (table 11). Concentrations of $NO_2 + NO_3$ ranged from 6.8 mg/L in the sample from LY 3607 to 31 mg/L in LY 3606 (table 11). The abundance of NO_3 in these lysimeters samples, relative to NO_2 and NH_3 and large concentrations of dissolved Fe in LY 3604 and LY 3605 may indicate disequilibrium between the redox species. Large concentrations of Fe in samples from

LY 3604 and LY 3605 (1,400 and 2,600 µg/L) and large values of alkalinity (489 and 572 mg/L) may indicate oxidation of organic matter and reduction of Fe in the nearby landfilled area. The concentrations of dissolved oxygen larger than 1.0 mg/L detected in samples from LY 3604, LY 3606, and LY 3607 probably are the result of contamination with atmospheric oxygen during sampling. Equilibrium-speciation calculations made assuming concentrations of dissolved Fe were in equilibrium with $Fe(OH)_3$ indicated pE values ranging from 2.6 in the sample from LY 3605 to 4.9 in the sample from LY 3607. Except for LY 3606, samples from all four of these lysimeters seem to be in equilibrium with calcite. Concentrations of Li and U in samples from these lysimeters were small compared to concentrations in the lysimeters west of raffinate pit 4. The small concentrations of Li indicate these lysimeters contained a small component of water from raffinate pit 3, probably less than a few percent. Mineralogic controls on U concentrations are not indicated because the solutions are undersaturated with UO_2 and other U minerals.

Attempts to collect samples from lysimeters located adjacent to raffinate pit 1 (fig. 26) were unsuccessful because the lysimeters were dry except for less than 40 mL (milliliters) removed from the shallowest lysimeter (LY 3608). This lysimeter samples an interval between 2.5 and 6.5 ft below the land surface. The specific conductance of this sample (12,700 µS/cm) was much larger than values measured in the other lysimeters, indicating a large component of raffinate water probably from raffinate pit 1.

During 1989 the USDOE completed construction of a diversion pond and ditch north of raffinate pit 3 to collect and divert runoff around the contaminated soils within Ash pond. This structure was constructed in a topographic low (characteristically marshy and filled with cattails) northeast of lysimeters LY 3604, LY 3605, LY 3606, and LY 3607 (fig. 26). Water-quality analyses from the diversion pond indicate increased concentrations of Na, SO_4, Cl, $NO_2 + NO_3$, and U (table 13) and slightly increased concentrations of Li. A possible source of the increased constituent concentrations is seepage from raffinate pit 3 because the concentrations of U in samples from the diversion pond (31 to 499 µg/L) were comparable to those in the surface water and interstitial water in raffinate pit 3 (41 to 610 µg/L; table 6). The concentrations of U in samples from the diversion

ABBREVIATIONS AND SYMBOLS USED IN TABLE 13

Q	Discharge, instantaneous, in cubic feet per second
SC	Specific conductance, in microsiemens per centimeter at 25 degrees Celsius
pH	In standard units
Temp	Temperature, in degrees Celsius
Ca	Calcium, dissolved, in milligrams per liter
Mg	Magnesium, dissolved, in milligrams per liter
Na	Sodium, dissolved, in milligrams per liter
K	Potassium, dissolved, in milligrams per liter
HCO_3 (IT)	Bicarbonate, incremental titration, in milligrams per liter
CO_3 (FET)	Carbonate, fixed endpoint titration, in milligrams per liter
CO_3 (IT)	Carbonate, incremental titration, in milligrams per liter
Alk (IT)	Alkalinity, incremental titration, total as $CaCO_3$, in milligrams per liter
SO_4	Sulfate, dissolved, in milligrams per liter
Cl	Chloride, dissolved, in milligrams per liter
F	Fluoride, dissolved, in milligrams per liter
Br	Bromide, dissolved, in milligrams per liter
SiO_2	Silica, dissolved, in milligrams per liter
DS	Dissolved solids, residue at 180 degrees Celsius, in milligrams per liter
NO_2+NO_3	Nitrite plus nitrate, dissolved as nitrogen, in milligrams per liter
NO_2	Nitrite, dissolved as nitrogen, in milligrams per liter
NH_3	Ammonia, dissolved as nitrogen, in milligrams per liter
P	Phosphorus, dissolved, in milligrams per liter
PO_4	Orthophosphate, dissolved as phosphorous, in milligrams per liter
Al	Aluminum, dissolved, in micrograms per liter
As	Arsenic, dissolved, in micrograms per liter
Ba	Barium, dissolved, in micrograms per liter
Be	Beryllium, dissolved, in micrograms per liter
B	Boron, dissolved, in micrograms per liter
Cd	Cadmium, dissolved, in micrograms per liter
Cr	Chromium, dissolved, in micrograms per liter
Co	Cobalt, dissolved, in micrograms per liter
Cu	Copper, dissolved, in micrograms per liter
Fe	Iron, dissolved, in micrograms per liter
Pb	Lead, dissolved, in micrograms per liter
Li	Lithium, dissolved, in micrograms per liter
Mn	Manganese, dissolved, in micrograms per liter
Mo	Molybdenum, dissolved, in micrograms per liter
Ni	Nickel, dissolved, in micrograms per liter
Se	Selenium, dissolved, in micrograms per liter
Ag	Silver, dissolved, in micrograms per liter
Sr	Strontium, dissolved, in micrograms per liter
V	Vanadium, dissolved, in micrograms per liter
Zn	Zinc, dissolved, in micrograms per liter
U	Uranium, dissolved, in micrograms per liter
TOC	Total organic carbon, in milligrams per liter
--	No data
<	Less than

Table 13. Water quality of samples from the Ash pond diversion structure

Date	Time	Q	SC	pH (onsite)	pH (laboratory)	Temp	Ca	Mg	Na	K	HCO₃ (IT)
10-05-89	0920	--	480	8.3	--	14.0	--	--	--	--	139
11-03-89	1150	--	494	8.7	8.3	8.5	43	19	32	4.2	150
1-10-90	1045	--	400	8.3	8.0	4.5	37	15	27	3.9	136
3-29-90	1030	0.0	380	8.8	7.6	9.0	43	12	20	3.9	115
2-14-91	1000	.07	755	8.0	7.8	3.0	75	18	50	3.4	175

Date	CO₃ (FET)	CO₃ (IT)	Alk (IT)	SO₄	Cl	F	Br	SiO₂	DS	NO₂+NO₃	NO₂	NH₃
10-05-89	--	11	131	--	--	--	--	--	--	--	--	--
11-03-89	9	--	--	86	21	0.50	0.040	8.2	294	<0.10	<0.01	<0.01
1 10-90	--	0	112	82	17	.30	<.010	7.8	264	<.10	<.01	.01
3-29-90	--	9	108	53	7.1	.10	--	7.6	264	7.5	.09	.02
2-14-91	--	0	144	68	7.9	<.10	.020	1.7	484	39	.17	.02

Date	P	PO₄	Al	As	Ba	Be	B	Cd	Cr	Co	Cu	Fe
10-05-89	--	--	--	--	--	--	--	--	--	--	--	--
11-03-89	<.01	--	10	<1	57	<5	60	<1.0	<1	<3	<1	9
1 10-90	<.01	--	10	<1	68	<5	50	<1.0	<1	<3	<10	8
3-29-90	.02	--	40	<1	46	<5	40	2.0	<5	<3	<10	47
2-14-91	<.01	<.01	<10	<1	130	<5	30	<1.0	2	<3	2	25

Date	Pb	Li	Mn	Mo	Ni	Se	Ag	Sr	V	Zn	U	TOC
10-05-89	--	--	--	--	--	--	--	--	--	--	74	--
11-03-89	<1	15	46	10	2	<1	<1.0	220	<6	18	31	--
1-10-90	<10	15	29	<10	<10	<1	<1.0	180	<6	3	79	--
3-29-90	20	5	4	<10	20	1	2.0	140	<6	6	480	--
2-14-91	<1	13	52	10	<1	2	<1.0	260	<6	39	499	5.9

pond, however, were larger than those concentrations in samples from lysimeters located between the diversion pond and raffinate pit 3 (table 11). The large U concentrations in the diversion ponds compared with those values within raffinate pit 3 and the lysimeters in this area may indicate additional sources of U because concentrations of other common raffinate constituents, such as Ca, Mg, NO_2 + NO_3, Li, and Sr, are small compared to U. Another source of increased U concentrations in samples from the diversion pond could be related to rainfall infiltration moving through U-contaminated materials within the landfilled area north of raffinate pit 3 or runoff from U-contaminated surficial soils in the vicinity. Molar ratios of SO_4/Li in the diversion pond (378 to 766) are larger than those within raffinate pit 3 (10.7 to 367), indicating additional sources of SO_4 other than raffinate pit 3. Although the movement of water from raffinate pit 3 through the overburden to the diversion pond is likely, additional data are needed to more accurately assess the effect of the raffinate pits and other contaminated materials on the water quality of the diversion pond.

MIGRATION OF CONTAMINANTS WITHIN THE SHALLOW AQUIFER

Background values of specific conductance and concentrations of Ca, Mg, Na, SO_4, Cl, NO_2 + NO_3, Li, Sr, and U in the shallow aquifer were determined by Kleeschulte and Imes (in press). They defined the background concentration of a given constituent as the 95 percentile of sample values from monitoring wells not affected by the WSCP site. Comparison of background constituent concentrations determined by Kleeschulte and Imes (in press) to water-quality data from monitoring wells sampled by the USGS (figs. 11 and 13) indicate samples from a number of monitoring wells are contaminated. The first two parts of this section discusses the geochemical controls and conceptual models for sources of contaminants within the shallow aquifer. The third part of the section discusses the water quality and sources of contaminants in Burgermeister spring.

Quality of Water from Contaminated Monitoring Wells and Piezometers

Samples from 41 monitoring wells and 1 piezometer completed in the shallow aquifer had

concentrations of at least one constituent larger than background concentrations (table 14). Samples were collected from these wells between 1984 and 1991. The number of times the USGS has sampled each well and the number of times a constituent exceeded the background concentration are listed in table 14. In addition, a column in the table indicates if the USDOE or U.S. Army has detected nitroaromatic compounds in a sample from the well at any time.

Twenty-four monitoring wells and one piezometer onsite and six monitoring wells offsite sampled by the USGS are considered contaminated. Eleven additional monitoring wells in the table are considered suspect or are thought to be contaminated from sources other than the WSCP. A monitoring well or piezometer was considered suspect if samples contained constituent concentrations that were only slightly larger than the background concentrations or if the only constituents concentrations larger than background concentrations were those constituents commonly associated with the aquifer materials.

Because large natural sources of specific conductance, and Ca, Mg, and Sr can exist in carbonate aquifers, the four monitoring wells onsite having only these constituents larger than background concentrations (MW-2004, MW-2019, MW-2021, and MW-2022; fig. 13) probably have a natural origin of these constituents. Two other monitoring wells located onsite (MW-2016 and MW-3010) and two monitoring wells on the August A. Busch Memorial Wildlife Area (USGS-1 and USGS-3; fig. 11) did not contain larger than background concentrations of NO_2 + NO_3 (a common constituent in the raffinate pits) and other constituent concentrations were only slightly larger than background concentrations (Kleeschulte and Imes, in press). Constituents in these monitoring wells also probably have a natural origin. Analyses of a sample from MW-2016 by the USDOE before the well was abandoned indicated concentrations of NO_2 + NO_3 as large as 85 mg/L (MK-Ferguson Company and Jacobs Engineering Group, 1989a). Although the concentration of NO_3 in the sample collected by the USGS from monitoring well MW-2016 was less than the upper limit of background concentrations, the Li concentration (21 µg/L; Kleeschulte and Cross, 1990) was larger than the background concentration in one of the three samples. Another monitoring well onsite, MW-2011, also contained concentrations of NO_2 + NO_3 larger than background concentrations.

Table 14. Summary of monitoring wells and piezometers sampled by the U.S. Geological Survey that contain larger than background concentrations of selected inorganic constituents

[Number in table is the number of times a constituent exceeded the background concentration; value in parentheses is the background constituent concentration determined by M.J. Kleeschulte and J.L. Imes (U.S. Geological Survey, written commun., 1991); SC, specific conductance; μS/cm, microsiemens per centimeter at 25 degrees Celsius; Ca, calcium; mg/L, milligrams per liter; Mg, magnesium; Na, sodium; SO$_4$, sulfate; Cl, chloride; NO$_3$, nitrate; Li, lithium; μg/L, micrograms per liter; Mo, molybdenum; Sr, strontium; U, uranium; N-Ar, nitroaromatic compound; --, constituent did not exceed the background concentration; X, detection of at least one nitroaromatic compound in one or more samples]

Well (figs. 13 and 15)	Number of samples	SC (651 μS/cm)	Ca (82 mg/L)	Mg (47 mg/L)	Na (30 mg/L)	SO$_4$ (32 mg/L)	Cl (8.4 mg/L)	NO$_3$ (1.6 mg/L)	Li (13 μg/L)	Mo (10 μg/L)	Sr (220 μg/L)	U (3.0 μg/L)	N-Ar[a]
Army Well[b]	5	--	--	--	--	3	2	--	--	--	--	--	--
USGS-1[b]	7	1	2	--	2	--	--	--	1	--	--	--	X[c]
USGS-3[b]	7	--	--	--	--	--	--	--	1	--	2	--	X[c]
USGS-5	9	3	2	--	--	--	--	--	1	--	--	5	--
USGS-6	9	--	--	--	--	--	--	--	--	--	--	2	--
USGS-8	8	1	--	--	--	--	1	8	--	--	--	1	--
USGS-9[d]	7	--	--	--	--	--	1	7	--	--	--	--	--
MW-2001	2	1	1	--	--	--	--	2	--	--	--	--	X
MW-2002	1	1	1	1	1	1	--	1	1	--	1	--	X
MW-2003	3	3	3	3	3	3	3	3	3	--	3	1	X
MW-2004[b]	2	1	--	--	--	--	--	--	--	--	--	--	X
MW-2005	3	3	1	--	--	--	--	3	3	--	--	--	X
MW-2006	3	3	3	3	3	1	3	3	3	--	--	--	X
MW-2007	1	--	--	--	--	--	--	--	--	--	--	1	X
MW-2008	1	1	1	--	--	1	1	1	--	--	--	--	X
MW-2009	1	1	1	--	1	1	1	--	--	--	--	--	X
MW-2010	1	1	1	--	1	1	1	--	--	--	--	--	X
MW-2011[b]	1	--	--	--	--	--	--	1	--	--	--	--	X
MW-2012	1	1	1	--	1	1	1	--	--	--	--	--	X
MW-2013	1	1	1	--	1	--	1	--	1	--	--	--	X
MW-2014	1	1	1	--	1	1	1	1	--	--	--	--	X
MW-2015	1	1	1	1	--	1	--	--	1	--	1	--	X
MW-2016[b,e]	3	--	--	--	--	--	--	--	1	--	--	--	X
MW-2017	1	1	1	1	1	1	1	--	1	--	1	1	X
MW-2018	1	1	--	--	1	--	--	--	1	--	1	--	X
MW-2019[b]	1	--	--	1	--	--	--	--	--	--	--	--	X
MW-2020[f]	3	3	2	2	2	2	2	--	2	--	2	3	X
MW-2021[b]	1	1	--	1	--	--	--	--	--	--	--	--	--
MW-2022[b]	1	--	--	1	--	--	--	--	--	--	--	--	X
MW-3003	2	2	2	2	2	1	1	2	2	2	2	2	X
MW-3004	1	1	1	--	1	1	--	1	1	--	1	--	--
MW-3006	2	1	--	1	1	1	--	1	2	1	1	--	X
MW-3007[g]	3	3	3	3	3	3	3	3	3	1	3	2	X
MW-3008	4	4	4	4	4	3	4	4	4	--	4	3	X
MW-3009[e]	5	5	1	1	--	4	--	4	1	--	--	5	X
MW-3010[b]	3	3	--	3	--	--	--	--	2	--	2	--	--
MW-3013	1	1	1	1	--	1	--	1	1	--	1	--	X
MW-3018	1	1	1	1	1	1	1	1	1	--	1	1	X
GT64-P	1	1	1	1	1	1	1	1	1	--	1	1	--
MW-4001	1	1	1	--	--	1	--	1	--	--	--	--	X
MW-4006	3	--	--	--	--	3	--	3	--	--	--	--	X
MW-4013	1	1	1	1	--	1	1	1	1	--	--	--	X

[a] Data obtained from MK-Ferguson Company and Jacobs Engineering Group (1990c). Concentration was not used to determine if well was contaminated.

[b] Well apparently is not contaminated by the Weldon Spring chemical plant and those constituents identified as increased probably have a natural origin.

[c] Data obtained from International Technology Corporation (1989); concentration was not used to determine if well was contaminated.

[d] Contamination from sources other than the Weldon Spring chemical plant and Weldon Spring ordnance works operations.

[e] Well abandoned.

[f] Only values of SC and U reported for one sample collected during 1986.

[g] Uranium data missing for one analysis.

The sources of larger than background concentrations of Cl (4.0 to 10.0 mg/L) and $NO_2 + NO_3$ (2.7 to 3.3 mg/L) in samples from monitoring well USGS-9 (fig. 11) probably were caused by a nearby horse stable, dog kennel, and maintenance shed containing stored fertilizers. The Army well, located on the U.S. Army property west of the site, contained slightly increased concentrations of SO_4 (8.3 to 10 mg/L) and Cl (31 to 35 mg/L). Unlike the other wells, this well is open to lower parts of the shallow aquifer (Fern Glen Limestone) as well as the upper part of the confining layer (Chouteau Group, Bushberg Sandstone, and the lower part of the Sulphur Springs Group). The increased concentrations of SO_4 and Cl may be related to different lithologies in these units.

Of the remaining monitoring wells that are considered contaminated, four wells (MW-4013, USGS-5, USGS-6, and USGS-8) are located within troughs that trend toward Burgermeister spring (figs. 11 and 13). As previously indicated, these troughs correlate with ground-water troughs that extend from the chemical plant site to the north towards Burgermeister spring (fig. 12). The water quality in these monitoring wells represents the migration of contaminants in the shallow aquifer from the chemical plant site northward toward Burgermeister spring along preferential paths within these troughs and ground-water troughs. A sample from monitoring well MW-4013 contained concentrations of $NO_2 + NO_3$ (65 mg/L) and Li (52 μg/L), much larger than the background concentrations of 1.6 mg/L and 13 μg/L (Kleeschulte and Cross, 1990). This well also contained larger than background concentrations of Ca, Mg, SO_4, and Cl; however, U concentrations were not larger than the background concentrations. Samples from monitoring well USGS-5 contained larger than background concentrations of Ca (71 to 87 mg/L), Li (less than 4 to 15 μg/L), and U (1.0 to 4.2 μg/L). Two samples from monitoring well USGS-6 contained U concentrations larger than background concentrations (3.0 and 4.0 μg/L). Water from monitoring well USGS-8 had concentrations of $NO_2 + NO_3$ (2.3 to 9.8 mg/L) consistently larger than background concentrations, and one value of specific conductance (660 μS/cm), Cl (12 mg/L), and U (3.3 μg/L) larger than background concentrations. The increased concentrations of $NO_2 + NO_3$ in this well may be caused by fertilizer application on fields surrounding this well and not because of the WSCP.

Monitoring wells MW-4001 and MW-4006 are immediately west of the raffinate pits on the U.S. Army property and water from these wells may represent a combination of relict contamination from the production of military ordnance in addition to contaminants migrating westward from the raffinate pits. The remaining monitoring wells and piezometer identified as contaminated (table 14) are located onsite (fig. 13). Samples from nearly all of these wells contained detectable concentrations of nitroaromatic compounds, and the largest concentrations were detected in monitoring wells MW-2006, MW-2013, and MW-4009 (MK-Ferguson Company and Jacobs Engineering Group, 1990c). These monitoring wells are located near former TNT production areas (figs. 2 and 13). Monitoring wells MW-4001, MW-4006, and MW-4013 also contained large concentrations of nitroaromatic compounds (MK-Ferguson Company and Jacobs Engineering Group, 1990c). Only one of the monitoring wells onsite (MW-3006) identified as contaminated was a deep well completed within the unweathered limestone.

Some of the largest specific conductance values and constituent concentrations were detected in samples from monitoring well MW-3007 before it was abandoned (table 15). This well was located near the northwest corner of raffinate pit 4 and was completed during 1983 as an open-hole from the top of bedrock with no annular seal (fig. 28). Because of the large open interval and the potential for inducing shallow contaminants deeper into the shallow aquifer, the USDOE replaced this well with a piezometer (GT64-P) and two clustered monitoring wells (MW-3003 and MW-3006). The piezometer is completed in the weathered limestone, monitoring well MW-3003 is completed in the weathered and unweathered limestone, and MW-3006 is a deep well completed only within the unweathered limestone (fig. 28).

Water-quality data from the abandoned well MW-3007, the clustered monitoring wells, and piezometer (MW-3006, MW-3003, and GT64-P, in order of decreasing depth) indicate the largest constituent concentrations generally were in samples from MW-3007 (table 15). Monitoring well MW-3006 generally contained the smallest constituent concentrations; monitoring well MW-3003 and piezometer GT64-P generally contained intermediate concentrations. The concentrations of constituents in these monitoring wells generally were larger than those detected in raffinate pit 4, which indicate the probable

ABBREVIATIONS AND SYMBOLS USED IN TABLE 15

SC	Specific conductance, in microsiemens per centimeter at 25 degrees Celsius
pH	In standard units
Temp	Temperature, in degrees Celsius
DO	Dissolved oxygen, in milligrams per liter
Ca	Calcium, dissolved, in milligrams per liter
Mg	Magnesium, dissolved, in milligrams per liter
Na	Sodium, dissolved, in milligrams per liter
K	Potassium, dissolved, in milligrams per liter
HCO_3 (IT)	Bicarbonate, incremental titration, in milligrams per liter
Alk (FET)	Alkalinity, fixed endpoint titration, total as $CaCO_3$, in milligrams per liter
Alk (IT)	Alkalinity, incremental titration, total as $CaCO_3$, in milligrams per liter
SO_4	Sulfate, dissolved, in milligrams per liter
Cl	Chloride, dissolved, in milligrams per liter
F	Fluoride, dissolved, in milligrams per liter
Br	Bromide, dissolved, in milligrams per liter
SiO_2	Silica, dissolved, in milligrams per liter
NO_2	Nitrite, dissolved as nitrogen, in milligrams per liter
NO_2+NO_3	Nitrite plus nitrate, dissolved as nitrogen, in milligrams per liter
NH_3	Ammonia, dissolved as nitrogen, in milligrams per liter
P	Phosphorus, dissolved, in milligrams per liter
Al	Aluminum, dissolved, in micrograms per liter
As	Arsenic, dissolved, in micrograms per liter
Ba	Barium, dissolved, in micrograms per liter
Be	Beryllium, dissolved, in micrograms per liter
B	Boron, dissolved, in micrograms per liter
Cd	Cadmium, dissolved, in micrograms per liter
Cr	Chromium, dissolved, in micrograms per liter
Co	Cobalt, dissolved, in micrograms per liter
Cu	Copper, dissolved, in micrograms per liter
Fe	Iron, dissolved, in micrograms per liter
Fe^{2+}	Iron, ferrous, dissolved, in micrograms per liter
Pb	Lead, dissolved, in micrograms per liter
Li	Lithium, dissolved, in micrograms per liter
Mn	Manganese, dissolved, in micrograms per liter
Mo	Molybdenum, dissolved, in micrograms per liter
Ni	Nickel, dissolved, in micrograms per liter
Se	Selenium, dissolved, in micrograms per liter
Sr	Strontium, dissolved, in micrograms per liter
V	Vanadium, dissolved, in micrograms per liter
Zn	Zinc, dissolved, in micrograms per liter
U	Uranium, dissolved, in micrograms per liter
DOC	Dissolved organic carbon, in milligrams per liter
--	No data available
>	Greater than
<	Less than

Table 15. Water-quality data from clustered monitoring wells and piezometer near raffinate pit 4

[Monitoring well MW-3007 is abandoned; the remaining wells and piezometer are listed in order of decreasing depth]

Sample location (fig. 13)	Date	SC	pH	Temp	DO	Ca	Mg	Na	K	HCO₃ (IT)
MW-3007	2-18-86	6,600	6.8	14.5	--	800	320	330	1.9	--
	6-18-86	7,000	7.0	15.5	--	820	280	340	13	270
	12-17-87	7,000	7.0	12.5	--	670	250	340	15	--
MW-3006	5-10-89	461	7.3	15.5	--	22	16	37	35	--
	6-12-90	698	7.2	14.5	<0.05	64	52	19	1.3	493
MW-3003	5-10-89	3,850	6.8	14.0	--	320	140	230	10	340
	6-12-90	3,360	6.8	15.0	1.4	270	150	180	10	379
GT64-P	6-14-90	3,960	7.0	16.0	>1.0	450	100	270	4.8	305

Sample location (fig. 13)	Date	Alk (FET)	Alk (IT)	SO₄	Cl	F	Br	SiO₂	NO₂	NO₂ + NO₃
MW-3007	2-18-86	210	--	190	35	<0.10	--	11	0.070	920
	6-18-86	217	--	320	22	.20	--	10	.050	930
	12-17-87	219	--	270	24	.10	--	7.4	.040	940
MW-3006	5-10-89	198	--	71	1.3	.30	--	.18	< .010	.310
	6-12-90	399	404	23	4.6	.20	0.021	12	< .010	14.0
MW-3003	5-10-89	280	--	200	13	.20	--	10	.190	440
	6-12-90	303	310	25	6.1	<.10	.030	10	.230	387
GT64-P	6-14-90	248	250	130	18	<.10	.070	12	1.10	410

Table 15. Water-quality data from clustered monitoring wells and piezometer near raffinate pit 4--Continued

Sample location (fig. 13)	Date	NH_3	P	Al	As	Ba	Be	B	Cd
MW-3007	2-18-86	--	--	--	--	--	--	--	--
	6-18-86	--	0.080	--	--	--	--	--	--
	12-17-87	--	--	--	--	--	--	--	--
MW-3006	5-10-89	0.030	.490	<10	1	<2	1	20	<1.0
	6-12-90	.021	.050	<10	3	170	<.5	<10	<1.0
MW-3003	5-10-89	.080	.030	<10	<1	300	<10	50	<1.0
	6-12-90	.020	.080	<10	<1	100	<10	30	<1.0
GT64-P	6-14-90	<.010	.030	<10	<1	<100	<10	20	<1.0

Sample location (fig. 13)	Date	Cr	Co	Cu	Fe	Fe^{2+}	Pb	Li	Mn
MW-3007	2-18-86	--	--	--	--	--	--	1,700	--
	6-18-86	--	--	--	--	--	--	1,700	--
	12-17-87	--	--	--	--	--	--	1,600	--
MW-3006	5-10-89	20	<3	<1	6	90	<1	45	2
	6-12-90	1	<3	<1	110	60	1	18	200
MW-3003	5-10-89	2	1	1	20	<10	1	740	180
	6-12-90	2	1	1	20	<10	<1	600	220
GT64-P	6-14-90	3	1	7	30	--	1	1,100	30

Table 15. Water-quality data from clustered monitoring wells and piezometer near raffinate pit 4--Continued

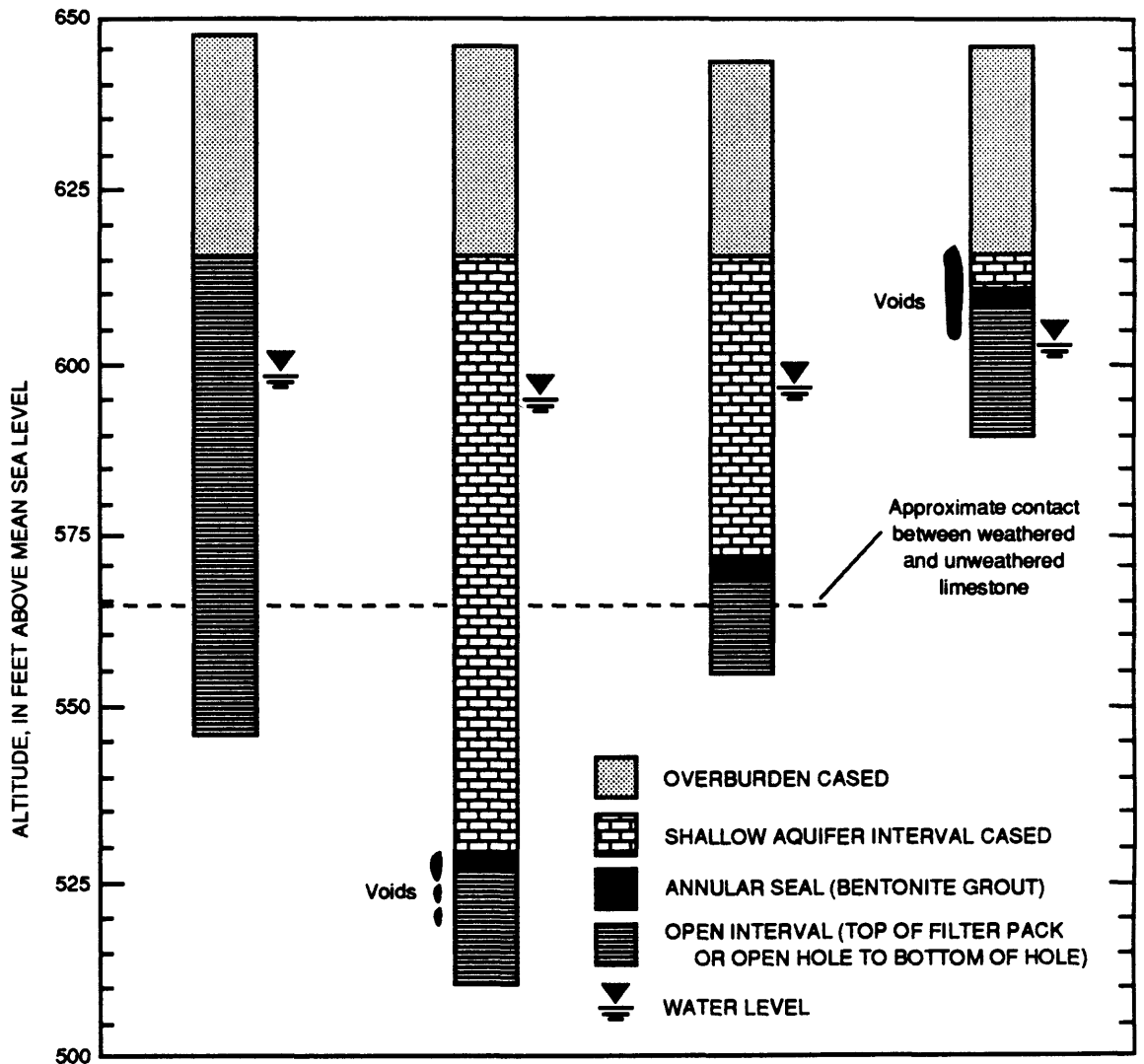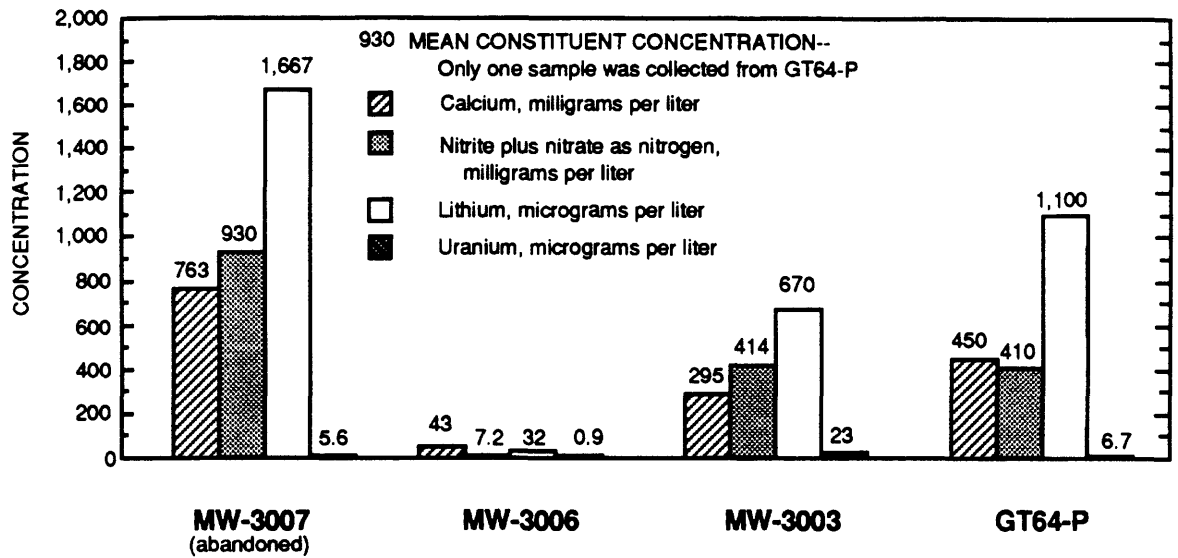| Sample location (fig. 13)	Date	Mo	Ni	Se	Sr	V	Zn	U	DOC
MW-3007	2-18-86	33	--	--	1,600	1	--	--	--
	6-18-86	--	--	--	1,500	1	--	6.0	--
	12-17-87	--	--	--	1,500	--	--	5.1	1.0
MW-3006	5-10-89	<10	<1	<1	26	<6	3	--	.3
	6-12-90	0	6	<1	230	<6	8	.90	.2
MW-3003	5-10-89	17	17	8	830	<1	40	17	--
	6-12-90	11	16	7	790	<1	20	23	.5
GT64-P	6-14-90	10	2	12	950	1	90	6.7	4.2

Figure 28. Concentration of selected constituents as a function of well construction in clustered monitoring wells near raffinate pit 4.

source is raffinate pit 3. The mean concentrations of Ca, NO_2 + NO_3, Li, and U and water-level and well-completion data are shown in figure 28. The large constituent concentrations in samples from monitoring well MW-3007 can be attributed to this well being open to the uppermost part of the weathered limestone. In addition, because the well contains no annular seal, it also may have received inflow from the overlying residuum, as well as from the residuum-weathered limestone contact. The general decrease in constituent concentrations with increasing depth in this well cluster indicates the largest concentrations of contaminants probably are being transported laterally within the upper part of the weathered bedrock or near the residuum-weathered bedrock contact. Although water-quality data from the well cluster at this location indicate less contamination within the unweathered limestone, the decrease in hydraulic head with depth (fig. 28) indicates the potential for additional contaminants to migrate into the unweathered limestone.

A trilinear diagram of samples from monitoring wells that contain larger than background constituent concentrations at the site and adjacent U.S. Army property is given in figure 29. Also shown on this diagram are the general plotting positions of the raffinate pits, interstitial-water samples from raffinate pit 3, and the uncontaminated monitoring wells. Hem (1985) indicates that the composition of any mixture of two waters A and B will plot along a straight line between A and B providing no chemical reactions occur as a result of the mixing. Samples from many of the contaminated monitoring wells identified in table 14 generally plot between samples from the uncontaminated monitoring wells and raffinate pit 3 or interstitial-water samples from raffinate pit 3. This indicates that, in general, mixing of these raffinate pit sources and uncontaminated ground-water could approximate the observed major element chemistry of those monitoring well samples plotting in this region; however, this does not necessarily indicate that all these monitoring wells are contaminated by the raffinate pits. For example, Cl concentrations in samples from monitoring well MW-2006 (200 mg/L to 250 mg/L; Kleeschulte and Cross, 1990) were larger than the Cl concentrations detected in samples from raffinate pit 3 (19 to 71 mg/L and concentrations of NO_2 + NO_3 in the well are relatively small (6.4 to 13 mg/L; Schumacher, 1990). Because of the large Cl concentrations, small concentrations of NO_2 + NO_3,

and the proximity of this monitoring well to Frog pond, which has Cl concentrations ranging from 160 to 500 mg/L (Kleeschulte and Cross, 1990), it is unlikely that the raffinate pits are contributing large quantities of constituents to this well. Frog pond and its outflow also contained large concentrations of Na (110 to 300 mg/L) and U (200 to 410 µg/L). The molar ratios of Na to Cl in Frog pond and the outflow from Frog pond range from 0.82 to 1.05, indicating the source for the large Na and Cl concentrations probably is from runoff from a road salt storage pile just east of the WSCP. The molar ratios of Na to Cl in monitoring well MW-2006 (0.49 to 0.59) probably are smaller because of exchange reactions involving Na for Ca and Mg within the overburden and residuum.

Water-quality samples from monitoring well MW-2020, which plot between the uncontaminated monitoring wells and raffinate pit 3 (fig. 29), contained concentrations of Ca (130 mg/L), Na (54 mg/L), SO_4 (260 mg/L), Li (40 µg/L), and U (5 to 49 µg/L) larger than background. Because this well does not contain larger than background concentrations of NO_2 + NO_3 and because it is located along the ground-water divide east of the raffinate pits (fig. 9), it probably is not receiving substantial quantities of constituents from the raffinate pits.

The plotting position of samples from monitoring well MW-3006 has shifted from between the uncontaminated monitoring wells and raffinate pit 4 (5-10-89) to just inside the region of uncontaminated monitoring wells (6-12-90; fig. 29). This shift may reflect an increase in a component derived from raffinate pit 3 between the two samples; however, the larger concentrations of K (potassium) and Cr in the sample collected during 1989 were anomalous. The USDOE conducted aquifer tracer tests in the vicinity of this well using KBr (potassium bromide) and it is possible this could have had some effect on this sample from the well.

Geochemical Controls on Contaminant Concentrations Within the Shallow Aquifer

Calcite equilibrium generally is achieved in the uncontaminated and contaminated monitoring wells as shown in a plot of calcite SI as a function of Ca concentration (fig. 30). The data points in the shaded area represent samples collected from the USGS monitoring wells on the August A. Busch Memorial

Interstitial-water samples raffinate pit 3

Surface of raffinate pit 2

Surface of raffinate pit 3

Surface of raffinate pit 1

SULFATE PLUS CHLORIDE PLUS NITRITE PLUS NITRATE

CALCIUM PLUS MAGNESIUM

MW-2020

MW-2006

MW-3006 (6-12-90)

Shaded area represents plotting position of uncontaminated monitoring wells in the shallow aquifer (fig.15)

MW-3006 (5-10-89)

Raffinate pit 4

SODIUM PLUS POTASSIUM

CARBONATE PLUS BICARBONATE

MAGNESIUM

CALCIUM

SULFATE

CHLORIDE PLUS NITRITE PLUS NITRATE

PERCENT

NORMALIZED MILLIEQUIVALENTS OF MAJOR IONS

EXPLANATION

MW-2006
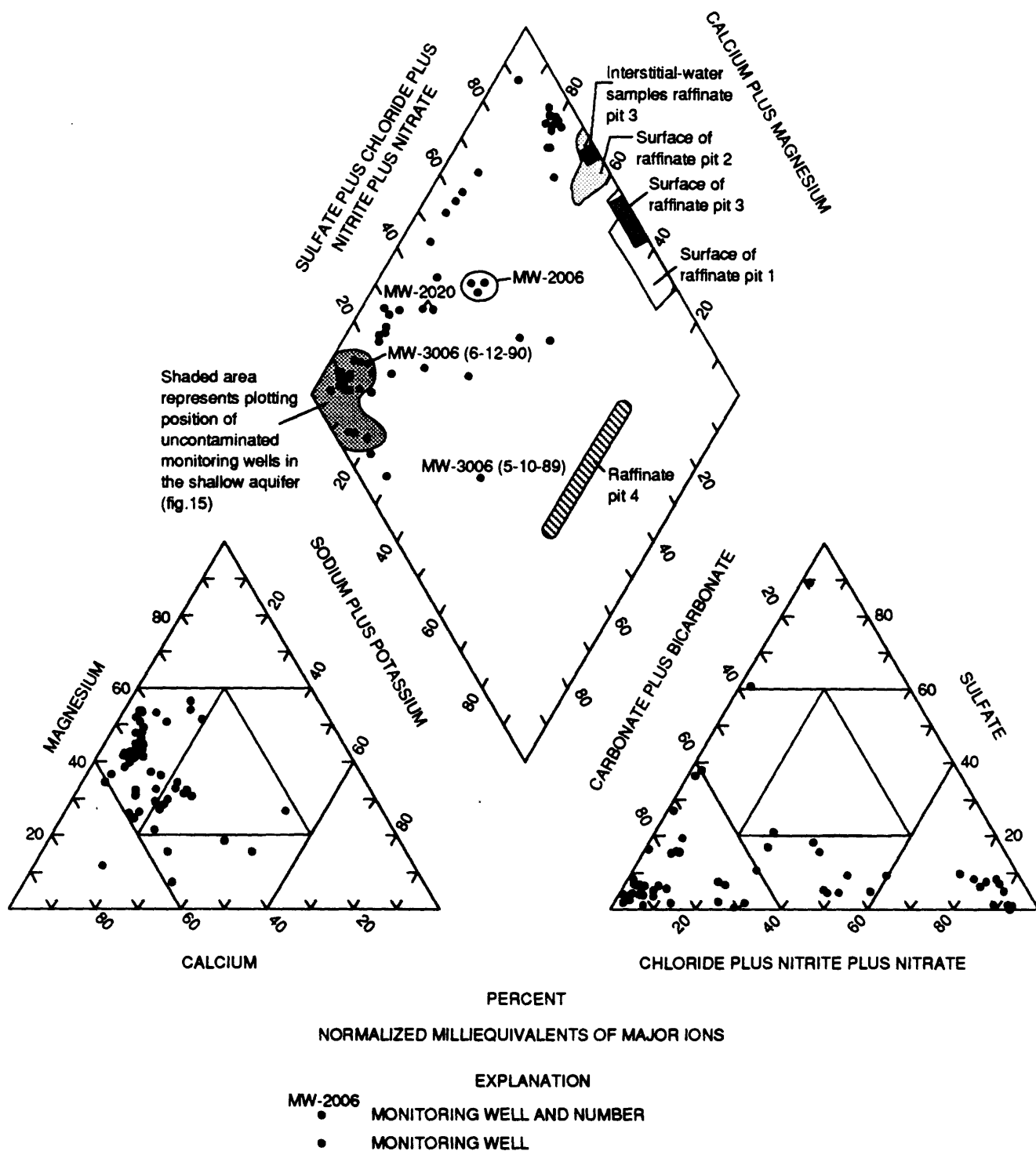●   MONITORING WELL AND NUMBER

●   MONITORING WELL

Figure 29. Trilinear diagram of major constituents in samples from contaminated monitoring wells in the shallow aquifer at the Weldon Spring chemical plant site and vicinity property.
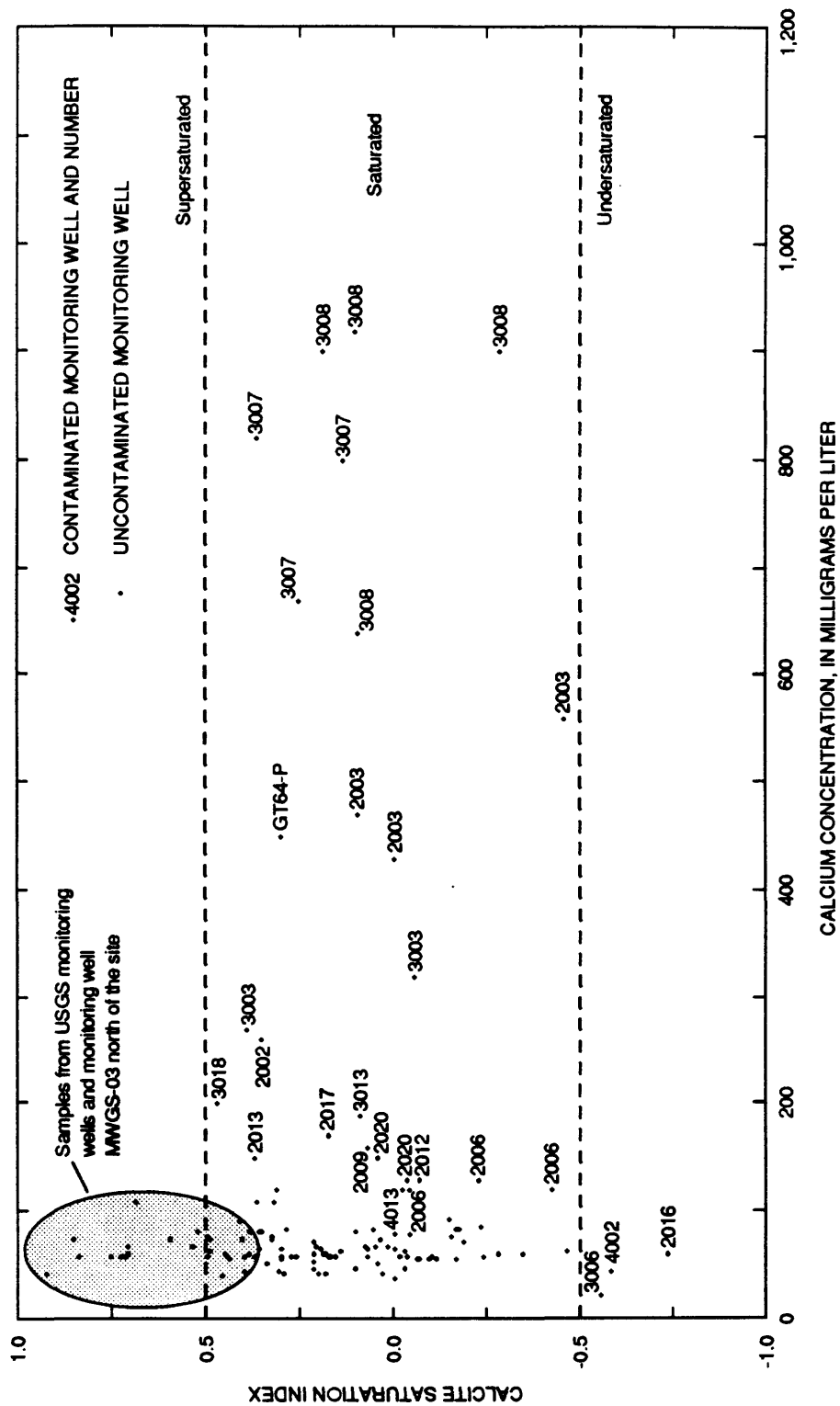
Figure 30. Calcite saturation index as a function of calcium concentration in samples from monitoring wells in the shallow aquifer.

Wildlife Area and one sample from MWGS-03 (fig. 11). Because the USGS monitoring wells are open from the top of unweathered limestone, they may be affected by conditions within the upper shallow aquifer or residuum. The plotting position of samples in figure 30 and the presence of calcite lining fractures and vugs within the shallow aquifer indicates precipitation of calcite within the shallow aquifer. The samples that have a Ca concentration greater than 200 mg/L in figure 30 are from contaminated monitoring wells and piezometers near raffinate pits 3 and 4 (MW-2002, MW-2003, MW-3003, MW-3007, MW-3008, and GT64-P). Samples from these monitoring wells and piezometer plot above the trend line in figure 18, which indicates sources of Ca other than dissolution of calcite by carbonic acid. The large Ca concentrations in these samples and apparent equilibrium with calcite indicate the precipitation of calcite as Ca-rich solutions migrating from the raffinate pits mix with HCO_3-rich ground water.

Results of equilibrium-speciation calculations on samples from several contaminated monitoring wells and piezometers, including MW-2003, MW-3003, MW-3007, MW-3008, and GT64-P are listed in table 16. The pE values were determined by assuming that the dissolved Fe is Fe^{2+} and is in equilibrium with $Fe(OH)_3$ at the measured temperature and pH value. The calculated pE values based on these assumptions are thought to represent the minimum pE values present in the system. All samples are at equilibrium with respect to calcite. Although dolomite saturation is· indicated, it probably is caused by dissolution of this mineral in the bedrock, because precipitation of dolomite does not readily occur under the geochemical conditions present in the shallow aquifer (Hem, 1985). The samples from monitoring well MW-2003 and the abandoned well MW-3007 were only slightly undersaturated with gypsum (SI values of -0.86 and -0.66), indicating that gypsum solubility could limit concentrations of SO_4 in these wells.

There are no expected mineral reactions limiting concentrations of Na and Li within the shallow aquifer, and these constituents generally behave in a conservative manner. Although the calculated predominate aqueous species of N is NH_4^+, substantial quantities of reduced N species were not detected in samples from any of the monitoring wells (Kleeschulte and Cross, 1990; Schumacher, 199C). The absence of reduced N species indicates NO_3 is not being reduced within the shallow aquifer and that the calculated pE

values probably are biased low. A possible explanation for the low calculated pE values is the assumption that the dissolved Fe is Fe^{2+} when it may actually be ferric Fe(III) oxide colloids. The absence of reduced N species indicate little microbial reduction of NO_3, and that NO_3 concentrations will persist in the shallow aquifer. Other than coprecipitation with Ca in calcite or small quantities of sorption onto carbonate minerals, no controls on concentrations of Sr are expected.

Although the laboratory sorption experiments indicate that all U should be removed within the overburden, two monitoring wells adjacent to raffinate pit 4, MW-3003 and MW-3009, contained concentrations of U of 17 and 110 µg/L (Schumacher, 1990). Piezometer GT64-P and monitoring well MW-3008 also contained concentrations of U (6.7 and 7.0 µg/L) larger than background concentrations. The increased U concentrations in these wells indicates saturation of available sorption sites, preferential flow paths, or stabilization of U in solution by carbonate or phosphate within the overburden, or a combination of these processes. Equilibrium-speciation calculations (table 16) indicate the predominate species of U in samples from these four monitoring wells are $UO_2(CO_3)_2^{2-}$ and $UO_2(HPO_4)_2^{2-}$. At the calculated pE values, U(VI) was not reduced to U(IV) and all samples were undersaturated with respect to UO_2 and several other U(VI) minerals. To determine the maximum concentration of U stable in these samples, the concentration of U was increased to 1,000 µg/L and the calculations were made again. In all cases, the solubilities of the U compounds listed were not exceeded, indicating that dissolved U concentrations may be stable in the shallow aquifer in excess of 1,000 µg/L. The calculations do not account for sorption reactions, such as those observed in the overburden; however, these are probably insignificant in the shallow aquifer. Although U can sorb onto calcite, this capacity is small (Carroll and Bruno, 1991) and is unlikely to substantially affect U concentrations in the shallow aquifer.

A simple mass-balance approach using NO_3 as a conservative tracer was used to investigate the source of contaminants in monitoring wells at the WSCP site in more detail (table 17). Based on results of the previous section describing the geochemistry of the lysimeters, the source of NO_3 was assumed to be raffinate pit 3. Nitrate was used as the conservative tracer because it is associated primarily with raffinate pit 3 and substantial NO_3 reduction does not appear to

ABBREVIATIONS AND SYMBOLS USED IN TABLE 16

pH	In standard units	NO_3	Nitrate, dissolved, in milligrams per liter
Temp	Temperature, in degrees Celsius	PO_4	Orthophosphate, dissolved as phosphorous, in milligrams per liter
pE	In standard units		
Ca	Calcium, dissolved, in milligrams per liter	Al	Aluminum, dissolved, in micrograms per liter
Mg	Magnesium, dissolved, in milligrams per liter	Ba	Barium, dissolved, in micrograms per liter
Na	Sodium, dissolved, in milligrams per liter	Fe	Iron, dissolved, in micrograms per liter
K	Potassium, dissolved, in milligrams per liter	Li	Lithium, dissolved, in micrograms per liter
HCO_3 (IT)	Bicarbonate, incremental titration, in milligrams per liter	Mn	Manganese, dissolved, in micrograms per liter
		Sr	Strontium, dissolved, in micrograms per liter
SO_4	Sulfate, dissolved, in milligrams per liter	V	Vanadium, dissolved, in micrograms per liter
Cl	Chloride, dissolved, in milligrams per liter	U	Uranium, dissolved, in micrograms per liter
F	Fluoride, dissolved, in milligrams per liter	<	Less than
SiO_2	Silica, dissolved, in milligrams per liter	--	No data available
		>	Greater than

Table 16. Results of equilibrium-speciation calculations on samples from selected contaminated monitoring wells at the Weldon Spring chemical plant site and vicinity property

[pE determined by assuming dissolved iron is ferrous and in equilibrium with ferrihydrite]

Property or constituent	GT64-P (6-14-90)	MW-2002 (8-02-89)	MW-2003 (6-06-89)	MW-2005 (6-06-89)	MW-3003 (5-10-89)
pH	7.0	7.2	6.2	6.9	6.8
Temp	16.0	15.0	14.5	14.2	14.0
pE	3.8	3.3	4.3	4.7	4.6
Ca	450	260	560	86	320
Mg	100	85	190	45	140
Na	270	110	240	17	230
K	4.8	2.0	12	1.8	10
HCO_3	305	350	300	360	340
SO_4	130	100	220	7.0	200
Cl	18	11	21	2.5	13
F	.10	.10	.10	.10	.20
SiO_2	12	15	11	9.4	10
NO_3	1,810	974	3,010	160	1,950
PO_4	.09	.12	.06	.12	.09
Al	<10	<10	<10	<10	<10
Ba	<100	300	300	170	300
Fe	30	30	40	5.0	20
Li	1,100	450	1,000	39	740
Mn	30	<10	20	<1	180
Sr	950	360	1,100	120	830
V	1.0	1	<1	<6	<1
U	6.7	1.8	3.0	1.0	17
Uranium maximum[a]	>1,000	>1,000	>1,000	>1,000	>1,000

Calculated predominant aqueous species

Nitrogen	NH_4^+	NH_4^+	NH_4^+	NH_4^+	NH_4^+
Uranium	$UO_2(CO_3)_2^{2-}$	$UO_2(CO_3)_3^{4-}$	$UO_2(CO_3)_2^{2-}$	$UO_2(HPO_4)_2^{2-}$	$UO_2(CO_3)_2^{2-}$ $UO_2(HPO_4)_2^{2-}$

Saturation indices

Calcite	0.33	0.40	0.15	-0.22	0.01
Dolomite	.23	.49	.04	-.53	-.14
Siderite	-1.66	-1.39	-1.80	-2.37	-2.02
Strontianite	-1.85	-1.96	-2.04	-2.57	-2.06
Gypsum	-1.09	-1.31	-.86	-2.71	-1.02
Celestite	-2.06	--	--	--	--
Barite	.24	.75	.87	-.38	.96
SiO_2 (amorphous)	-.91	-.80	-.93	-.99	-.97
Quartz	.42	.53	.41	.35	.38
$Fe(OH)_3$ (amorphous)	.00	.00	-.02	.00	.00
Rhodochrosite	-1.39	-1.61	-1.82	-2.44	-.78
Uraninite	-6.81	-8.90	-7.70	-9.59	-7.67
Uraninite (amorphous)	-12.0	-14.0	-12.8	-14.6	-12.7
Coffinite	-7.34	-9.92	-8.19	-10.2	-8.25
Carnotite	-7.92	-9.91	-7.44	-8.81	-6.23
Schoepite	-5.11	-5.86	-5.45	-6.20	-4.85
Autunite	-9.99	--	--	--	--
Sodium autunite	-8.39	--	--	--	--
Tyuyamunite	-5.78	-7.29	-6.09	-6.57	-4.98

Table 16. Results of equilibrium-speciation calculations on samples from selected contaminated monitoring wells at the Weldon Spring chemical plant site and vicinity property--Continued

Property or constituent	MW-3006 (6-12-90)	MW-3007 (6-18-86)	MW-3008 (6-06-89)	MW-3009 (6-06-89)	MW-4013 (6-01-90)
pH	7.2	7.0	6.2	7.5	7.0
Temp	14.5	15.5	15.0	15.0	13.5
pE	2.6	3.6	4.6	3.3	--
Ca	64	820	900	57	120
Mg	52	280	240	39	52
Na	19	340	260	10	29
K	1.3	13	2.6	.5	5.7
HCO_3	493	270	300	200	387
SO_4	23	320	43	65	40
Cl	4.6	22	20	1.8	9.9
F	.20	.20	.10	.20	.20
SiO_2	12	10	12	8.4	8.3
NO_3	62	4,120	4,870	106	288
PO_4	.15	.24	.03	.03	1.8
Al	<10	--	<10	<10	<10
Ba	170	--	500	450	150
Fe	110	--	40	<3	3.0
Li	18	1,700	170	8	52
Mn	200	--	<20	8	3.0
Sr	230	1,500	2,900	110	140
V	<6	1.0	<1	<6	1.0
U	.90	6.0	7.0	110	2.1
Uranium maximum[a]	>1,000	>1,000	>1,000	>1,000	>1,000

Calculated predominant aqueous species

Nitrogen	NH_4^+	NH_4^+	NH_4^+	NH_4^+	NH_4^+
Uranium	$UO_2(CO_3)_2^{2-}$ $UO_2(CO_3)_3^{4-}$	$UO_2(CO_3)_3^{4-}$	$UO_2(CO_3)_2^{2-}$	$UO_2(CO_3)_2^{2-}$	$UO_2(HPO_4)_2^{2-}$

Saturation indices

Calcite	0.05	0.41	0.22	-0.09	-0.01
Dolomite	.24	.56	.08	-.14	-.21
Siderite	-.60	-1.60	-1.94	-2.25	-2.55
Strontianite	-1.89	-1.82	-1.76	-2.30	-2.43
Gypsum	-2.34	-.66	-1.47	-1.88	-1.87
Celestite	--	-1.69	-2.27	-2.90	-3.10
Barite	.09	--	.28	1.01	.27
SiO_2 (amorphous)	-.91	-.98	-.89	-1.06	-1.04
Quartz	.42	.36	.44	.29	.30
$Fe(OH)_3$ (amorphous)	.00	.00	.00	.00	.00
Rhodochrosite	-.10	--	-1.95	-1.52	-2.20
Uraninite	-6.07	-6.70	-7.77	-5.01	-11.2
Uraninite (amorphous)	-11.2	-11.8	-12.9	-10.1	-16.5
Coffinite	-6.61	-7.30	-8.28	-5.69	-12.1
Carnotite	-11.5	-7.56	-8.13	-6.24	-12.5
Schoepite	-6.37	-5.37	-5.06	-3.39	-7.83
Autunite	--	-9.81	-10.5	-8.50	-12.9
Sodium autunite	--	-8.22	-9.20	-8.89	-12.6
Tyuyamunite	-9.03	-6.08	-5.22	-3.03	-11.2

[a] Maximum uranium concentration in solution assuming mineral equilibrium controls.

Table 17. Measured and simulated water quality in selected contaminated monitoring wells at the Weldon Spring chemical plant site and vicinity property

[mg/L, milligrams per liter; µg/L, micrograms per liter; SI, saturation index; --, no data]

Property or constituent	GT64-P		MW-2002		MW-2003		MW-2005		MW-3003	
	6-14-90	Simulated	8-02-89	Simulated	6-06-89	Simulated	6-06-89	Simulated	5-10-89	Simulated
pH, standard units	7.0	7.1	7.2	7.2	6.2	6.9	6.9	7.1	6.8	6.9
Calcium, mg/L	450	400	260	220	560	550	86	67	320	350
Magnesium, mg/L	100	100	85	68	190	190	45	45	140	140
Sodium, mg/L	270	300	110	160	240	310	17	30	230	190
Potassium, mg/L	4.8	18	2.0	9.4	12	25	1.8	2.4	10	16
Bicarbonate, mg/L	305	340	350	350	300	310	360	360	340	320
Sulfate, mg/L	130	74	100	48	220	97	7.0	27	200	70
Chloride, mg/L	18	6	11	3.5	21	7.7	2.5	2.2	13	5.5
Nitrate, mg/L	1,810	2,000	974	1,000	3,010	3,000	160	150	1,950	1,870
Lithium, µg/L	1,100	63-213	450	34-110	1,000	90-310	39	10-21	740	58-200
Strontium, µg/L	950	1,190	360	700	1,100	1,630	120	290	830	1,100
Uranium, µg/L	6.7	3	1.8	2	3.0	4	1.0	1	17	3
Percentage of raffinate pit 3 water	--	5.5	--	2.7	--	8.0	--	.4	--	4.8
Calcite SI	.33	.4	.40	.26	.15	.15	-.22	-.22	.01	.01
Quantity of calcite precipitated (moles per liter)		3.35×10^{-4}		3.35×10^{-4}		6.94×10^{-4}		4.56×10^{-4}		7.73×10^{-4}

Table 17. Measured and simulated water quality in selected contaminated monitoring wells at the Weldon Spring chemical plant site and vicinity property--Continued

Property or constituent	MW-3006		MW-3007		MW-3008		MW-3009		MW-4013	
	6-12-90	Simulated	6-18-86	Simulated	6-06-89	Simulated	3-15-89, 6-06-89	Simulated	6-01-90	Simulated
pH, standard units	7.2	7.3	7.0	7.0	6.2	6.8	7.3, 7.5	7.2	7.0	7.2
Calcium, mg/L	64	66	820	753	900	880	94, 57	65	120	96
Magnesium, mg/L	52	43	280	280	240	240	55, 39	44	52	54
Sodium, mg/L	19	18	340	340	260	720	20, 10	23	29	52
Potassium, mg/L	1.3	1.8	13	34	2.6	41	1.0, .5	2.02	5.7	3.6
Bicarbonate, mg/L	493	380	270	320	300	300	190, 200	370	387	360
Sulfate, mg/L	23	25	320	126	43	140	46, 65	26	40	30
Chloride, mg/L	4.6	2	22	9.9	20	11	3.4, 1.8	2	9.9	2.5
Nitrate, mg/L	62	76	4,120	4,100	4,870	4,850	370, 106	100	288	300
Lithium, µg/L	18	8-18	1,700	120-420	170	142-490	16, 8	9-17	52	14-36
Strontium, µg/L	230	260	1,500	2,160	2,900	2,510	200, 110	270	140	360
Uranium, µg/L	.9	1	6.0	6	7.0	6	57, 110	1	2.1	1.3
Percentage of raffinate pit 3 water	--	.2	--	11	--	--	--	[a].3	--	.8
Calcite SI	.05	.05	.41	.26	.22	.26	-.09	-.09	-.01	-.01
Quantity of calcite precipitated (moles per liter)	1.56×10^{-4}		4.32×10^{-4}		6.16×10^{-4}		3.00×10^{-4}		3.59×10^{-4}	

[a] Percentage of raffinate pit 4 water.

occur within the raffinate pits or the ground water. Lithium was not used as a conservative tracer because of the large variability of Li concentrations within the raffinate pits (tables 4 and 6) and large concentrations of Li in both raffinate pits 3 and 4. Sodium was not used because of the potential for exchange reactions involving Na at mineral surfaces. An interstitial-water sample from 9 ft deep (sample 5; table 6) was used to approximate the raffinate pit 3 component. The water quality of a given monitoring-well sample was simulated by mixing an appropriate quantity of uncontaminated water with water from raffinate pit 3 or 4 to yield the derived NO_3 concentrations. Because variability exists in the concentration of Li in the interstitial-water samples, a range of Li concentrations from 1,000 to 3,600 $\mu g/L$ was used. Solid-phase controls included in the simulations were calcite equilibrium (based on data shown in fig. 30) and Na for Mg exchange.

The simulations indicate that the chemistry in monitoring wells MW-2002, MW-2005, MW-3006, MW-3009, and MW-4013 generally can be approximated by mixing uncontaminated ground water with interstitial water from raffinate pit 3, or raffinate pit 4 (in the case of MW-3009), and precipitation of small quantities (less than 4.6×10^{-4} moles or about 50 mg/L) of calcite. The simulations corroborate previous assumptions that raffinate pit 3 contributes the largest quantity of contaminants to the ground water. Some Na for Mg exchange was required to simulate the concentrations of Na and Mg in samples from monitoring wells MW-2003, MW-3003, MW-3007, MW-3008, and MW-4013, and piezometer GT64-P; however, simulated Na concentrations in monitoring well MW-3008 remained anomalously large. The exchange of Na for Mg was not indicated in the laboratory experiments. However, the Na/Mg ratios in the interstitial water from raffinate pit 3 were larger than those in the solutions used in the laboratory experiments. The exchange of Na for Mg in the simulations also could be an artifact of using NO_3 as the conservative tracer. Concentrations of Cl and SO_4 generally were underestimated. Large SO_4 concentrations in these monitoring wells probably are the result of relict contamination from the production of military ordnance (Schumacher and Stollenwerk, 1991) in addition to migration of contaminants from the raffinate pits. Similar to simulations of water quality in the overburden, the small simulated concentrations of Cl are the result of unusually small Cl

concentrations in the uncontaminated component used in the simulations. However, the small Cl concentrations (less than 25 mg/L) as compared to large concentrations of other major constituents in the most contaminated wells (MW-2003, MW-3003, MW-3007, MW-3008) and piezometer GT64-P indicate the raffinate pits do not contribute substantial quantities of Cl to the shallow aquifer. The large concentrations of Li in monitoring wells MW-2002, MW-2003, MW-3003, and MW-3007, and piezometer GT64-P were anomalous and were largely underestimated in the simulations, probably indicating additional unidentified sources of Li. These wells are located in the same general area (northwest of raffinate pit 4), which may indicate a common source for the Li in these wells.

Differences between measured and simulated constituent concentrations also can be attributed to the calculation of the raffinate pit 3 component by assuming it is the single source of $NO_2 + NO_3$. Sorption of U was not required in the simulations because of the large quantity of dilution of the raffinate pit source terms. Because of the variable constituent concentrations within the interstitial water in raffinate pit 3, probable additional sources of relict contamination, and the large quantity of dilution involved, the simulations are at best simplified approximations and indicate one possible estimation of the observed water quality in a given monitoring well at one point in time. The numerical values should not be considered unique or absolute.

Water Quality and Migration of Contaminants to Burgermeister Spring

Burgermeister spring is located about 1 mi north of the WSCP site along a small tributary to lake 34 on the August A. Busch Memorial Wildlife Area (fig. 8). The USGS has collected continuous discharge record at Burgermeister spring since March 1985 and continuous specific conductance data since July 1987. An inverse relation exists between daily mean discharge and daily mean specific conductance (fig. 31). The discharge hydrograph indicates about 5 months of low flow from July through November and the largest values of specific conductance generally occurred during this period. Kleeschulte and Emmett (1987) indicated that Burgermeister spring responds rapidly to precipitation and becomes turbid. At least
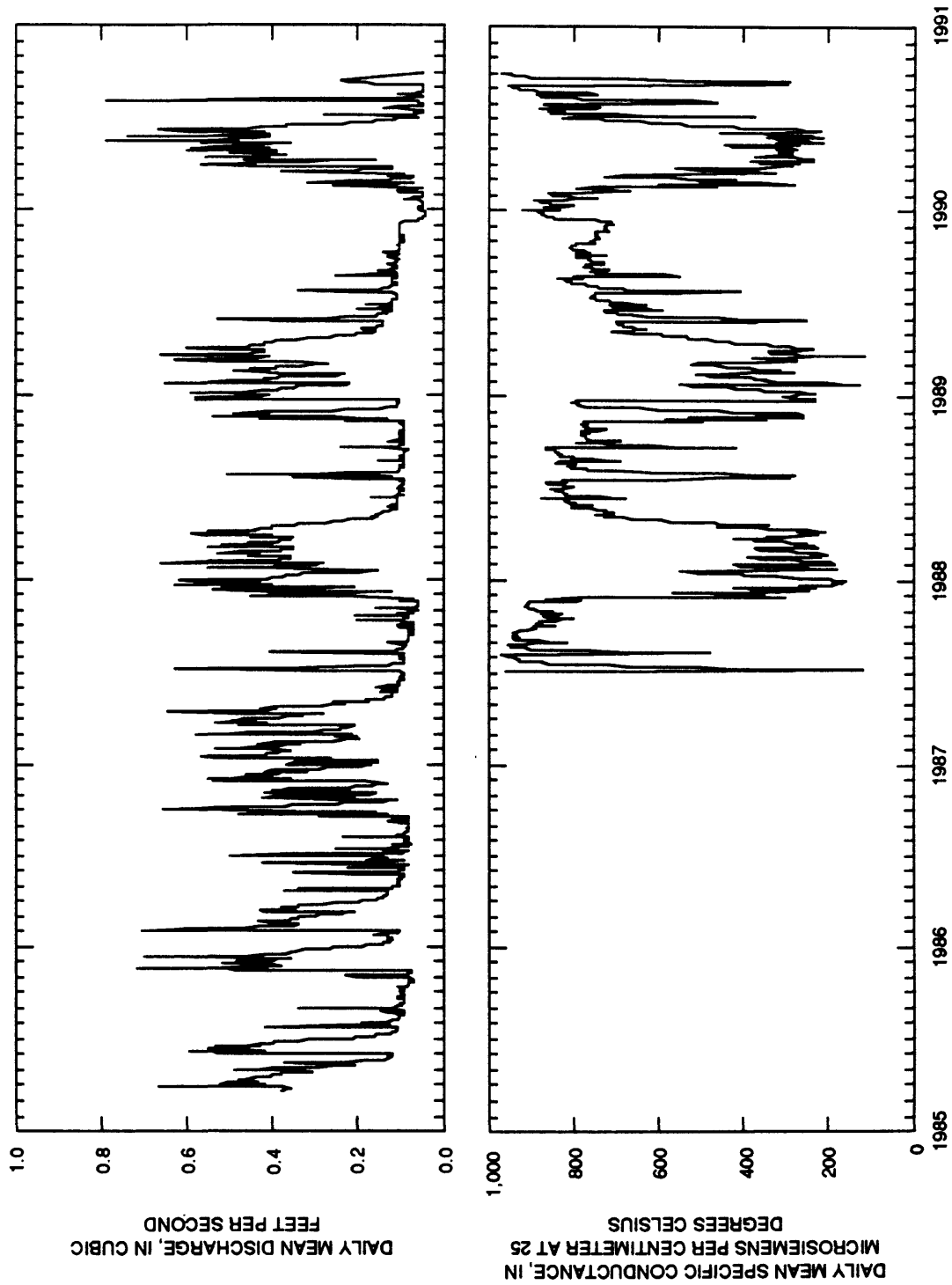
Figure 31. Daily mean discharge from March 1985 to October 1990 and daily mean specific conductance from June 1987 to October 1990 at Burgermeister spring.

two sources of flow to Burgermeister spring are indicated in figure 31--a large specific conductance ground-water component predominating during low base-flow periods from about July through November diluted by a small specific conductance runoff component during storm events and high base-flow periods from about December through June.

Water-quality samples collected by the USGS since 1984 indicate that in addition to increased concentrations of U (26 to 250 µg/L, Kleeschulte and others, 1986; Kleeschulte and Cross, 1990; Schumacher, 1990), Burgermeister spring contained values of specific conductance (208 to 1,090 µS/cm), and concentrations of Ca (29 to 120 mg/L), Na (5 to 47 mg/L), SO_4 (24 to 63 mg/L), Cl (3.3 to 37 mg/L), $NO_2 + NO_3$ (2.3 to 54 mg/L as N), and Li (less than 4 to 77 µg/L) larger than background concentrations for springs as determined by Kleeschulte and Imes (in press). Identification of the source of contamination at Burgermeister spring is difficult because of the large number of potential sources (raffinate pits, Ash pond, Frog pond, relict contamination from military ordnance production, or other unknown sources), potentially large dilution ratios, and uncertainty in the ground-water flow system within the shallow aquifer. Kleeschulte and Emmett (1987) indicated that increased concentrations of $NO_2 + NO_3$ and Li in Burgermeister spring could be the result of seepage from the raffinate pits and the U could be transported from the site through surface-water sources, such as losing streams. The east fork of the west tributary of. Schote Creek is a losing stream reach that receives runoff from the Ash pond and raffinate pit area (fig. 8). Outflow from Ash pond into this tributary has contained large concentrations of U (590 to 4,000 µg/L) relative to Na (14 to 19 mg/L), Cl (3.0 to 6.5 mg/L), $NO_2 + NO_3$ (0.96 to 12 mg/L as N), and Li (6 to 20 µg/L; Kleeschulte and Cross, 1990). Dye injected by the DGLS into the east fork of the west tributary of Schote Creek downstream from Ash pond emerged between 12 and 24 hours later in Burgermeister spring (Missouri Department of Natural Resources, 1991; fig. 8). The positive dye trace indicates the potential for the large concentrations of U in the outflow from Ash pond to contribute U to Burgermeister spring. Another possible source for U is seepage to the ground water from the raffinate pits, especially raffinate pit 4, because the largest concentration of U in ground water at the site (110 µg/L) was detected in a monitoring well (MW-3009) adjacent to this pit (Schumacher, 1990).

Although the outflow from Ash pond contained large concentrations of U, it does not contain sufficient concentrations of Ca, Na, SO_4, Cl, $NO_2 + NO_3$, and Li to generate those detected at Burgermeister spring. The largest known potential source of Na and Cl is the east tributary of Schote Creek. Outflow from Frog pond flows into the east tributary of Schote Creek, then into lake 36 and Schote Creek (fig. 8). Outflow from Frog pond contained large concentrations of Na (as much as 300 mg/L) and Cl (as much as 500 mg/L) and moderate concentrations of U (up to 410 µg/L; Kleeschulte and Cross, 1990). A recent sample (February 1991; M.J. Kleeschulte, U.S. Geological Survey, written commun., 1991) contained the largest concentrations of Na and Cl measured by the USGS in the outflow from Frog pond (610 and 1,300 mg/L). The large concentrations of Na and Cl probably are related to runoff from a road-salt pile located immediately upstream from Frog pond. The stream reach between Frog pond and lake 36 did not lose flow; however, the reach between lake 36 and lake 35 did lose flow (Kleeschulte and Emmett, 1986). In addition, a dye trace performed by the DGLS indicated a subsurface connection between Schote Creek and the tributary that contains Burgermeister spring (locally referred to as tributary 6300) because dye injected upstream from lake 35 emerged directly downstream from lake 34 (fig. 8). The outflow from lake 36 contained large concentrations of both Na and Cl (as large as 83 and 130 mg/L; Kleeschulte and Cross, 1990) related to discharges from Frog pond. It is possible that the east tributary of Schote Creek contributes Na and Cl to Burgermeister spring through losing stream reaches between lake 36 and lake 35 or possibly through seepage from the bottom of lake 36.

The only known sources containing concentrations of $NO_2 + NO_3$ and Li large enough to affect Burgermeister spring are raffinate pits 1, 2, and 3. Raffinate pits 1 and 2 lie south of the ground-water divide at the site; consequently, raffinate pit 3 is the most likely source of the $NO_2 + NO_3$ and Li in Burgermeister spring. The larger than background concentrations of $NO_2 + NO_3$, Li, and U in low base-flow samples from Burgermeister spring and monitoring well MW-4013, larger than background concentrations of Li and U in monitoring well USGS-5 and U in USGS-6, and good agreement between measured and simulated constituent concentrations in a sample from MW-4013 indicate the migration of contaminants from the raffinate pits northward within

the bedrock troughs (fig. 11) towards Burgermeister spring.

Four water-quality samples were collected from Burgermeister spring during 1989; two during a high-base-flow period (March 16 and June 7), and two during a low-base-flow period (August 2 and November 2). Generally, values of specific conductance and concentrations of Ca, Na, SO_4, Cl, $NO_2 + NO_3$, and Li were largest at smaller discharges and concentrations of U were largest at larger discharges (table 18). This indicates a base-flow source for Ca, Na, SO_4, Cl, $NO_2 + NO_3$, and Li and a runoff source for U. The tendency for U concentrations to decrease during low-flow periods may be related to the lack of flow in the losing stream segment downstream from Ash pond and decreased U concentrations entering this stream since the completion of the diversion structure around Ash pond in April 1989. Total U concentrations entering this drainage during 1988 averaged about 2,200 µg/L as compared to about 213 µg/L in the fall of 1989, indicating the effectiveness of this structure (MK-Ferguson Company and Jacobs Engineering Group, 1990c). However, as previously discussed, concentrations of U in the diversion structure have tended to increase since its completion (table 13), indicating additional runoff sources of U other than those identified within Ash pond.

Based on water-level data and ground-water-quality data, discharge and water-quality data of streams and springs, water-quality data from the raffinate pits and surface impoundments, and dye trace information, a conceptual model for the major sources of contamination at Burgermeister spring was derived. During low-base flow, the water probably is a mixture of a Na-Cl rich component from the east tributary of Schote Creek, a NO_3-Li rich component from raffinate pit 3, and possibly a U-Li rich component from raffinate pit 4 mixing with an uncontaminated ground-water component. At high-base flow an additional U-rich component probably is derived from the Ash pond drainage.

Based on the conceptual model, the water quality at Burgermeister spring was simulated at both low-base flow (August 2, 1989) and higher flow (March 16, 1989) by mixing the various sources using PHREEQE. In these simulations, most constituents were assumed to be conservative and the quantity of the raffinate pit 3 component was adjusted based on comparison of observed and simulated concentrations

of NO_3 in samples from Burgermeister spring. Calcite equilibrium was fixed only in the low base-flow simulation. The uncontaminated component of base flow at Burgermeister spring was approximated by the mean constituent concentrations in the Rearing pond spring (fig. 8), locally known as spring 6601. Water-quality data for this spring are given in Kleeschulte and Cross (1990). The raffinate pit 3 component was approximated by interstitial-water samples collected from pit 3 during 1989 (sample 5; Schumacher, 1990). A sample collected from the outflow of lake 36 (March 22, 1988) was used to represent the Na-Cl rich component from the east tributary of Schote Creek. The effect of seepage from raffinate pit 4 on the U concentration at low-base flow was simulated by adding increasing quantities of a component from raffinate pit 4 (surface sample collected from raffinate pit 4 on March 13, 1989; Schumacher, 1990). The maximum quantity of the raffinate pit 4 component was constrained by the simulated concentration of Li. During high base-flow conditions, an additional input of a U-rich water was approximated by a sample from the outflow of Ash pond (collected April 4, 1988; Kleeschulte and Cross, 1990).

Results from the simulations of water quality at Burgermeister spring generally compare favorably with the measured values (table 19). Slight overestimation of Ca, Mg, Na, and HCO_3 concentrations in the high base-flow simulation probably was caused by approximating the uncontaminated runoff component using water quality of the Rearing pond spring rather than a smaller specific conductance component more approximating rainwater. The largest discrepancies in the simulation were between the measured and simulated concentrations of SO_4; the simulated concentrations were consistently smaller, which is related to small SO_4 concentration of the uncontaminated component (19 mg/L) relative to the upper limit of background concentrations (Kleeschulte and Imes, in press) for wells and springs (32 and 54 mg/L). The simulated concentrations of U at Burgermeister spring during low flow ranged from about 4 µg/L, assuming no raffinate pit 4 component, to 88 µg/L, assuming a small component of raffinate pit 4 water. Additional simulations assuming no component from raffinate pit 4 indicated that seepage from the bottom of Ash pond could generate the U concentrations at low flow (about 74 µg/L); however, the concentrations of Li were underestimated (less than 13 µg/L), indicating raffinate

ABBREVIATIONS USED IN TABLE 18

Q	Discharge, instantaneous, in cubic feet per second
SC	Specific conductance, in microsiemens per centimeter at 25 degrees Celsius
pH	In standard units
Eh	Oxidation reduction potential, in millivolts
Temp	Temperature, in degrees Celsius
DO	Dissolved oxygen, in milligrams per liter
Ca	Calcium, dissolved, in milligrams per liter
Mg	Magnesium, dissolved, in milligrams per liter
Na	Sodium, dissolved, in milligrams per liter
K	Potassium, dissolved, in milligrams per liter
HCO_3 (IT)	Bicarbonate, incremental titration, in milligrams per liter
Alk (IT)	Alkalinity, incremental titration, total as $CaCO_3$, in milligrams per liter
SO_4	Sulfate, dissolved, in milligrams per liter
Cl	Chloride, dissolved, in milligrams per liter
F	Fluoride, dissolved, in milligrams per liter
Br	Bromide, dissolved, in milligrams per liter
SiO_2	Silica, dissolved, in milligrams per liter
DS	Dissolved solids, residue at 180 degrees Celsius, in milligrams per liter
NO_2	Nitrite, dissolved as nitrogen, in milligrams per liter
NO_2 total	Nitrite, total as nitrogen, in milligrams per liter
NO_2+NO_3	Nitrite plus nitrate, dissolved as nitrogen, in milligrams per liter
NO_2+NO_3 total	Nitrite plus nitrate, total, in milligrams per liter
NH_3	Ammonia, dissolved as nitrogen, in milligrams per liter
NH_3 total	Ammonia, total as nitrogen, in milligrams per liter
P	Phosphorus, dissolved, in milligrams per liter
P total	Phosphorus, total as nitrogen, in milligrams per liter
PO_4	Orthophosphate, dissolved as phosphorous, in milligrams per liter
Al	Aluminum, dissolved, in micrograms per liter
As	Arsenic, dissolved, in micrograms per liter
Ba	Barium, dissolved, in micrograms per liter
Be	Beryllium, dissolved, in micrograms per liter
B	Boron, dissolved, in micrograms per liter
Cd	Cadmium, dissolved, in micrograms per liter
Cr	Chromium, dissolved, in micrograms per liter
Co	Cobalt, dissolved, in micrograms per liter
Cu	Copper, dissolved, in micrograms per liter
Fe	Iron, dissolved, in micrograms per liter
Fe^{2+}	Iron, ferrous, dissolved, in micrograms per liter
Pb	Lead, dissolved, in micrograms per liter
Li	Lithium, dissolved, in micrograms per liter
Mn	Manganese, dissolved, in micrograms per liter
Mo	Molybdenum, dissolved, in micrograms per liter
Ni	Nickel, dissolved, in micrograms per liter
Se	Selenium, dissolved, in micrograms per liter
Ag	Silver, dissolved, in micrograms per liter
Sr	Strontium, dissolved, in micrograms per liter
V	Vanadium, dissolved, in micrograms per liter
Zn	Zinc, dissolved, in micrograms per liter
Ra	Radium-226, dissolved, planchet count, in picocuries per liter
U	Uranium, dissolved, in micrograms per liter
TOC	Total organic carbon, in milligrams per liter
DOC	Dissolved organic carbon, in milligrams per liter
Trit	Tritium, total, in picocuries per liter
--	No data available
<	Less than

Table 18. Water-quality data from Burgermeister spring, 1989

Date	Time	Q	Sc	pH	pH (lab)	Eh	Temp	DO	Ca	Mg	Na	K	HCO₃ (IT)
3-16-89	1100	0.41	372	6.5	7.4	364	8.5	--	43	9.6	13	2.4	110
6-07-89	0945	.15	663	6.8	7.3	431	11.0	--	73	18	29	2.8	190
8-02-89	0815	.13	749	6.3	7.2	510	10.5	8.2	75	20	33	3.0	220
11-02-89	0830	.09	802	6.9	7.0	--	12.5	7.7	81	22	37	3.0	220

Date	Alk (IT)	SO₄	Cl	F	Br	SiO₂	DS	NO₂	NO₂+NO₃	NH₃	P	P total	PO₄
3-16-89	94	34	10	0.20	--	9.2	200	<0.010	8.20	0.010	0.020	0.040	0.010
6-07-89	155	45	11	.20	0.040	11	356	<.010	20.0	.010	.020	.020	.030
8-02-89	176	57	23	.20	.060	12	435	<.010	21.0	.020	.040	.040	.030
11-02-89	176	63	30	.20	.070	12	454	<.010	27.0	.020	.030	--	--

Date	Al	As	Ba	Be	B	Cd	Cr	Co	Cu	Fe	Fe²⁺	Pb	Li
3-16-89	<10	<1	77	<0.5	30	<1	<1	<3	10	8	0	<5	10
6-07-89	<10	<1	120	<.5	40	<1	<1	<3	1	4	0	<1	28
8-02-89	<10	<1	120	<.5	80	<1	1	<3	1	3	10	<1	35
11-02-89	<10	1	130	<.5	60	<1	1	<3	2	8	--	2	34

Date	Mn	Mo	Ni	Se	Ag	Sr	V	Zn	Ra	U	TOC	DOC	Trit
3-16-89	1	<1	<1	<1	<1.0	110	<6	6	<0.1	180	3.6	2.8	38
6-07-89	2	<1	<1	<1	<1.0	160	<6	11	--	150	2.2	2.7	--
8-02-89	<1	<1	<1	1	<1.0	170	<6	7	--	84	1.6	1.6	--
11-02-89	2	<1	2	1	<1.0	170	<6	37	--	63	--	--	--

Table 19. Measured and simulated water quality in Burgermeister spring at low- and high-base flow

[mg/L, milligrams per liter; μg/L, micrograms per liter; --, no data]

Physical property of constituent	Low-base flow (8-02-89)		High-base flow (3-16-89)	
	Measured	Simulated	Measured	Simulated
pH, standard units	7.2	7.5	7.4	7.1
Calcium, mg/L	75	65	43	52
Magnesium, mg/L	20	12	9.6	12
Sodium, mg/L	33	37	13	15
Potassium, mg/L	3.0	3.1	2.4	2
Sulfate, mg/L	57	26	34	19
Chloride, mg/L	23	24	10	10
Bicarbonate, mg/L	220	190	110	210
Nitrate, as nitrogen, mg/L	93	97	36	27
Lithium, μg/L	35	29-36	10	12 -14
Strontium, μg/L	170	140	110	120
Uranium, μg/L	84	88	180	160
Percentage of selected components				
Uncontaminated ground water		71.3		75.4
Raffinate pit 3 (interstitial water)		.2		.2
Raffinate pit 4		3.0		2.1
Ash pond outflow		.0		4.0
Lake 36 outflow		25.5		18.3

pit 4 is a more likely source of the U concentration in Burgermeister spring at low-base flow than seepage from Ash pond. Results from these simulations are non-unique, are not intended to represent actual onsite conditions, and are best used as general indicators of contaminant sources in Burgermeister spring based on the available hydrologic and water-quality data. Additional water-quality data and quantitative dye traces along the east and middle forks of the west tributary of Schote Creek are needed to confirm these results.

SUMMARY AND CONCLUSIONS

Investigations were conducted by the U.S. Geological Survey at the Weldon Spring chemical plant site to determine the geochemistry of the shallow aquifer and geochemical controls on the migration of uranium and other constituents from the raffinate pits. Water-quality analyses from monitoring wells at and in the vicinity of the Weldon Spring chemical plant site indicate that the water in the shallow aquifer is a calcium magnesium bicarbonate type water that is at equilibrium with respect to calcite and slightly supersaturated with respect to dolomite. The U.S. Department of Energy has conceptually subdivided the shallow aquifer into an upper weathered limestone unit and a lower unweathered limestone unit. Iron oxide staining on fracture surfaces and measurable concentrations of dissolved oxygen, small concentrations of dissolved iron, and abundance of oxidized forms of nitrogen in the ground-water samples indicate that moderately oxidizing conditions exist within the weathered limestone unit of the shallow aquifer. In addition to the presence of fresh pyrite in core samples, dissolved oxygen concentrations were smaller and dissolved iron concentrations generally were larger in samples from monitoring wells in the unweathered limestone, indicating a decrease in the pE of the system with depth. Ratios of calcium to magnesium decrease from a median value of about 0.98 in shallow monitoring wells to 0.79 in the deeper monitoring wells. The presence of drusy calcite crystals within vugs and along fractures in the shallow aquifer indicates that the small calcium/magnesium ratios are related to the precipitation of calcite in addition to dissolution of dolomite, which may increase in abundance in the deeper part of the shallow aquifer.

Relations between concentrations of calcium, magnesium, strontium, and bicarbonate indicate weathering of the shallow aquifer by carbonic acid rather than mineral acid dissolution or hydrolysis. Stable carbon isotopic analyses indicate that carbonic acid is derived from a source containing δ^{13} C ratios of about -10.6 to -13.9, indicating C4-type organic matter. Comparison of hydraulic conductivity, water-level, and geochemical data from the shallow aquifer indicate that much of the recharge at the site may be moving laterally above the unweathered part of the shallow aquifer to vicinity springs and streams.

Water-quality samples from the surface of the raffinate pits indicated large concentrations of calcium, magnesium, sodium, potassium, sulfate, nitrite plus nitrate, lithium, molybdenum, strontium, vanadium, and uranium. Interstitial-water and sludge samples were collected from raffinate pit 3 to determine the geochemical environment within the sludge, the chemistry of solutions entering the ground water from the bottom of the raffinate pits, and the solid phase mineralogy and chemistry. Concentrations of most constituents in the interstitial water of raffinate pit 3 increased with increasing depth below the water-sediment interface. Concentrations of selenium increased from less than the detection limit of 1 microgram per liter in the surface water to more than 4,000 micrograms per liter at 9 feet below the sediment-water interface. Nitrate comprised more than 97 percent of the nitrogen species in the interstitial water at all depths. Equilibrium-speciation calculations indicate that interstitial-water samples generally were undersaturated with respect to uraninite and supersaturated with respect to two uranium-vanadium minerals (carnotite and tyuyamunite). Solid-phase analyses of sludge samples indicated large variations in mineralogy, however, generally confirmed the equilibrium-speciation calculations. Shallow sludge samples (less than 4.5 feet deep) contained large quantities of apatite and trace quantities of carnotite. Deeper sludge samples (4.5 to 9 feet) contained large quantities of gypsum (40 to 75 percent) and sellaite (magnesium fluoride, 10 to 40 percent), and lesser quantities of apatite (5 to 15 percent), quartz (5 to 10 percent), and goethite (about 5 percent). Fission track radiography and scanning electron microscopy identified scattered grains of carnotite and an unidentified uranium-rich phase containing about 76 percent uranium by weight. No reduced U(IV) minerals were identified. Equilibrium-

speciation calculations indicate that nitrate and uranium were not reduced and attenuated within the raffinate pits and can be expected to migrate into the overburden where sorption reactions and dilution may affect their distribution.

Laboratory sorption experiments (batch) were performed to evaluate the effect of solution pH and equilibration time on the sorption of several raffinate constituents. No significant sorption of calcium, sodium, sulfate, nitrate, or lithium was observed. Substantial quantities of Mo(VI) and U(VI) were sorbed by the Ferrelview Formation and clay till. Larger quantities of Mo(VI) and U(VI) were sorbed by the Ferrelview Formation. The sorption behavior of both Mo(VI) and U(VI) was consistent with sorption controlled by oxyhydroxides, rather than by clay minerals. The K_d values at neutral pH for Mo(VI) ranged from 6.9 to 11 milliliters per gram for solutions in contact with the Ferrelview Formation to 2.1 to 2.9 milliliters per gram for solutions in contact with the clay till. At neutral pH values, the U(VI) K_d for solutions in contact with the Ferrelview Formation ranged from milliliters per gram of solid as compared to 10.7 to 26 milliliters per gram for solutions in contact with the clay till. The large range in Mo(VI) and U(VI) K_d values with pH values indicate the inability of the K_d model to accurately simulate the laboratory sorption data; therefore, the surface complexation approach was used. A diffuse-layer surface complexation model was used to simulate the sorption of Mo(VI) and U(VI) in the laboratory sorption experiments. Model simulations indicate that the sorption of Mo(VI) was only a function of pH value, and Mo(VI) was completely removed from solutions in contact with either overburden unit at pH less than about 5. Sorption of U(VI) was a function of pH value and carbonate concentration, with sorption of U(VI) decreasing with increasing pH value or carbonate concentration. At a pH larger than pH 5.5, the model indicated that U(VI) remaining in solution was complexed with carbonate and present as $UO_2(CO_3)_2^{2-}$ and $UO_2(CO_3)_3^{4-}$.

The water quality of samples from overburden lysimeters near raffinate pit 4 can be modeled as a mixture of water from raffinate pits 3 and 4 and an uncontaminated component in a system at equilibrium with ferrihydrite and calcite. Concentrations of uranium are limited by dilution and sorption. The conceptual model for contamination of lysimeters west of raffinate pit 4 is the migration of contaminants from

raffinate pit 3 through the unsaturated Ferrelview Formation and the clay till into the residuum where mixing with uncontaminated ground water and lateral migration westward beneath raffinate 4 occurs. The source of contaminants in the conceptual model was verified by simulations using the geochemical code PHREEQE. The simulations also indicate that precipitation of calcite is likely, as calcium-rich solutions migrating from raffinate pit 3 mix with bicarbonate-rich ground water and water from raffinate pit 4. Additional sources of sulfate other than the raffinate pits are indicated by the model. A potential source of this sulfate is relict contamination of soils and ground water from the manufacturing of military ordnance at the Weldon Spring ordnance works before 1946.

Water-quality data collected by the U.S. Geological Survey from monitoring wells in the shallow aquifer indicate that 24 monitoring wells at the chemical plant site and 6 wells located on vicinity property are contaminated. The source of these contaminants is the raffinate pits. Constituents that had no sorption in the laboratory experiments, such as nitrate, were detected most frequently and in the largest concentrations in the ground water. Those constituents readily sorbed, such as molybdenum and uranium, should be completely sorbed within the overburden and were detected infrequently in the ground water. However, the presence of increased uranium concentrations in several monitoring wells near the raffinate pits indicate the presence of preferential flow paths, saturation of available sorption sites, or formation of weakly sorbed uranium carbonate complexes within the overburden. Simulations of water quality in several contaminated bedrock monitoring wells using the geochemical code PHREEQE indicate that the water quality can be generated by mixing water from raffinate pits 3 and 4 with an uncontaminated ground-water component, and allowing for equilibrium with calcite. These simulations indicate that raffinate pit 3 is the most likely source of increased concentrations of calcium, sodium, nitrite plus nitrate, and lithium in these wells and that raffinate pit 4 is the largest source of uranium.

Water-level and ground-water-quality data, discharge and water-quality data from streams and springs, water-quality data from the raffinate pits and surface-water impoundments, dye-trace information, and the results of simulations using the geochemical code PHREEQE indicate that contaminants in

Burgermeister spring were derived from several sources. At low-base flow Burgermeister spring contained increased concentrations of sodium, chloride, nitrite plus nitrate, lithium, and uranium. The increased concentrations of sodium and chloride probably are the result of flows from the east tributary of Schote Creek that are lost to the subsurface in Schote Creek upstream from lake 35 on the August A. Busch Memorial Wildlife Area. A subsurface connection exists between this reach and Burgermeister spring. This tributary contained large concentrations of sodium and chloride derived from storage of road salt in the upper part of the basin. Increased concentrations of nitrite plus nitrate, lithium, and small quantities of uranium at base flow were the result of seepage from the raffinate pits (predominately raffinate pits 3 and 4) migrating through preferential pathways within bedrock troughs that extend northward from the raffinate pit area to Burgermeister spring. Several shallow bedrock monitoring wells located within this bedrock trough between Burgermeister spring and the chemical plant also contained increased concentrations of several of these constituents. Concentrations of uranium in Burgermeister spring tended to increase at larger flows because of runoff containing large concentrations of uranium from Ash pond and the Ash pond diversion structure entering the east fork of the west tributary of Schote Creek. This tributary loses flow to the subsurface and is hydrologically connected to Burgermeister spring.

REFERENCES CITED

Ball, J.W., Nordstrom, D. K., and Zachmann, O.W., 1987, WATEQ4F--A personal computer Fortran translation of the geochemical model WATEQ2 with revised data base: U.S. Geological Survey Open-File Report 87-50, 108 p.

Bechtel National, Inc., 1984, Geological report for the Weldon Spring raffinate pits site: U.S. Department of Energy, Oak Ridge Operations Office, 46 p. with appendices.

_____ 1987, Hydrogeological characterization report for the Weldon Spring chemical plant: U.S. Department of Energy, Oak Ridge Operations Office, 98 p. with appendices.

Carlston, C.W., 1964, Use of tritium in hydrologic research-problems and limitations: International Association of Scientific Hydrology, v. IX, no. 3, p. 39-43.

Carman, J.D., 1991, Aquifer characteristics of the shallow Burlington-Keokuk Limestone at the Weldon Spring site, in Proceedings of the Geosciences Workshop: U.S. Department of Energy, Oak Ridge Operations Office, p. 155-203.

Carroll, S. A., and Bruno, Jordi, 1991, Mineral-solution interactions in the U(VI)-CO_2-H_2O: Radiochemical Acta, v. 52/53, p. 187-193.

Cathcart, J.B., 1978, Uranium in phosphate rock, in Geology and resources of uranium deposits: U.S. Geological Survey Professional Paper 988-A, 6 p.

Cotton, F.A., and Wilkinson, Geoffrey, 1972, Advanced inorganic chemistry--A comprehensive text: New York, International Publishers, 1,145 p.

Deines, P., 1980, The isotopic composition of reduced organic carbon, in Fritz, P. and Fontes, J.C. eds. Handbook of environmental isotope geochemistry: New York, Elsevier Scientific Publishing Company, 545 p.

Dzombak, P.A., and Morel, F.M.M., 1990, Surface complexation modeling: New York, John Wilson, 893 p.

Fenneman, N.M., 1938, Physiography of eastern United States: New York, McGraw-Hill, 714 p.

Fraser-Brace Engineering Company, 1941, As-constructed pipeline drawings: Atlas Powder Co., 1941 and 1942.

Freeze, R.A., and Cherry, J.A., 1979, Groundwater: Englewood Cliffs, N.J., Prentice-Hall, Inc., 604 p.

Gilbert, M.J., 1991, Introduction to the geology of the Weldon Spring site, in Proceedings of the Geosciences Workshop: U.S. Department of Energy, Oak Ridge Operations Office, p. 17-40.

Harrington C.D., and Ruehle, A.E., eds., 1959, Uranium production technology: Princeton, N.J., D. Van Nostrand Co., Inc., 579 p.

Heir, K.S., and Billings, G.K., 1970, Lithium, in Wedepohl, K.H., ed., Handbook of geochemistry: Berlin, Springer-Verlag, v. II-1, p. 311-313.

Hem, J.D., 1985, Study and interpretation of the chemical characteristics of natural water (3d ed.): U.S. Geological Survey Water-Supply Paper 2254, 263 p.

Hendry, M.J., 1988, Do isotopes have a place in ground-water studies?: National Water Well Journal, v. 26, no. 4, p. 410-415.

Howe, W.B., and Heim, G.E., Jr., 1968, The Ferrelview Formation (Pleistocene) of Missouri: Rolla, Missouri Division of Geology and Land Survey Report of Investigations 42, 32 p.

Hsi, C.D., 1981, Sorption of uranium (UI) by iron oxides: Golden, Colorado School of Mines, unpublished Ph.D dissertation, 154 p.

International Technology Corporation, 1989, Draft--Remedial investigation, Weldon Spring training area: v. 1, 171 p.

Kelly, W.P., 1948, Cation exchange in soils: New York, Reinhold Publishing Corp., 114 p.

Kharaka, Y.K., Gunter, W.D., Aggarwal, P.K., Perkins, E.H., and DeBraal, J.D., 1988, SOLMINEQ.88--A computer program for geochemical modeling of water-rock interactions: U.S. Geological Survey Water-Resources Investigations Report 88-4227, 420 p.

Kleeschulte, M.J., and Cross, P.W., 1990, Hydrologic data for the Weldon Spring chemical plant site and vicinity property, St. Charles County, Missouri--1986-89: U.S. Geological Survey Open-File Report 90-552, 117 p.

Kleeschulte, M.J., and Emmett, L.F., 1986, Compilation and preliminary interpretation of hydrologic data for the Weldon Spring radioactive waste disposal sites, St. Charles County, Missouri--A progress report: U.S. Geological Survey Water-Resources Investigations Report 85-4272, 71 p.

_____ 1987, Hydrology and water quality at the Weldon Spring radioactive waste-disposal sites, St. Charles County, Missouri: U.S. Geological Survey Water-Resources Investigations Report 87-4169, 65 p.

Kleeschulte, M.J., Emmett, L.F., and Barks, J.H., 1986, Hydrologic data for the Weldon Spring radioactive waste-disposal sites, St. Charles County, Missouri--1984-1986: U.S. Geological Survey Open-File Report 88-488, 61 p.

Kleeschulte, M.J., and Imes, J.L., in press, Geohydrology, water quality, and simulation of ground-water flow at the Weldon Spring Chemical Plant and vicinity, St. Charles County, Missouri, 1987-90: U.S. Geological Survey Open-File Report 93-648, pending publication as a U.S. Geological Survey Water-Supply Paper.

Langmuir, D.L., 1978, Uranium solution-mineral equilibria at low temperatures with applications to sedimentary ore deposits: Geochemica et Cosmochimica Acta, v. 42, p. 547-569.

Langmuir, D.L., and Chatham, J.R., 1980, Ground water prospecting for sandstone-type uranium deposits--A preliminary comparison of the merits of mineral-solution equilibria, and single-element tracer methods: Journal of Geochemical Exploration, v. 13, p. 201-219.

Lenhard, L.A., Belcher, F.H., and Holt, J.N., 1967, Weldon Spring raffinate pits and quarry task force report: U.S. Department of Energy, Oak Ridge Operations Office, 21 p.

Lindburgh, R.D., and Runnells, D.D., 1984, Ground water redox reactions--An analysis of equilibrium state applied to Eh measurements and geochemical modeling: Science, v. 225, p. 925-927.

Lowdon, J.A., and Dyck, W., 1974, Seasonal variations in the isotope ratios of carbon maple leaves and other plants: Canadian Journal of Earth Science, v. 11, p. 79-88.

Missouri Department of Natural Resources, 1991, Shallow ground water investigations at Weldon Spring, Missouri--Final report for fiscal years 1988-90: Rolla, Missouri Division of Geology and Land Survey, 36 p. with appendices and plates.

MK-Ferguson Company and Jacobs Engineering Group, 1989a, Weldon Spring site remedial action project--Draft phase II ground-water quality assessment for the Weldon Spring site, chemical plant, and surrounding vicinity properties: U.S. Department of Energy, Oak Ridge Operations Office, revision B, 78 p.

_____1989b, Weldon Spring site remedial action project--Chemical soil investigation report for the Weldon Spring chemical plant/raffinate pits, phase II: U.S. Department of Energy, Oak Ridge Operations Office, revision 0, 56 p.

_____1989c, Waste assessment chemical characterization of the Weldon Spring site raffinate pits: U.S. Department of Energy, Oak Ridge Operations Office, revision 0, 68 p.

_____1989d, Waste assessment radiologic characterization of the Weldon Spring site raffinate pits: U.S. Department of Energy, Oak Ridge Operations Office, revision 0, 68 p.

_____1989e, Weldon Spring site remedial action project--Draft remedial investigation report: U.S. Department of Energy, Oak Ridge Operations Office, revision B.

_____1990a, Weldon Spring site remedial action project--Draft suitability of the Weldon Spring site for potential location of a disposal facility: U.S. Department of Energy, Oak Ridge Operations Office, revision A, 75 p.

_____1990b, Aquifer characteristics data for the Weldon Spring site chemical plant/raffinate pits and vicinity property: U.S. Department of Energy, Oak Ridge Operations office, revision 0, 111 p.

_____1990c, Annual site environmental monitoring report 1989: U.S. Department of Energy, Oak Ridge Operations Office, revision 1, 173 p.

_____1990d, Ground water classification for the Weldon Spring site remedial action project: U.S. Department of Energy, Oak Ridge Operations Office, revision 0.

M.K. Ferguson Company and Jacobs Engineering Group, 1991, Site suitability data on potential location of a disposal facility--Collapse potential and permeability: U.S. Department of Energy, Oak Ridge Operations Office, revision 0.

National Oceanic and Atmospheric Administration, 1988, Climatological data annual summary--Missouri: Asheville, N.C., v. 92, no. 13, 36 p.

Parkhurst, D.L., Thorstenson, D.C., and Plummer, N.L., 1980, PHREEQE--A computer program for geochemical calculations· U.S. Geological Survey Water-Resources Investigations 80-96, revised and reprinted in 1987, 193 p.

Roberts, C.M., 1951, Preliminary investigation of ground-water occurrences in the Weldon Spring area, St. Charles County, Missouri, with further notes on Problems of the Weldon Spring Area, Missouri, by C.V., Theis: U.S. Geological Survey Open-File Report 82-1008, 36 p.

Rueff, A.W., 1977, Minerals, in The resources of St. Charles County, Missouri--Land, water, and minerals: Rolla, Missouri Division of Geology and Land Survey, p. 83-107.

Ryckman, Edgerley, Tomlinson, and Assoc., 1978, Weldon Spring chemical plant survey and assessment: Aberdeen Proving Ground, Maryland, U.S. Army, Office of the Project Manager for Chemical Demilitarization and Installation Restoration, 79 p.

Schumacher, J.G., 1990, Geochemical data for the Weldon Spring chemical plant site and vicinity property, St. Charles County, Missouri--1989-1990: U.S. Geological Survey Open-File Report 90-351, revised in 1991, 45 p.

Schumacher, J.G., and Stollenwerk, K.G., 1991, Geochemical controls on contaminant migration at the Weldon Spring chemical plant site, in Proceedings of the Geosciences Workshop: U.S. Department of Energy, Oak Ridge Operations Office, p. 87-140.

Stumm, Werner, and Morgan, J.J., 1981, Aquatic chemistry--An introduction emphasizing chemical equilibria in natural waters (2d ed.): New York, John Wiley and Sons, 780 p.

Taylor, P.A., Napier, J.M., Scheitlin, F.M., and Strandberg, G.W., 1979, Chemical analysis of ponds 3 and 4 at Weldon Spring, Missouri: U.S. Department of Energy, Oak Ridge Operations Office, 10 p.

Thompson, T.L., 1986, Paleozoic succession in Missouri--Part 4, Mississippian System: Rolla, Missouri Division of Geology and Land Survey Report of Investigations 70, 182 p.

Weidner, R.B., and Boback, M.W., 1982, Weldon Spring storage site environmental monitoring report for 1979 and 1980: Cincinnati, National Lead Company of Ohio, Inc., Feed Material Production Center, 54 p.

Whitfield, J.W., Briller, K.G., and Krummel, W.J., 1989, Geologic map of the Weldon Spring 7-1/2 minute Quadrangle, St. Charles County, Missouri: Rolla, Missouri Division of Geology and Land Survey.